

HERWIG 6.5: an event generator for Hadron Emission Reactions With Interfering Gluons (including supersymmetric processes)*

Gennaro Corcella

Max-Planck-Institut für Physik, Werner-Heisenberg-Institut, Munich
E-mail: corcella@mppmu.mpg.de

Ian G. Knowles

Department of Physics and Astronomy, University of Edinburgh, UK
E-mail: knowles@supanet.com

Giuseppe Marchesini

Dipartimento di Fisica, Università di Milano-Bicocca, and
I.N.F.N., Sezione di Milano, Italy
E-mail: Giuseppe.Marchesini@mi.infn.it

Stefano Moretti

Theory Division, CERN, and IPPP, University of Durham, UK
E-mail: Stefano.Moretti@cern.ch

Kosuke Odagiri

Theory Group, KEK, Japan
E-mail: odagirik@post.kek.jp

Peter Richardson

Department of Applied Mathematics and Theoretical Physics and
Cavendish Laboratory, University of Cambridge, UK
E-mail: richardn@hep.phy.cam.ac.uk

Michael H. Seymour

Department of Physics and Astronomy, University of Manchester, UK
E-mail: M.Seymour@r1.ac.uk

Bryan R. Webber

Cavendish Laboratory, University of Cambridge, UK
E-mail: webber@hep.phy.cam.ac.uk

ABSTRACT: HERWIG is a general-purpose Monte Carlo event generator, which includes the simulation of hard lepton-lepton, lepton-hadron and hadron-hadron scattering and soft hadron-hadron collisions in one package. It uses the parton-shower approach for initial- and final-state QCD radiation, including colour coherence effects and azimuthal correlations both within and between jets. This article updates the description of HERWIG published in 1992, emphasising the new features incorporated since then. These include, in particular, the matching of first-order matrix elements with parton showers, a more correct treatment of spin correlations and heavy quark decays, and a wide range of new processes, including many predicted by the Minimal Supersymmetric Standard Model, with the option of R-parity violation. At the same time we offer a brief review of the physics underlying HERWIG, together with details of the input and control parameters and the output data, to provide a self-contained guide for prospective users of the program. This version of the manual (version 3) is updated to HERWIG version 6.5, which is expected to be the last major release of Fortran HERWIG. Future developments will be implemented in a new C++ event generator, HERWIG++.

KEYWORDS: Supersymmetric Standard Model, QCD, Phenomenological Models, Hadronic Colliders.

*Work supported in part by the U.K. Particle Physics and Astronomy Research Council, by the Italian Ministero della Università e Ricerca Scientifica, and by the E.U. Fourth Framework Programme ‘Training and Mobility of Researchers’, Network ‘Quantum Chromodynamics and the Deep Structure of Elementary Particles’, contract FMRX-CT98-0194 (DG 12 - MIHT). Research of G.C. supported by grant number DE-FG02-91ER40685 from the U.S. Department of Energy.

Contents

| | |
|--|-----------|
| 1. Introduction | 4 |
| 2. Using HERWIG | 6 |
| 3. Physics simulated by HERWIG | 7 |
| 3.1 Elementary hard subprocess | 7 |
| 3.2 Parton showers | 8 |
| 3.2.1 Final-state showers | 8 |
| 3.2.2 Initial-state showers | 11 |
| 3.2.3 Matrix-element corrections | 12 |
| 3.3 Heavy flavour production and decay | 13 |
| 3.4 Gauge and Higgs boson decays | 15 |
| 3.5 Supersymmetry | 17 |
| 3.5.1 Data input | 19 |
| 3.5.2 Processes | 21 |
| 3.5.3 Related changes | 22 |
| 3.6 Spin correlations | 23 |
| 3.7 Hadronization | 24 |
| 3.7.1 Cluster model | 24 |
| 3.7.2 Underlying soft event | 27 |
| 3.7.3 Minimum bias processes | 27 |
| 3.8 Spacetime structure | 29 |
| 3.8.1 Particle decays | 29 |
| 3.8.2 Parton showers | 30 |
| 3.8.3 Hadronization | 30 |
| 3.8.4 Colour rearrangement | 30 |
| 3.8.5 B - \bar{B} mixing | 31 |
| 4. Processes | 32 |
| 4.1 Beams | 32 |
| 4.1.1 Parton distributions | 33 |
| 4.2 Summary of subprocesses | 34 |
| 4.2.1 Treatment of quark masses | 40 |
| 4.2.2 Couplings | 41 |
| 4.3 Lepton-antilepton Standard Model processes | 41 |
| 4.3.1 IPROC=100–127: hadron production | 42 |
| 4.3.2 IPROC=150–250: lepton and electroweak boson production | 42 |

| | | |
|--------|--|----|
| 4.3.3 | IPROC=300–499: Higgs boson production | 43 |
| 4.3.4 | IPROC=500–559: two-photon/photon-boson processes | 43 |
| 4.3.5 | IPROC=600–656: four jet production | 43 |
| 4.4 | Lepton-antilepton supersymmetric processes (MSSM) | 44 |
| 4.4.1 | IPROC=700–799: gaugino, slepton and/or squark production | 44 |
| 4.5 | Other lepton-antilepton non-Standard-Model processes | 45 |
| 4.5.1 | IPROC=800–899: R-parity violating SUSY processes | 45 |
| 4.5.2 | IPROC=900–999: MSSM Higgs production processes | 46 |
| 4.5.3 | IPROC=1000–1199: SM and MSSM Higgs associated production | 46 |
| 4.6 | Hadron-hadron Standard Model processes | 46 |
| 4.6.1 | IPROC=1300–1499: Drell-Yan processes | 46 |
| 4.6.2 | IPROC=1500: QCD $2 \rightarrow 2$ processes | 47 |
| 4.6.3 | IPROC=1600–1699: Higgs boson production by parton fusion | 48 |
| 4.6.4 | IPROC=1700–1706: heavy quark production | 48 |
| 4.6.5 | IPROC=1800: QCD direct photon plus jet production | 48 |
| 4.6.6 | IPROC=1900–1999: Higgs production by weak boson fusion | 48 |
| 4.6.7 | IPROC=2000–2008: single top production | 49 |
| 4.6.8 | IPROC=2100–2170: electroweak boson plus jet production | 49 |
| 4.6.9 | IPROC=2200: direct photon pair production | 49 |
| 4.6.10 | IPROC=2300–2399: Higgs boson plus jet production | 49 |
| 4.6.11 | IPROC=2400–2450: colour singlet exchange | 50 |
| 4.6.12 | IPROC=2500–2599: Higgs boson plus top quark pair production | 50 |
| 4.6.13 | IPROC=2600–2799: Higgs plus weak boson production | 50 |
| 4.6.14 | IPROC=2800–2825: Gauge boson pair production | 50 |
| 4.6.15 | IPROC=2850–2880: Gauge boson pairs using MC@NLO | 51 |
| 4.6.16 | IPROC=2900–2916: $Q\bar{Q}Z$ production | 51 |
| 4.7 | Hadron-hadron supersymmetric processes (MSSM) | 51 |
| 4.7.1 | IPROC=3000–3030: sparton, gaugino and/or slepton production | 52 |
| 4.7.2 | IPROC=3110–3178: charged Higgs plus squark pair production | 53 |
| 4.7.3 | IPROC=3210–3298: neutral Higgs plus squark pair production | 53 |
| 4.7.4 | IPROC=3310–3375: Higgs pair and Higgs-W/Z production | 53 |
| 4.7.5 | IPROC=3410–3450: Higgs boson plus heavy quark production | 54 |
| 4.7.6 | IPROC=3500: charged Higgs boson from bq -initiated processes | 54 |
| 4.7.7 | IPROC=3610–3630: parton fusion to neutral Higgs | 54 |
| 4.7.8 | IPROC=3710–3720: weak boson fusion to neutral Higgs | 54 |
| 4.7.9 | IPROC=3811–3899: Higgs plus heavy quark pair production | 54 |
| 4.8 | Other hadron-hadron non-Standard-Model processes | 55 |
| 4.8.1 | IPROC=4000–4199: R-parity violating SUSY processes | 55 |
| 4.8.2 | IPROC=4200–4299 : graviton resonance production | 55 |
| 4.9 | Photon-hadron and photon-photon processes | 56 |
| 4.9.1 | IPROC=5000–5520: pointlike photon-hadron processes | 56 |

| | | |
|-----------|--|------------|
| 4.9.2 | IPROC=6000–6010: pointlike photon-photon processes | 57 |
| 4.10 | Baryon number violating processes | 57 |
| 4.10.1 | IPROC=7000–7999: generated by the HERBVI package | 57 |
| 4.11 | Minimum bias soft hadron-hadron collisions | 57 |
| 4.11.1 | IPROC=8000: minimum bias soft hadron-hadron event | 57 |
| 4.12 | Deep inelastic lepton scattering | 57 |
| 4.12.1 | IPROC=9000–9006: neutral current | 58 |
| 4.12.2 | IPROC=9010–9016: charged current | 58 |
| 4.12.3 | IPROC=9100–9130: $\mathcal{O}(\alpha_S)$ neutral current processes | 58 |
| 4.12.4 | IPROC=9140–9144: charged-current heavy quark production | 59 |
| 4.12.5 | IPROC=9500–9599: Higgs production by weak boson fusion | 59 |
| 4.13 | Including new subprocesses | 59 |
| 5. | Parameters | 61 |
| 6. | Control switches, constants and options | 63 |
| 6.1 | Negative weights option | 70 |
| 7. | Particle data | 71 |
| 8. | Structure and output | 77 |
| 8.1 | Main program | 77 |
| 8.2 | Form factor file | 79 |
| 8.3 | Event data | 80 |
| 8.3.1 | Status codes | 82 |
| 8.3.2 | Event weights | 83 |
| 8.4 | Error conditions | 84 |
| 8.5 | Sample output | 85 |
| 8.5.1 | Guide to sample output | 89 |
| 8.6 | Subroutine descriptions | 90 |
| 9. | Interfaces | 100 |
| 9.1 | Les Houches | 100 |
| 9.2 | CIRCE | 101 |
| 9.3 | TAUOLA | 102 |
| 9.4 | ISAWIG | 103 |
| 9.5 | HDECAY | 103 |
| 9.6 | MC@NLO | 104 |
| 9.7 | JIMMY | 104 |
| 9.8 | HERBVI | 104 |

1. Introduction

HERWIG is a general-purpose event generator for high-energy processes, with particular emphasis on the detailed simulation of QCD parton showers. The program provides a full simulation of hard lepton-lepton, lepton-hadron and hadron-hadron scattering and soft hadron-hadron collisions in a single package, and has the following special features:

- Initial- and final-state QCD jet evolution with soft gluon interference taken into account via angular ordering;
- Colour coherence of (initial and final) partons in all hard subprocesses, including the production and decay of heavy quarks and supersymmetric particles;
- Azimuthal correlations within and between jets due to gluon interference and polarization;
- A cluster model for jet hadronization based on non-perturbative gluon splitting, and a similar cluster model for soft and underlying hadronic events;
- A space-time picture of event development, from parton showers to hadronic decays, with an optional colour rearrangement model based on space-time structure.

Several of these features were already present in HERWIG version 5.1 and were described accordingly in some detail in ref. [1]. This was in turn based on the work of refs. [2–14]. In the present article we concentrate therefore on the new features incorporated into HERWIG since 1992. The most important of these are the matching of first-order matrix elements with parton showers [15–20], a more correct treatment of spin correlations [21] and heavy quark decays, again including matrix element matching [19], and a wide range of new hard processes. In particular HERWIG now includes the production and decay of supersymmetric particles, with or without the assumption of R-parity conservation [22].

The precise HERWIG version described here is 6.500, which we shall generally refer to as “version 6” in the following.

Let us recall briefly the main features of a generic hard, i.e. high momentum transfer, process of the type simulated by HERWIG. It can be divided notionally into four components, corresponding roughly to increasing scales of distance and time:

1. *Elementary hard subprocess.* A pair of incoming beam particles or their constituents interact to produce one or more primary outgoing fundamental objects. This can be computed exactly to lowest order in perturbation theory. The hard momentum transfer scale Q together with the colour flow of the subprocess set the boundary conditions for the initial- and final-state parton showers, if there are any.

2. *Initial- and final-state parton showers.* A parton constituent of an incident beam hadron with low spacelike virtuality can radiate timelike partons. In the process it decreases its energy to a fraction x of that of the beam and increases its spacelike virtuality, which is bounded in absolute value by the scale Q of the hard subprocess. This initial-state emission process leads to the evolution of the structure function $F(x, Q)$ of the incident hadron. On a similar time-scale, an outgoing parton with large timelike virtuality can generate a shower of partons with lower virtuality. The amount of emission depends on the upper limit on the virtuality of the initiating parton, which is again controlled by the momentum transfer scale Q of the hard subprocess. Timelike partons from the initial-state emission may in turn initiate parton showering. The coherence of soft gluon emission from different parton showers is controlled by the colour flow of the subprocess. Within the showers, it is simulated by angular ordering of successive emissions.

3. *Heavy object decays.* Massive produced objects such as top quarks, electroweak gauge and Higgs bosons, and possibly non-Standard Model (e.g. SUSY) particles, can decay on time-scales that may be shorter than or comparable to that of the QCD parton showers. Depending on their nature and the decay mode, they may also initiate parton showers before and/or after decaying.

4. *Hadronization process.* In order to construct a realistic simulation one needs to combine the partons into hadrons. This applies to the constituent partons of incoming hadronic beams as well as to the outgoing products of parton showering, which give rise to hadronic jets. This hadronization process takes place at a low momentum transfer scale, for which the strong coupling α_s is large and perturbation theory is not applicable. In the absence of a firm theoretical understanding of non-perturbative processes, it must be described by a phenomenological model. The model adopted in HERWIG is intended to disrupt as little as possible the event structure established in the parton showering phase. Showering is terminated at a low scale, $Q_0 < 1$ GeV, and the *preconfinement* property of perturbative QCD [23, 24] is exploited to form colour-neutral clusters [4] which decay into the observed hadrons. Initial-state partons are incorporated into the incoming hadron beams through a soft, non-perturbative “forced branching” phase of spacelike showering. The remnants of incoming hadron, i.e. those constituent partons which do not participate in the hard subprocess, undergo a soft “underlying event” interaction modelled on soft minimum bias hadron-hadron collisions.

After a brief, practical section on the use of HERWIG, in the following sections we discuss each of these components in turn, concentrating on the new features since version 5.1.

2. Using HERWIG

The latest version of the program, together with all relevant information, is always available via the official HERWIG web page:

<http://hepwww.rl.ac.uk/theory/seymour/herwig/>

which is also mirrored at CERN:

<http://home.cern.ch/seymour/herwig/>

The program is written in Fortran and the user has to modify the main program HWIGPR to generate the type and number of events required. See section 8.1 for a sample main program. The program operates by setting up parameters in common blocks and then calling a sequence of subroutines to generate an event. Parameters not set explicitly in the block data HWUDAT or in HWIGPR are set to default values in the main initialisation routine HWIGIN. Output data are delivered in the LEP standard common block HEPEVT [25, 26]. Note that all real variables accessible to the user, including those in HEPEVT, are of type DOUBLE PRECISION.

Since version 6.3, to take account of the increased energy and complexity of interactions at LHC and future colliders, the default value of the parameter NMXHEP, which sets the array sizes in the standard /HEPEVT/ common block, has been increased to 4000.

To generate events the user must first set up the beam particle names PART1, PART2 (type CHARACTER*8) and momenta PBEAM1, PBEAM2 (in GeV/c), a process code IPROC and the number of events required MAXEV.

See section 4 for beams and processes available.

All analysis of generated events (histogramming, etc.) should be performed by the user-provided routines HWABEG (to initialise the run), HWANAL (to analyse an event) and HWAEND (to terminate the run).

A detailed event summary is printed out for the first MAXPR events (default MAXPR = 1). Setting IPRINT = 2 lists the particle identity codes, properties and decay schemes used in the program.

The programming language is standard Fortran 77 as far as possible. However, the following may require modification for running on some computers

- Most common blocks are inserted by INCLUDE 'HERWIG65.INC' statements — the file HERWIG65.INC is part of the standard program package.
- Many common blocks are initialised by BLOCK DATA HWUDAT. Although BLOCK DATA is standard Fortran 77, it can cause linkage problems for some systems.
- Variables of type DOUBLE COMPLEX are used, which may be called COMPLEX*16 on some systems.

In the `INCLUDE` file, common blocks have been regrouped so that all commons that were present in version 6.1 are unchanged. All new variables since version 6.1 are in separate common blocks, which are frozen after each version.

It is anticipated that version 6.5, with minor modifications in the series 6.5xx, will be the *last Fortran version* of HERWIG. Substantial physics improvements will be included in the new C++ event generator HERWIG++ [27], to be released in 2003. Watch for progress on the HERWIG++ web page:

<http://www.hep.phy.cam.ac.uk/~gieseke/Herwig++/>

3. Physics simulated by HERWIG

3.1 Elementary hard subprocess

In HERWIG version 6 there is a fairly large library of QCD, electroweak and supersymmetric elementary subprocesses. These are listed and discussed in section 4.

The hard subprocess plays an important rôle in defining the phase space of any associated initial- and final-state parton showers. As discussed in ref. [1] and references therein, the parton showers are branching processes in which the branchings are ordered in angle from a maximum to a minimum value determined by the cut-off Q_0 . The maximum value is determined by the elementary subprocess and is due to interference among soft gluons. The general result [6, 7, 28] is that the initial and final branchings are approximately confined within cones around the incoming and outgoing partons from the elementary subprocess. For the branching of parton i , the aperture of the cone is defined by the direction of the other parton j that is colour-connected to i . The relation between soft gluon interference and the colour connection structure of the elementary subprocess leads to many detectable effects in hadronic final states. For recent examples, see e.g. refs. [29, 30].

For a general process there are various contributions with different colour connections. The HERWIG library of elementary subprocesses includes the separate colour connection contributions. In general there is some ambiguity in the separation of contributions which are suppressed by inverse powers of the number of colours N_c . In earlier versions of HERWIG, these sub-leading terms were divided amongst the various colour connection contributions according to the recipe in ref. [7]. In version 6 the following improved prescription [31] has been followed, for both the QCD and SUSY QCD subprocesses. The matrix element squared $|\mathcal{M}_i|^2$ for each colour connection is computed in the limit $N_c \rightarrow \infty$ and the corresponding contribution is defined as

$$\frac{|\mathcal{M}_i|^2}{\sum_j |\mathcal{M}_j|^2} |\mathcal{M}|^2,$$

where $|\mathcal{M}|^2$ represents the sum over all colour connections *including terms sub-leading in N_c* . This ensures that each colour connection contribution is positive-definite and

has the correct pole structure, while the sum of contributions yields the exact (Born-level) cross section.

Parton emission into phase space regions which are outside the above-mentioned angular cones, called in the following “dead zones”, do not contribute to leading order and often not even to next-to-leading order. However, for a more complete description of the event it is also necessary to take into account emission into these “dead zones”, which may be done using exact fixed-order matrix elements (see the following sections).

Another important function of the elementary subprocess is to set up the polarizations of any electroweak bosons, heavy (e.g. SUSY) particles or gluon jets that may be involved. These polarizations give rise to angular asymmetries and correlations in boson decays and jet fragmentation. They are included in HERWIG for many of the subprocesses provided, using the approach of refs. [9, 10, 21] to generate all correlations in decays, and in jet fragmentation to leading-logarithmic accuracy.

3.2 Parton showers

3.2.1 Final-state showers

Final-state parton showering in HERWIG is generated by a *coherent branching algorithm* with the following properties:

1. The energy fractions are distributed according to the leading-order Dokshitzer-Gribov-Lipatov-Altarelli-Parisi (DGLAP) splitting functions.
2. The full available phase space is restricted to an angular-ordered region. Such a restriction is the result of interference and correctly takes important infrared singularities into account. At each branching, the angle between the two emitted partons is smaller than that of the previous branching.
3. The emission angles are distributed according to the Sudakov form factors, which sum the virtual corrections and unresolved real emissions. The Sudakov form factor normalizes the branching distributions to give the probabilistic interpretation needed for a Monte Carlo simulation. This fact is a consequence of unitarity and of the infrared finiteness of inclusive quantities.
4. The azimuthal angular distribution in each branching is determined by two effects:
 - (a) for a soft emitted gluon the azimuth is distributed according to the eikonal dipole distribution [7];
 - (b) for non-soft emission one finds azimuthal correlations due to spin effects. See [9, 10] for the method used to implement these correlations in full, to leading collinear logarithmic accuracy, in HERWIG.

5. In each branching the scale of α_s is the relative transverse momentum of the two daughter partons.
6. In the case of heavy flavour production the mass of the quark modifies the angular-ordered phase space. The most important effect is that the soft radiation in the direction of the heavy quark is depleted. One finds that emission within an angle of order M/E is suppressed, M and E being the mass and energy of the heavy quark: this is known as the “dead cone” [32].

Specifically, the HERWIG parton shower evolution is done in terms of the parton energy fraction z and an angular variable ξ . In the parton splitting $i \rightarrow jk$, $z_j = E_j/E_i$ and $\xi_{jk} = (p_j \cdot p_k)/(E_j E_k)$. Thus $\xi_{jk} \simeq \frac{1}{2}\theta_{jk}^2$ for massless partons at small angles. The values of z are chosen according to the DGLAP splitting functions and the distribution of ξ values is determined by the Sudakov form factors. Angular ordering implies that each ξ value must be smaller than the ξ value for the previous branching of the parent parton.

The parton showers are terminated as follows. For partons there is a cutoff of the form $Q_i = m_i + Q_0$, where m_i ($i = 1, \dots, 6$ for d, u, s, c, b, t) is set by the relevant mass parameter `RMASS(i)` and Q_0 is set by the quark and gluon virtuality cutoff parameters `VQCUT` and `VGCUT` (see section 5). Showering from any parton stops when a value of ξ below Q_i^2/E_i^2 is selected for the next branching. For heavy quarks, the condition $\xi > Q_i^2/E_i^2$ corresponds to the “dead cone” mentioned above. At this point the parton is put on mass-shell or given a small non-zero effective mass in the case of gluons.¹ Working backwards from these on-shell partons, one can now construct the virtual masses of all the internal lines of the shower and the overall jet mass, from the energies and opening angles of the branchings. Finally one can assign the azimuthal angles of the branchings, including EPR-type correlations (from Einstein-Podolski-Rosen [33]), and deduce completely all the 4-momenta in the shower.

Next the parton showers are used to replace the (on mass-shell) partons that were generated in the original hard process. This is done in such a way that the jet 3-momenta have the same directions as the original partons in the c.m. frame of the hard process, but they are boosted to conserve 4-momentum taking into account their extra masses.

The main improvements in the final-state emission algorithm of HERWIG version 6, relative to version 5.1, are as follows.

The Sudakov form factors can be calculated using the one-loop or two-loop α_s , according to the variable `SUDORD` (default = 1). The parton showering still incorporates the two-loop α_s in either case but if `SUDORD` = 1 this is done using a veto algorithm, whereas if `SUDORD` = 2 no vetoes are used in the final-state evolution. The usefulness of this option is discussed briefly in section 8.2.

¹The quark mass parameters should also be thought of as effective or constituent masses rather than current quark masses.

Matrix element corrections have been introduced into final-state parton showers in e^+e^- and deep inelastic processes [15, 16], in heavy flavour decays [19] and in Drell-Yan processes [20] (see section 3.2.3).

In HERWIG, the angular-ordering constraint, which is derived for soft gluon emission, is applied to all parton shower vertices, including $g \rightarrow q\bar{q}$. In versions before 6.1, this resulted in a severe suppression (an absence in fact) of configurations in which the gluon energy is very unevenly shared between the quarks. For light quarks this is irrelevant, because in this region one is dominated by gluon emissions, which are correctly treated. However, for heavy quarks this energy sharing (or equivalently the quarks' angular distribution in their rest frame) is a directly measurable quantity and was badly described. Related to this was an inconsistency in the calculation of the Sudakov form factor for $g \rightarrow q\bar{q}$. This was calculated using the entire allowed kinematic range (with massless kinematics) for the energy fraction, $0 \leq z \leq 1$, while the z distribution generated was actually confined to the angular-ordered region, $z, 1-z \geq m/E\sqrt{\xi}$.

In version 6, these defects are corrected as follows. We generate the E, ξ and z values for the shower as before. We then apply an *a posteriori* adjustment to the kinematics of the $g \rightarrow q\bar{q}$ vertex during the kinematic reconstruction. At this stage, the masses of the q and \bar{q} showers are known. We can therefore guarantee to stay within the kinematically allowed region. In fact, the adjustment we perform is purely of the angular distribution of the q and \bar{q} showers in the g rest frame, preserving all the masses and the gluon four-momentum. Therefore we do not disturb the kinematics of the rest of the shower at all.

Although this cures the inconsistency above, it actually introduces a new one: the upper limit for subsequent emission is calculated from the generated E, ξ and x values, rather than from the finally-used kinematics. This correlation is of NNLL importance, so we can formally neglect it. It would be manifested as an incorrect correlation between the masses and directions of the produced q and \bar{q} jets. This is, in principle, physically measurable, but it seems less important than getting the angular distribution itself right. In fact the solution we propose maps the old angular distribution smoothly onto the new, so the sign of the correlation will still be preserved, even if the magnitude is wrong. Even with this modification, the HERWIG kinematic reconstruction can only cope with particles that are emitted into the forward hemisphere in the showering frame. Thus one cannot populate the whole of kinematically-allowed phase space. Nevertheless, we find that this is usually a rather weak condition and that most of phase space is actually populated.

Using this procedure, we find that the predicted angular distribution for secondary b quarks at LEP energies is well-behaved, i.e. it looks reasonably similar to the leading-order result $(1 + \cos^2 \theta^*)$, and has relatively small hadronization corrections.

Real photon emission is included in timelike parton showering. The infrared

photon cutoff is `VPCUT`, which defaults to 0.4 GeV. Agreement with LEP data is satisfactory if showering is used together with the matrix element correction to produce photons in the back-to-back region. The results are insensitive to `VPCUT` variations in the range 0.1–1.0 GeV. Setting `VPCUT` greater than the total c.m. energy switches off such emission. As an expedient way of improving the efficiency of photon final-state radiation studies, the electromagnetic coupling `ALPHEM` can be multiplied by a factor `ALPFAC` (default = 1) for all quark-photon vertices in jets, and in the ‘dead zone’ in e^+e^- . Results at small photon-jet separation become sensitive to `ALPFAC` above about 5.

3.2.2 Initial-state showers

The theoretical analysis of initial-state showering is more complex than the final-state case. The most relevant parameters of the hard subprocess are the hard scale Q and the energy fraction x of the incoming parton after the emission of initial state radiation. For lepton-hadron processes x corresponds to the Bjorken variable, while for hadron-hadron processes x is related to Q^2/s where s is the c.m. energy squared.

The main result is that for any value of x , even for x small [34], the initial-state emission process factorizes and can be described as a *coherent branching* process suitable for Monte Carlo simulations. The properties which characterize this process include all those discussed above for the final-state emission. However, in the initial-state case the angular-ordering restriction on the phase space applies to the angles θ_i between the directions of the incoming hadron and the emitted partons i .

For large x , the coherent branching algorithm sums correctly [13] not only the leading but also the next-to-leading contributions. This accuracy allows us to identify the relation between the QCD scale used in the Monte Carlo program and the fundamental parameter $\Lambda_{\overline{\text{MS}}}$. This is achieved by using the one-loop Altarelli-Parisi splitting functions and the two-loop expression for α_s with the following universal relation between the scale parameter Λ_{phys} [13] used in the simulation and $\Lambda_{\overline{\text{MS}}}$ (here, N_f is the number of flavours)

$$\Lambda_{\text{phys}} = \exp\left(\frac{67 - 3\pi^2 - 10N_f/3}{2(33 - 2N_f)}\right) \Lambda_{\overline{\text{MS}}} \simeq 1.569 \Lambda_{\overline{\text{MS}}} \quad \text{for } N_f = 5.$$

Therefore a Monte Carlo simulation with next-to-leading accuracy can be used to determine $\Lambda_{\overline{\text{MS}}}$ from semi-inclusive data at large momentum fractions.²

In the case of small values of x , the initial state branching process has additional properties, which are not yet included fully in `HERWIG`. This was discussed in ref. [1] and the situation remains unchanged since version 5.1.

The initial-state branching algorithm in `HERWIG` is of the *backward evolution* type. It proceeds from the elementary subprocess, at a hard scale set by colour co-

²This applies also to final-state emission, i.e. to jet fragmentation at large values of the jet momentum fraction.

herence (see section 3.1), back to the hadron scale, set here by the spacelike cutoff parameter `QSPAC`. At this point there is a forced non-perturbative stage of branching which ensures that the emitting parton fits smoothly with the valence parton distributions of the incoming hadron.

Matrix-element corrections have been introduced into initial-state parton showers in deep inelastic [16] and Drell-Yan processes [20], as discussed in the following subsection.

To avoid double-counting of hard parton emission, all radiation at transverse momenta greater than the hard process scale `EMSCA` is vetoed. In the case of initial-state radiation, this affects all events, while for final-state radiation it only affects those events in which the two jets have a rapidity difference of more than about 3.4.

In the backward evolution of initial-state radiation for photons the “anomalous” branching $q\bar{q} \leftarrow \gamma$ is included. Variables `ANOMSC(1,IBEAM)` and `ANOMSC(2,IBEAM)` record the evolution scale and transverse momentum, respectively, at which an anomalous splitting was generated in the backward evolution of beam `IBEAM`. If zero, then no such splitting was generated.

The treatment of forced branching of gluons and sea (anti-)quarks in backward evolution has been improved, by allowing it to occur at a random scale between the spacelike cutoff `QSPAC` and the infrared cutoff, instead of exactly at `QSPAC` as before. A new option `ISPAC = 2` allows the freezing of structure functions at the scale `QSPAC`, while evolution continues to the infrared cutoff. The default, `ISPAC = 0` is equivalent to previous versions, in which perturbative evolution stops at `QSPAC`.

The width of the (gaussian) intrinsic transverse momentum distribution of valence partons in incoming hadrons at scale `QSPAC` is set by the parameter `PTRMS` (default value zero). The intrinsic transverse momentum is chosen before the initial state cascade is performed and is held fixed even if the generated cascade is rejected. This is done to avoid correlation between the amount of perturbative and non-perturbative transverse momentum generated.

It is possible to completely switch off initial-state emission, by setting `NOSPAC = .TRUE.`, in which case only the forced splitting of non-valence partons is generated.

3.2.3 Matrix-element corrections

One of the new features of `HERWIG 6` is the matching of first-order matrix elements with parton showers.

The `HERWIG` parton showers are performed in the soft or collinear approximation and emission is allowed only in regions of the phase space satisfying the condition $\xi < 1$ or $\xi < z^2$, for the final- (timelike branching) and initial-state (spacelike branching) radiation respectively, where ξ and z are the showering variables defined above.

The emission is entirely suppressed inside the so-called dead zones ($\xi > 1$ or $\xi > z^2$), corresponding to hard and/or large-angle parton radiation. According to the exact matrix elements, the radiation in the dead zones is suppressed, since it

is not soft or collinear logarithmically enhanced, but it is not completely absent as happens in the HERWIG standard shower algorithm. The HERWIG parton cascades need to be supplemented by matrix-element corrections for a full description of the physical phase space.

The method of matrix-element corrections to the HERWIG parton showers is discussed in [16,17]. The radiation in the dead zones is generated according to the exact first-order matrix element (‘hard correction’); the shower in the already-populated region of the phase space is corrected by the use of the exact $\mathcal{O}(\alpha_S)$ amplitude any time an emission is capable of being the ‘hardest so far’ (‘soft correction’³).

By ‘hardest-so-far’, we mean the radiation of a parton whose transverse momentum relative to the splitting one is larger than all those previously emitted. This is not always the first emission, as angular ordering does not necessarily imply ordering in transverse momentum. As shown in [16], if we corrected only the first emission, we would have problems in the implementation of the Sudakov form factor whenever a subsequent harder emission occurs, as we would find that the probability of hard radiation would depend on the infrared cutoff, which is clearly unphysical. Using the $\mathcal{O}(\alpha_S)$ result for the hardest-so-far emission in the already-filled phase space as well as in the dead zone allows one to have matching over the boundary of the dead zone itself.

Since the fraction of events which receive a hard correction is typically small, we neglect multiple hard emissions in the dead zones and rely on the first-order result plus showering in those regions.

Our method is quite different from the one used to implement matrix-element corrections in JETSET [35], where the parton shower probability is applied over the whole phase space and the first-order amplitude is used only to correct the first emission.

Following these general prescriptions, matrix-element corrections have been implemented in some e^+e^- processes [15] (including $e^+e^- \rightarrow WW/ZZ$), deep inelastic lepton scattering [18], top quark decay [19], and Drell-Yan processes [20]. Those for the process $gg \rightarrow$ Higgs are now in progress [36].

The variables `HARDME` (default = `.TRUE.`) and `SOFTME` (default = `.TRUE.`) allow respectively the application of hard and soft matrix-element corrections to the HERWIG parton cascades.

3.3 Heavy flavour production and decay

Heavy quark decays are treated as secondary hard subprocesses. Top quarks and any hypothetical heavier quarks always decay before hadronization. Heavy-flavoured hadrons are split into collinear heavy quark and spectator and the former decays independently. After decay, parton showers may be generated from coloured decay

³We point out that in the expression ‘soft correction’, ‘soft’ refers to the phase space where such corrections are applied and not to the amplitude, since we still use the ‘hard’ exact matrix element for the soft correction as well.

products, in the usual way. See ref. [11] for details of the treatment of colour coherence in these showers.

In HERWIG version 6 matrix-element corrections to the simulation of top quark decays are available. The routine HWBTOP implements the hard corrections; HWBRAN has been modified to implement the soft corrections. Since the dead zone includes part of the soft singularity, a cutoff is required: only gluons with energy above GCUTME (default value 2 GeV) in the top rest frame are corrected. Physical quantities are not strongly dependent on GCUTME in the range 1 to 5 GeV, after the typical experimental cuts are applied. For more details see ref. [19].

The structure of the program has been altered so that the secondary hard sub-process and subsequent fragmentation associated with each partonic heavy hadron decay appear separately in the event record. Thus top quark decays are treated individually as are any subsequent bottom hadron partonic decays. Note that the statement CALL HWDHOB, which deals with the decays of all heavy objects (including SUSY particles), must appear in the main program between the calls to HWBGEN and HWCFOR, in order to carry out any decays before hadronization.

The partonic decay fractions of heavy quarks are specified in the decay tables like the decay modes of other particles. This permits different decays to be given to individual heavy hadrons. Changes to the decay table entries can be made on an event by event basis if desired. Partonic decays of charm hadrons and quarkonium states are also now supported. The order of the products in a partonic decay mode is significant. For example, if the decay is $Q \rightarrow W + q \rightarrow (f + \bar{f}') + q$ occurring inside a $Q\bar{s}$ hadron, the required orderings are:

$$\begin{aligned}
 Q + \bar{s} &\rightarrow (f + \bar{f}') + (q + \bar{s}) \\
 &\text{or } (q + \bar{f}') + (f + \bar{s}) \quad (\text{'colour rearranged'}).
 \end{aligned}$$

In both cases the $(V - A)^2$ matrix element-squared is proportional to $(p_Q \cdot p_2)(p_1 \cdot p_3)$, where p_1 etc. correspond to the ordering given. Decays of heavy-flavoured hadrons to exclusive non-partonic final states are also supported. No check is made against double counting from partonic modes. However this is not expected to be a major problem for the semi-leptonic and two-body hadronic modes supplied.

The default masses of the c and b quarks have been lowered to 1.55 and 4.95 respectively: this corresponds to the mass of the lightest meson minus the u or d quark mass. This increases the number of heavy mesons, and hence total multiplicities, and slightly softens their momentum spectrum. The rate of photoproduced charm states increases and $B-\pi$ momentum correlations become smoother. The default top quark mass is $174.3 \text{ GeV}/c^2$. The same value is used in the production and decay matrix elements and for all kinematics. Note that higher-order corrections are not fully included, and so the HERWIG top mass does not necessarily correspond to that defined in any particular rigorous scheme (e.g. the pole mass or the $\overline{\text{MS}}$ running

mass). However, since it is probably the decay kinematics that are most sensitive to this parameter, it should be close to the pole mass. See subsection 4.2.1 for notes on the treatment of quark masses in various processes.

3.4 Gauge and Higgs boson decays

The total decay widths of the electroweak gauge bosons $V = W, Z$ are specified by the input parameters **GAMW** and **GAMZ**. Their branching fractions to various final states are computed automatically from the other SM input parameters. Which decays actually occur is controlled as follows. The variable **MODBOS**(i) controls the decay of the i th gauge boson per event (table 1).

| MODBOS(i) | W^\pm Decay | Z^0 Decay |
|---------------|-----------------|-----------------------|
| 0 | all | all |
| 1 | $q\bar{q}$ | $q\bar{q}$ |
| 2 | $e\nu$ | e^+e^- |
| 3 | $\mu\nu$ | $\mu^+\mu^-$ |
| 4 | $\tau\nu$ | $\tau^+\tau^-$ |
| 5 | $e\nu + \mu\nu$ | $e^+e^- + \mu^+\mu^-$ |
| 6 | all | $\nu\bar{\nu}$ |
| 7 | all | $b\bar{b}$ |
| > 7 | all | all |

Table 1: W, Z decays.

All entries of **MODBOS** default to 0. Bosons which are produced in pairs (i.e. from VV pair production, or Higgs decay)

are symmetrized in **MODBOS**(i) and **MODBOS**($i + 1$). For processes which directly produce gauge bosons, the event weight includes the branching fraction to the requested decay, but this is only true for Higgs production if decay to W^+W^-/Z^0Z^0 is forced (**IPROC** = 310, 311 but not 399, etc.). Users can thus force $Z \rightarrow b\bar{b}$ decays, with **MODBOS**(i) = 7. For example, **IPROC** = 250, **MODBOS**(1) = 7, **MODBOS**(2) = 0 gives Z^0Z^0 production with one Z^0 decaying to $b\bar{b}$.

The spin correlations in the decays are handled in one of two ways:

1. The diagonal members of the spin density matrix are stored in **RHOHEP**(i , **IHEP**), where $i = 1, 2, 3$ for helicity = $i - 2$ in the centre-of-mass frame of their production, for processes where this matrix is diagonal (i.e. there is no interference between spin states).
2. The correlations in the decay are handled directly by the production routine where (1) is not possible.

The processing of the parton showers in hadronic W and Z decays is handled in the rest frame of the vector boson if **WZRFR** is **.TRUE.** (the default), otherwise in the lab frame. In the latter case, which was the default in earlier versions, the initial cone angles of the showers depend on the velocity of the boson, which leads to a slight Lorentz non-invariance of decay distributions.

The total decay width of the SM Higgs boson is computed from its input mass **RMAS**(201) and stored as **GAMH**. Its decay branching fractions are also computed and stored in **BRHIG**(**I**): **I** = 1–6 for $d\bar{d}, \dots, t\bar{t}$; **I** = 7–9 for $e^+e^-, \dots, \tau^+\tau^-$; **I** = 10,11,12

for W^+W^- , Z^0Z^0 , $\gamma\gamma$. Non-SM Higgs bosons, on the other hand, such as those in supersymmetric models, have to have their widths and decay tables provided as input data (see section 3.5.1). To avoid any ambiguity, the SM Higgs boson has a distinct identity code in **HERWIG** and is represented by the special symbol H_{SM}^0 .

There are two choices for the treatment of the SM Higgs width, both controlled by the variable **IOPHIG**:

$$\text{IOPHIG} = 2I + J,$$

where I and J are both zero or one. Whenever a Higgs boson is generated, its mass is chosen from a distribution that, for heavy SM Higgs bosons, can be rather broad. The choice of I makes a significant difference to the physical meaning of the distribution generated: for $I = 0$, the cross section corresponds to the tree level process containing an s -channel Breit-Wigner resonance for the Higgs boson with a running Higgs width. As discussed in [37], this neglects important contributions from interference with non-resonant diagrams and can violate unitarity at high energy, so $I = 1$ (the default) uses the improved prescription of [37]. This replaces the s -channel propagator by an effective propagator that sums the interference terms to all orders. This increases the cross section below resonance and decreases it above, causing an overall increase in cross section. More details can be found in [37].

The variable J is a more technical parameter that does not affect the physical results, only the method by which they are generated: $J = 1$ (the default) generates the mass according to a fixed-width Breit-Wigner resonance, while $J = 0$ biases the distribution more towards higher masses. In either case, the appropriate jacobian factor is included in the event weight, so that the physical cross section is independent of J .

In all the above cases, the SM Higgs mass distribution is restricted to the range $[m_{\text{H}} - \text{GAMMAX} \times \Gamma_{\text{H}}, m_{\text{H}} + \text{GAMMAX} \times \Gamma_{\text{H}}]$. **GAMMAX** defaults to 10, but in the non-perturbative region $m_{\text{H}} \gtrsim 1 \text{ TeV}$ should be reduced to protect against poor weight distributions. These considerations do not affect the distribution noticeably for $m_{\text{H}} \lesssim 500 \text{ GeV}$, and **GAMMAX** can safely be increased if necessary.

For a SUSY Higgs, the width is never large enough for unitarity to be violated and these issues are unimportant. In this case, the mass distribution is chosen according to a fixed-width Breit-Wigner resonance, like that of any other SUSY particle.

The SM Higgs decays that can occur are normally controlled by the process code **IPROC**, as in **IPROC** = 300 + **ID** for example: **ID**= 1–6 for quarks, 7–9 for leptons, 10/11 for W^+W^-/Z^0Z^0 pairs, and 12 for photons. In addition **ID**= 0 gives quarks of all flavours, and **ID**= 99 gives all decays. For each process, the average event weight is the cross section in nb times the branching fraction to the requested decay. The branching ratios to quarks use the next-to-leading logarithm corrections, those to W^+W^-/Z^0Z^0 pairs allow for one or both bosons being off mass-shell.

All Higgs vertices include an optional enhancement factor to account for non-SM

and non-MSSM couplings. The amplitudes for all Higgs vertices are multiplied by the factor `ENHANC(ID)` where `ID` is the same as in `IPROC = 300 + ID` except the $\gamma\gamma H$ ‘vertex’ which is calculated from `ENHANC(6)` and `ENHANC(10)` for the top and W^\pm loops. This allows the simulation of the production of any chargeless scalar Higgs-like particle. Note however that pseudoscalar and charged Higgs bosons, and processes involving more than one Higgs particle (e.g. the decay $H^0 \rightarrow h^0 Z$) are not included this way (see section 4.7).

The array `ENHANC(ID)` is initialised as usual in `HWIGIN`. Note, however, that it will be overwritten if MSSM Higgs production is required by `IPROC`. In that case, as mentioned earlier, the Higgs widths and decay modes are simply read from an input particle data file (see section 3.5.1).

3.5 Supersymmetry

| Particle | | Spin | Particle | | Spin |
|---|-----------------|------|-------------------|----------------------|------|
| quark | q | 1/2 | squarks | $\tilde{q}_{L,R}$ | 0 |
| charged lepton | ℓ | 1/2 | charged sleptons | $\tilde{\ell}_{L,R}$ | 0 |
| neutrino | ν | 1/2 | sneutrino | $\tilde{\nu}$ | 0 |
| gluon | g | 1 | gluino | \tilde{g} | 1/2 |
| photon | γ | 1 | photino | $\tilde{\gamma}$ | 1/2 |
| neutral gauge boson | Z^0 | 1 | zino | \tilde{Z} | 1/2 |
| neutral Higgs bosons | h^0, H^0, A^0 | 0 | neutral Higgsinos | $\tilde{H}_{1,2}^0$ | 1/2 |
| charged gauge boson | W^\pm | 1 | wino | \tilde{W}^\pm | 1/2 |
| charged Higgs boson | H^\pm | 0 | charged Higgsino | \tilde{H}^\pm | 1/2 |
| graviton | G | 2 | gravitino | \tilde{G} | 3/2 |
| $\tilde{W}^\pm, \tilde{H}^\pm$ mix to form 2 chargino mass eigenstates $\tilde{\chi}_1^\pm, \tilde{\chi}_2^\pm$ $\tilde{\gamma}, \tilde{Z}, \tilde{H}_{1,2}^0$ mix to form 4 neutralino mass eigenstates $\tilde{\chi}_1^0, \tilde{\chi}_2^0, \tilde{\chi}_3^0, \tilde{\chi}_4^0$ \tilde{t}_L, \tilde{t}_R (and similarly $\tilde{b}, \tilde{\tau}$) mix to form the mass eigenstates \tilde{t}_1, \tilde{t}_2 | | | | | |

Table 2: SUSY particle content.

`HERWIG` now includes the production and decay of superparticles, as given by the Minimal Supersymmetric Standard Model (MSSM) [22]. The mass spectrum and decay modes, being read from input files (see below), are completely general. The particle content, listed in the following table (table 2), includes the gravitino/goldstino. For particles that mix, the subscripts label the mass eigenstates in the ascending order of mass. The two Higgs Doublet Model (2HDM) Higgs sector, intrinsic to the MSSM, is also included. The three neutral Higgs bosons are denoted by h^0 , H^0 and A^0 .

The SUSY particle names in `HERWIG` are as shown in table 3. `IDHW` is the `HERWIG` identity code and `IDPDG` is the corresponding Particle Data Group code [38].

| IDHW | NAME | IDPDG | IDHW | NAME | IDPDG | | |
|------|--------------------|------------|---------|------|--------------------|------------|---------|
| 401 | \tilde{d}_L | 'SSDL ' | 1000001 | 413 | \tilde{d}_R | 'SSDR ' | 2000001 |
| 402 | \tilde{u}_L | 'SSUL ' | 1000002 | 414 | \tilde{u}_R | 'SSUR ' | 2000002 |
| 403 | \tilde{s}_L | 'SSSL ' | 1000003 | 415 | \tilde{s}_R | 'SSSR ' | 2000003 |
| 404 | \tilde{c}_L | 'SSCL ' | 1000004 | 416 | \tilde{c}_R | 'SSCR ' | 2000004 |
| 405 | \tilde{b}_1 | 'SSB1 ' | 1000005 | 417 | \tilde{b}_2 | 'SSB2 ' | 2000005 |
| 406 | \tilde{t}_1 | 'SST1 ' | 1000006 | 418 | \tilde{t}_2 | 'SST2 ' | 2000006 |
| 425 | \tilde{e}_L | 'SSEL- ' | 1000011 | 437 | \tilde{e}_R | 'SSER- ' | 2000011 |
| 426 | $\tilde{\nu}_e$ | 'SSNUEL ' | 1000012 | 439 | $\tilde{\mu}_R$ | 'SSMUR- ' | 2000013 |
| 427 | $\tilde{\mu}_L$ | 'SSMUL- ' | 1000013 | 441 | $\tilde{\tau}_2$ | 'SSTAU2- ' | 2000015 |
| 428 | $\tilde{\nu}_\mu$ | 'SSNUMUL ' | 1000014 | | | | |
| 429 | $\tilde{\tau}_1$ | 'SSTAU1- ' | 1000015 | | | | |
| 430 | $\tilde{\nu}_\tau$ | 'SSNUTL ' | 1000016 | | | | |
| 449 | \tilde{g} | 'GLUINO ' | 1000021 | 458 | \tilde{G} | 'GRAVTINO' | 1000039 |
| 450 | $\tilde{\chi}_1^0$ | 'NTLINO1 ' | 1000022 | 451 | $\tilde{\chi}_2^0$ | 'NTLINO2 ' | 1000023 |
| 452 | $\tilde{\chi}_3^0$ | 'NTLINO3 ' | 1000025 | 453 | $\tilde{\chi}_4^0$ | 'NTLINO4 ' | 1000035 |
| 454 | $\tilde{\chi}_1^+$ | 'CHGINO1+' | 1000024 | 455 | $\tilde{\chi}_2^+$ | 'CHGINO2+' | 1000037 |
| 203 | h^0 | 'HIGGSLO ' | 26 | 204 | H^0 | 'HIGGSHO ' | 35 |
| 205 | A^0 | 'HIGGSAO ' | 36 | 206 | H^+ | 'HIGGS+ ' | 37 |

Table 3: SUSY particle names.

Antiparticles generally appear in sequence after the corresponding particles, e.g. antisquarks $\tilde{d}_L^* - \tilde{t}_1^*$ at IDHW = 407–412, $\tilde{d}_R^* - \tilde{t}_2^*$ at 419–424. They have 'BR' added to the name, e.g. 'SSDLBR ', or opposite charge, and negative PDG codes. A full list can be obtained using the print option `IPRINT = 2` (see section 6).

Note that the `HERWIG` particle labelling of the lightest MSSM Higgs boson departs from the PDG recommendation: it is given PDG code 26, to avoid confusion with the SM Higgs boson (PDG code 25) in our implementation (specifically, in our use of the array `ENHANC` for the MSSM processes: see the relevant Higgs sections for more details).

`HERWIG` does not contain any built-in models for SUSY scenarios beyond the MSSM, such as, Supergravity (SUGRA) or Gauge Mediated Symmetry Breaking (GMSB). In all cases the SUSY particle spectrum and decay tables must be provided just like those for any other particles. The subroutine `HWISSP`, if called, reads these from an input file. The production subprocesses are then generated by `HWHESP`, in lepton-antilepton collisions, `HWHSSP`, in hadron-hadron collisions, or by one of the \mathcal{R}_p production routines. The decays of the sparticles produced, as well as any top quarks or Higgs bosons, are then performed by `HWDHOB`.

3.5.1 Data input

A package `ISAWIG`, see section 9.4, has been created to work with `ISAJET` [39] to produce a file containing the SUSY particle masses, lifetimes and decay modes. This package takes the outputs of the `ISAJET SUGRA` or general MSSM programs and produces a data file in a format that can be read into `HERWIG` by the subroutine `HWISSP`. In principle the user can produce a similar file provided that the correct format is used, as explained below.

For the mixing terms of the MSSM lagrangian we follow the Haber-Kane [40,41] conventions, so that we differ from `ISAJET` on the sign for gaugino masses, the ordering and signs of the gaugino current eigenstates, the interchange of the rows and columns of the gaugino mixing matrices, and the sign of the neutral Higgs mixing angle α .

In addition to the decay modes included in the `ISAJET` package `ISAWIG` allows for the possibility of violating R-parity and includes the calculation of all 2-body squark and slepton, and 3-body gaugino and gluino R-parity violating (\mathcal{R}_p) decay modes.

It can happen that some of the SUSY particle decay modes generated by `ISAJET` are found to be kinematically forbidden in `HERWIG`, owing to the slightly different values assumed for the light quark masses. In this case a warning message is printed by `HERWIG` and these modes are deleted, the other branching ratios being rescaled accordingly. Such modes normally have negligible `ISAJET` branching ratios anyway, because of their tiny phase space.

The input file organisation expected by `HWISSP` is as follows. First the SUSY particle and top quark masses and lifetimes (in seconds) are given according to their `HERWIG` identity codes `IDHW`, for example:

```
65
401 927.3980    0.74510E-25
402 925.3307    0.74009E-25
....etc.
```

That is,

```
NSUSY = Number of SUSY + top particles
IDHW, RMASS(IDHW), RLTIM(IDHW)
repeated NSUSY times.
```

Next each particle's decay modes together with their branching ratios and matrix element codes are given as, for example:

```
6
401 0.18842796E-01    0 450    1    0    0    0
:      :              :  :      :    :    :
:      :              :  :      :    :    :
```

```

401  0.32755006E-02      0  457    2    0    0    0
6
402  0.94147678E-02      0  450    2    0    0    0
....etc.

```

That is,

Number of decay modes for a given particle IDK
 IDK(IM), BRFRAC(IM), NME(IM), IDKPRD(1-5, IM)
 repeated for each mode IM
 all repeated for each particle (NSUSY times).

The order in which the decay products appear is important in order to obtain appropriate showering and hadronization. The correct orderings are indicated in the table below (table 4).

New matrix element codes have been added for SUSY and Higgs decays:

- NME=200, describing the $1 \rightarrow 3$ body heavy-quark decays via a virtual H^\pm boson. A new function, HWDHWT, was introduced to this end. This can be used to emulate e.g. $t \rightarrow bH^+(\rightarrow f\bar{f}')$ decays.
- NME = 300 for three-body \mathcal{R}_p gaugino and gluino decays.

The indices i, j, k in \mathcal{R}_p gaugino/gluino decays refer to the ordering of the indices in the \mathcal{R}_p couplings in the superpotential. The convention is as in ref. [42].

Next a number of parameters derived from the SUSY lagrangian must be given. These are: the ratio of Higgs VEVs, $\tan\beta$, and the scalar Higgs mixing angle, α ; the mixing parameters for the Higgses, gauginos and the sleptons; the trilinear couplings; and the Higgsino mass parameter μ .

Finally the logical variable RPARTY must be set .FALSE. if R-parity is violated, and the \mathcal{R}_p couplings must also be supplied; otherwise not.

Details of the FORMAT statements employed can be found by examining the subroutine HWISSP.

HWISSP reads the data from UNIT = LRSUSY (default LRSUSY = 66). If the data are stored in a `fort.LRSUSY` file on a UNIX system⁴ no further action is required, but if the data are to be read from a file named `fname.dat` then appropriate OPEN and CLOSE statements must be added by hand:

```

OPEN(UNIT=LRSUSY,FORM='FORMATTED',STATUS='UNKNOWN',FILE='fname.dat')
CALL HWISSP CLOSE(UNIT=LRSUSY)

```

A number of sets of SUSY parameter files, produced using ISAJET, for the standard LHC SUGRA and GMSB points are available from the ISAWIG home page: <http://www.hep.phy.cam.ac.uk/~richardn/HERWIG/ISAWIG/>

⁴Or the equivalent, e.g. `fortLRSUSY.dat` on a VAX system.

| Decaying Particle | No. of products | Type of mode | Order of decay products | | |
|-------------------|-----------------|-----------------------------|---|---|--------|
| | | | 1st | 2nd | 3rd |
| top | 2 | two-body to Higgs | Higgs | bottom | |
| | 3 | three-body via Higgs/W | quarks or leptons from W/Higgs | | bottom |
| gluinos | 2 | without gluon | any order | | |
| | | with gluon | gluon | colour neutral | |
| | 3 | R-parity conserved | colour neutral | quark or antiquark | |
| squark or slepton | 2 | gaugino/gluino quark/lepton | gaugino gluino | quark lepton | |
| | 3 | weak | sparticle | particles from W decay | |
| squarks | 2 | lepton number violated | quark | lepton | |
| | | baryon number violated | quark | quark | |
| sleptons | 2 | lepton number violated | quark or antiquark | | |
| Higgs | 2 | (s)quark-anti(s)quark | (s)quark or anti(s)quark | | |
| | | (s)lepton-anti(s)lepton | (s)lepton or anti(s)lepton | | |
| | 3 | all three-body | colour neutral | quark or antiquark lepton or antilepton | |
| gaugino | 2 | squark-quark | quark or squark | | |
| | | slepton-lepton | lepton or slepton | | |
| | 3 | R-parity conserved | colour neutral | quark or antiquark lepton or antilepton | |
| gaugino or gluino | 3 | R-parity violating | particles in the order i, j, k as in the superpotential | | |

Table 4: SUSY decay product ordering.

3.5.2 Processes

The implementation of supersymmetric particle production processes in lepton-anti-lepton and hadron-hadron collisions is described in sections 4.4 and 4.7, respectively. As in SM processes, we do not include any higher-order QCD corrections to the relevant matrix elements, even though these are now known in many cases. This is in order to avoid double counting of corrections generated approximately by parton showering.

The procedure by which the MSSM matrix elements describing the elementary hard subprocesses are interfaced to the initial- and final-state parton showers is similar to that described in sections 3.1 and 3.2 for the SM case. However, at present showers are generated from partons but not from spartons, whose short lifetimes should make this a reasonable approximation.

We include matrix elements and spin correlations in all SUSY decays as described in [21]. Breit-Wigner mass distributions have been implemented for all unstable SUSY particles, according to their widths as given in the input file. For a list of the most relevant decay modes of MSSM particles, see ref. [22].

One difference between the SM and MSSM implementations of the Higgs decay channels should be mentioned. Whereas for the SM Higgs boson all decay rates are calculated by `HERWIG` itself, in terms of the other (known) parameters of the SM, in the case of the MSSM scalars these are passed to the generator through the data files.

A more detailed description of the new SUSY reactions in `HERWIG`, along with the relevant formulae for the hard scattering processes involved, can be found in [22].

We include the possibility of violating R-parity both in the decays of the sparticles and in the initial hard subprocess. The \mathcal{R}_p model we consider is specified by a spectrum which can be given in either the SUGRA, GMSB or a more general MSSM scenario, and a set of \mathcal{R}_p couplings at the weak scale. We include only the tri-linear couplings and not the bi-linear terms which mix the leptons and gauginos; a recent review of these models can be found in [43]. However we do include the possibility that more than one of the \mathcal{R}_p couplings can be non-zero. All the two-body squark and slepton and three-body gaugino and gluino decay modes, and resonant production processes in hadron-hadron collisions are included, as well as a range of production processes in e^+e^- collisions. A decay matrix element is implemented for the three-body decays. The colour structure of these events is very different from that of the MSSM [42], due to the presence of the baryon-number violating (\mathcal{B}) vertex. This means that a new subroutine `HWBRCN` is required to handle the colour connections between jets in this case. A full discussion of the colour connections in these processes and the matrix elements for the cross sections and decays can be found in [42].

3.5.3 Related changes

A large number of changes have been made in `HERWIG` to enable SUSY processes to be included in hadron-hadron collisions. The main changes are:

- The subroutine `HWDHQB` has been replaced by `HWDHOB` which does both heavy quark and SUSY particle decays.
- The subroutines `HWBCON`, `HWCGSP` and `HWCFOR` have been adapted to handle the colour connections found in normal SUSY decays.
- The subroutine `HWBRCN` has been included to deal with the inter-jet colour connections arising in \mathcal{R}_p SUSY. Also `HWCBVI`, `HWCBVT` and `HWCBCT` have been added to handle the hadronization of baryon number violating (\mathcal{B}) SUSY decays and processes. If the variable `RPARTY=.TRUE.` (default) then the old `HWBCON` colour connection code is used, else the new `HWBRCN`.

3.6 Spin correlations

In addition to the spin correlations in parton showers and vector boson decays discussed above, in versions 6.4 and higher spin correlation effects are included in processes where top quarks, τ leptons and SUSY particles are produced, as described in [21]. At the moment the effects are only calculated for the production of these particles in the following processes: IPROC=100-199, 700-799, 800-899, 1300-1399, 1400-1499, 1500-1599, 1700-1799, 2000-2099, 2800-2825, 3000-3030, 4000-4199. However, if these particles are produced in other processes, the spin correlation algorithm will still be used to perform their decays. The correlations are also included for the decay of the MSSM Higgs bosons, regardless of how they are produced.

The spin correlations are controlled by the logical variable⁵ SYSPIN [.TRUE.] which switches the correlations on. If required the correlations are initialised by the new routine HWISPN. This routine initialises the two, three and four body matrix elements.

The three and four body matrix elements can be used separately to generate the decay distributions without spin correlation effects. These are switched on by the switches THREEB [.TRUE.] for three body decay and FOURB [.FALSE.] for four body decays. The four body decays are only important in SUSY Higgs studies, and have small branching ratios. However, they take some time to initialise and are therefore switched off by default.

The initialisation of the spin correlations and/or decay matrix elements can be time consuming and we have therefore included an option to read/write the information. The information is written to unit LWDEC [88] and read from LRDEC [0]. If either are zero the data is not written/read. If IPRINT=2 then information on the branching ratios for the decay modes and the maximum weights for the matrix elements is outputted.

If the spin correlation (SYSPIN) or matrix element switches (THREEB, FOURB) are .TRUE., then the matrix element codes (NME entries) for the decays concerned are not used; the calculated matrix elements are used instead.

When we included spin correlations in HERWIG6.4 [21] we did not include either R-parity violating decays or decays producing gravitinos in the algorithm. This led to HERWIG stopping when such decays were included. This of course could be stopped by switching the spin correlations off, i.e. SYSPIN=.FALSE.. In version 6.5, we have included the relevant matrix elements for R-parity violating decays and hard processes and decays producing gravitinos. At the same time we have made changes so that at both the initialisation and event generation stages many of the terminal warnings which were caused by the code not having the correct matrix elements are now information-only warnings. If you still get terminal error messages from any of the spin correlation routines please let us know.

⁵Default values for input variables are shown in square brackets.

The effect of polarization for incoming leptonic beams in MSSM and \mathcal{R}_p SUSY processes has also been included. These effects are included both in the production of SUSY particles and via the spin correlation algorithm in their decays.

3.7 Hadronization

For a general hard process in hadron-hadron collisions, we have to consider: (a) the representation of the incoming partons as constituents of the incident hadrons; (b) the conversion of the emitted partons into outgoing hadrons; (c) the ‘underlying soft event’ associated with the presence of spectator partons.

The first of these is dealt with through the use of non-perturbative parton distribution functions, which are discussed below in section 4.1.1, and by the remnant hadronization model. The cluster model for hadron formation, remnant hadronization and the underlying event is as follows.

3.7.1 Cluster model

The preconfinement property mentioned in section 1 is used by HERWIG as the basis for a simple hadronization model which is local in colour and independent of the hard process and the energy [4, 7].

After the perturbative parton showering, all outgoing gluons are split non-perturbatively, into light quark-antiquark or diquark-antidiquark pairs (the default option is to disallow diquark splitting). At this point, each jet consists of a set of outgoing quarks and antiquarks (also possibly some diquarks and antidiquarks) and, in the case of spacelike jets, a single incoming valence quark or antiquark. The latter is replaced by an outgoing spectator carrying the opposite colour and the residual flavour and momentum of the corresponding beam hadron.

In the limit of a large number of colours, each final-state colour line can now be followed from a quark/anti-diquark to an antiquark/diquark with which it can form a colour-singlet cluster.⁶ By virtue of pre-confinement, these clusters have a distribution of mass and spatial size that peaks at low values, falls rapidly for large cluster masses and sizes, and is asymptotically independent of the hard subprocess type and scale.

The clusters thus formed are fragmented into hadrons. If a cluster is too light to decay into two hadrons, it is taken to represent the lightest single hadron of its flavour. Its mass is shifted to the appropriate value by an exchange of 4-momentum with a neighbouring cluster in the jet. Similarly, any diquark-antidiquark clusters with masses below threshold for decay into a baryon-antibaryon pair are shifted to the threshold via a transfer of 4-momentum to a neighbouring cluster.

⁶The situation when baryon number is violated is more complicated and is discussed in [44] for the Standard Model and in [42] for R-parity violating SUSY models.

Those clusters massive enough to decay into two hadrons, but below a fission threshold to be specified below, decay isotropically ⁷ into pairs of hadrons selected in the following way. A flavour f is chosen at random from among u , d , s , the six corresponding diquark flavour combinations, and c . For a cluster of flavour $f_1\bar{f}_2$, this specifies the flavours $f_1\bar{f}$ and $f\bar{f}_2$ of the decay products, which are then selected at random from tables of hadrons of those flavours. See section 7 for details of the hadrons included. The selected choice of decay products is accepted in proportion to the density of states (phase space times spin degeneracy) for that channel. Otherwise, f is rejected and the procedure is repeated.

The above method of selection for cluster decays is simple and fast but does not automatically satisfy constraints such as strong isospin symmetry. The decay rate into hadrons of a certain flavour depends on the average phase space for channels involving that flavour. Thus, for example, the existence of the η or η' , with the same quark content as the π^0 , leads to a slight reduction of direct π^0 production relative to π^+ and π^- . Quantitatively, the effect is too small to be observed even with the high statistics of the LEP1 data. However, the method can give rise to strange effects if the particle data tables are extended, and modifications to avoid this have been proposed [45].

In the decays of clusters to η or η' , the parameter `ETAMIX` gives the η_8/η_0 mixing angle in degrees (default = -20). Rates are not very sensitive to its exact value, as the η'/η suppression is dominated by mass effects in the cluster model. See section 7 for more details.

A fraction of clusters have masses too high for isotropic two-body decay to be a reasonable ansatz, even though the cluster mass spectrum falls rapidly (faster than any power) at high masses. These are fragmented using an iterative fission model until the masses of the fission products fall below the fission threshold. In the fission model the produced flavour f is limited to u , d or s and the product clusters $f_1\bar{f}$ and $f\bar{f}_2$ move in the directions of the original constituents f_1 and \bar{f}_2 in their c.m. frame. Thus the fission mechanism is not unlike string fragmentation [46].

In `HERWIG` there are three main fission parameters, `CLMAX`, `CLPOW` and `PSPLT`. The maximum cluster mass parameter `CLMAX` and `CLPOW` specify the fission threshold M_f according to the formula

$$M_f^{\text{CLPOW}} = \text{CLMAX}^{\text{CLPOW}} + (m_1 + m_2)^{\text{CLPOW}},$$

where m_1 and m_2 are the quark mass parameters `RMASS(i)` for flavours f_1 and f_2 (see section 3.2). The parameter `PSPLT` specifies the mass spectrum of the produced clusters, which is taken to be M^{PSPLT} within the allowed phase space. Provided the parameter `CLMAX` is not chosen too small (the default value is 3.35 GeV), the gross features of events are insensitive to the details of the fission model, since only a small

⁷Except for those containing a ‘perturbative’ quark when `CLDIR` = 1 — see below.

fraction of clusters undergo fission. However, the production rates of high- p_t or heavy particles (especially baryons) are affected, because they are sensitive to the tail of the cluster mass distribution. The default value of the power `CLPOW` is 2. Smaller values will increase the yield of heavier clusters (and hence of baryons) for heavy quarks, without affecting light quarks much. For example, the default value gives no b -baryons (for the default value of `CLMAX`) whereas `CLPOW` = 1.0 makes the ratio of b -baryons to b -hadrons about 1/4.

There is also a switch `CLDIR` for cluster decays. If `CLDIR` = 1 (the default) then a cluster that contains a ‘perturbative’ quark, i.e. one coming from the perturbative stage of the event (the hard process or perturbative gluon splitting) ‘remembers’ its direction. Thus when the cluster decays, the hadron carrying its flavour continues in the same direction (in the cluster c.m. frame) as the quark. This considerably hardens the spectrum of heavy hadrons, particularly of c - and b -flavoured hadrons. It also introduces a tendency for baryon-antibaryon pairs preferentially to align themselves with the event axis (the ‘TPC/2 γ string effect’ [47]). `CLDIR` = 0 turns off this option, treating clusters containing quarks of perturbative and non-perturbative origin equivalently. In the `CLDIR` = 1 option, the parameter `CLSMR` (default = 0.0) allows for a gaussian smearing of the direction of the perturbative quark’s momentum. The smearing is actually exponential in $1 - \cos \theta$ with mean `CLSMR`. Thus increasing `CLSMR` decorrelates the cluster decay from the initial quark direction.

The process of b -quark hadronization requires special treatment and the results obtained using `HERWIG` are still not fully satisfactory. Generally speaking, it is difficult to obtain a sufficiently hard B-hadron spectrum and the observed b -meson/ b -baryon ratio. These depend not only on the perturbative subprocess and parton shower but also on non-perturbative issues such as the fraction of b -flavoured clusters that become a single B meson, the fractions that decay into a B meson and another meson, or into a b -baryon and an antibaryon, and the fraction that are split into more clusters. Thus the properties of b -jets depend on the parameters `RMASS(5)`, `CLMAX`, `CLPOW` and `PSPLT` in a rather complicated way. In practice these parameters are tuned to global final-state properties and one needs extra parameters to describe b -jets.

A parameter `B1LIM` has therefore been introduced to allow clusters somewhat above the $B\pi$ threshold mass M_{th} to form a single B meson if

$$M < M_{\text{lim}} = (1 + \text{B1LIM})M_{\text{th}} .$$

The probability of such single-meson clustering is assumed to decrease linearly for $M_{\text{th}} < M < M_{\text{lim}}$. This has the effect of hardening the B spectrum if `B1LIM` is increased from the default value of zero. In addition, in version 6, the parameters `PSPLT`, `CLDIR` and `CLSMR` have been converted into two-dimensional arrays, with the first element controlling clusters that do not contain a b -quark and the second those that do. Thus tuning of b -fragmentation can now be performed separately from other

flavours, by setting `CLDIR(2) = 1` and varying `PSPLT(2)` and `CLSMR(2)`. By reducing the value of `PSPLT(2)`, further hardening of the B-hadron spectrum can be achieved.

3.7.2 Underlying soft event

In hadron-hadron and lepton-hadron collisions there are ‘beam clusters’ containing the spectators from the incoming hadrons. In the formation of beam clusters, the colour connection between the spectators and the initial-state parton showers is cut by the forced emission of a soft quark-antiquark pair. The underlying soft event in a hard hadron-hadron collision is then assumed to be a soft collision between these two beam clusters. In a lepton-hadron collision the corresponding ‘soft hadronic remnant’ is represented by a soft collision between the beam cluster and the adjacent cluster, i.e. the one produced by the forced emission mentioned above.

The model used for the underlying event is based on the minimum-bias $p\bar{p}$ event generator of the UA5 Collaboration [48], modified to make use of our cluster fragmentation algorithm. This model is explained in the following subsection.

Adding 10000 to the `HERWIG` process code `IPROC` suppresses the underlying event, in which case the beam clusters are simply fragmented like other clusters, without any soft collision. The parameter `PRSOFT` enables one to produce an underlying event in only a fraction `PRSOFT` of events (default = 1.0). Adding 10000 to `IPROC` is thus equivalent to setting `PRSOFT = 0`.

A parameter `BTCLM` is available to users to adjust the mass parameter equivalent to `PMBM1` (see below) in remnant cluster formation. Its default value, 1.0, is identical to previous versions. There is also an option for the special treatment of the splitting of clusters containing hadron (or photon) remnants. `IOPREM = 0` gives the fragments a gaussian mass spectrum typical of soft processes. When `IOPREM = 1` (default), the child containing the remnant is treated as before but the other cluster, containing a perturbative parton, is treated as a normal cluster, with mass spectrum M^{PSPLT} .

Two special remnant ‘particles’ have been defined: ‘`REMG`’ with `IDHW = 71`, `IDHEP = 98` and ‘`REMN`’ with `IDHW = 72`, `IDHEP = 99`. These are remnant photons and nucleons respectively. They are identical to photons and nucleons, except that gluons are labelled as valence partons and, for the nucleon, valence quark distributions are set to zero. They are used by an external package for simulating multi-parton interactions, called `JIMMY` [49]. See section 9.7 for further details.

3.7.3 Minimum bias processes

The minimum-bias event generator of the UA5 Collaboration [48] starts from a parametrization of the $p\bar{p}$ inelastic charged multiplicity distribution as a negative binomial distribution. In `HERWIG` version 6, the relevant parameters are made available to the user for modification, the default values being the UA5 ones as used in previous versions. These parameters are given in table 5.

| Name | Description | Default |
|-------|-------------------------------------|---------|
| PMBN1 | a in $\bar{n} = as^b + c$ | 9.110 |
| PMBN2 | b in $\bar{n} = as^b + c$ | 0.115 |
| PMBN3 | c in $\bar{n} = as^b + c$ | -9.500 |
| PMBK1 | a in $1/k = a \ln s + b$ | 0.029 |
| PMBK2 | b in $1/k = a \ln s + b$ | -0.104 |
| PMBM1 | a in $(M - m_1 - m_2 - a)e^{-bM}$ | 0.4 |
| PMBM2 | b in $(M - m_1 - m_2 - a)e^{-bM}$ | 2.0 |
| PMBP1 | p_t slope for d, u | 5.2 |
| PMBP2 | p_t slope for s, c | 3.0 |
| PMBP3 | p_t slope for qq | 5.2 |

Table 5: Soft/min.bias parameters.

The first three parameters control the mean charged multiplicity \bar{n} at c.m. energy \sqrt{s} as indicated. The next two specify the parameter k in the negative binomial charged multiplicity distribution,

$$P(n) = \frac{\Gamma(n+k)}{n! \Gamma(k)} \frac{(\bar{n}/k)^n}{(1 + \bar{n}/k)^{n+k}}.$$

The parameters PMBM1 and PMBM2 describe the distribution of cluster masses M in the soft collision. These soft clusters are generated using a flat rapidity distribution with gaussian shoulders. The transverse momentum distribution of soft clusters has the form

$$P(p_t) \propto p_t \exp\left(-b\sqrt{p_t^2 + M^2}\right),$$

where the slope parameter b depends as indicated on the flavour of the quark or diquark pair created when the cluster was produced. As an option, for underlying events the value of \sqrt{s} used to choose the multiplicity n may be increased by a factor **ENSOF** to allow for an enhanced underlying activity in hard events. The actual charged multiplicity is taken to be n plus the sum of the moduli of the charges of the colliding hadrons or clusters.

There is now also an interface to the multiple-interaction model **JIMMY** [49]. For this purpose, several routines have been added or modified. New are **HWHREM** for identifying and cleaning up the beam remnants and **HWSCT** to administer the extra scatters. Minor modifications to **HWBGEN** and **HWSBRN** suppress energy conservation

errors when `ISLENT = -1`; `HWSSPC` has an improved approximation for remnant mass at high energies; and `HWUPCM` improves safety against negative square roots.

3.8 Spacetime structure

The space-time structure of events is available for all types of subprocess. The production vertex of each parton, cluster, unstable resonance and final-state particle is supplied in the `VHEP` array of `/HEPEVT/`. Set `PRVTX = .TRUE.` to include this information when printing the event record (120 column format). The units are: x, y, z in mm and t in mm/ c . In the case of partons and clusters the production points are always given in a local coordinate system with its origin at the relevant hard subprocess. This helps to separate the fermi-scale partonic showers from millimetre-scale distances possible in particle decays, for example the partonic decays of heavy (c, b) hadrons. The vertices of hadrons produced in cluster decays are always corrected back into the laboratory coordinate system.

It is possible to vary the principal interaction point, assigned to the c.m. frame entry in `/HEPEVT/` (with `ISTHEP = 103`), by setting `PIPSMR = .TRUE.` The smearing is generated by the routine `HWRPIP` according to a triple gaussian given by parameters `VIPWID(I)` ($I = 1,2,3$ for x, y, z widths): the default values correspond to LEP1.

It is also possible to veto particle decays that would occur outside a specified volume by setting `MAXDKL = .TRUE.` Each putative decay is tested in `HWDXLM` and if the particle would have decayed outside the chosen volume it is frozen and labelled as final state. Using `IOPDKL = 1, 2` selects a cylindrical or spherical allowed region (centred about the origin): then parameters `DXRCYL`, `DXZMAX` or `DXRSPH` specify the dimensions of the region.

3.8.1 Particle decays

Lepton and hadron lifetimes (in seconds) are supplied in the array `RLTIM`. In the case of MSSM (s)particles, including Higgs states, `RLTIM` values are entered through the input files (see discussion in section 3.5.2). The lifetimes of heavy quarks (top and any hypothetical extra generations) and weak bosons (including the SM Higgs) are derived from their calculated or specified widths in `HWUDKS`, whilst light quarks and gluons are given an effective minimum width that acts as a lifetime cutoff — see below. All particles whose lifetimes are larger than `PLTCUT` are set stable.

The proper (i.e. rest-frame) time t^* at which an unstable lepton or hadron decays is generated according to the exponential decay law with mean lifetime $\langle t^* \rangle = \tau \equiv \text{RLTIM}$:

$$\text{Prob}(\text{proper time} > t^*) = \exp(-t^*/\tau).$$

The laboratory-frame decay time t and distance travelled d are obtained by applying a boost: $t = \gamma t^*$, $d = \beta \gamma t^*$ where $\beta = v/c$ and $\gamma = 1/\sqrt{1 - \beta^2}$. The production vertices of the daughter particles are then calculated by adding the distance travelled

by the mother particle as given above to its production vertex. The mean lifetime τ of a particle is set, taking into account its width and virtuality, by:

$$\tau(q^2) = \frac{\hbar\sqrt{q^2}}{\sqrt{(q^2 - M^2)^2 + (\Gamma q^2/M)^2}}.$$

This formula is used for all particles: light partons; heavy quarks and weak bosons, which have appreciable widths; resonances; and unstable leptons. It interpolates between $\tau = \hbar/\Gamma$ for a particle that is on mass-shell and $\tau = \hbar\sqrt{q^2}/(q^2 - M^2)$ for one that is far off mass-shell.

3.8.2 Parton showers

The above prescription, based on an exponential proper lifetime distribution, is also used to describe parton showers. For light quarks and gluons, whose natural widths are small, this could lead to unreasonably large distances being generated in the final, low virtuality steps of showering. To avoid this they are given a width $\Gamma = \text{VMIN2}/M$; the parameter `VMIN2` (default value 0.1 GeV^2) acts effectively as a lower limit on a parton's virtuality. This is particularly important for the forced splitting of gluons (see section 3.7.1), which uses $\tau = \hbar \text{RMASS}(13)/\text{VMIN2}$.

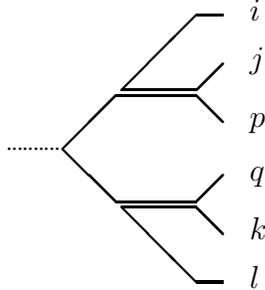
3.8.3 Hadronization

In the case of a cluster its initial production vertex is taken as the midpoint of a line perpendicular to the cluster's direction of travel and with its two ends on the trajectories of the constituent quark-antiquark pair. If such a cluster undergoes a forced splitting to two clusters the string picture is adopted. The vertex of the light quark pair is positioned so that the masses of the two daughter clusters would be the same as those for two equivalent string fragments. The production vertices of the daughter clusters are given by the first crossing of their constituent $q\bar{q}$ pairs. The production positions of primary hadrons from cluster decays are smeared, relative to the cluster position, according to a gaussian distribution of width $1/(\text{cluster mass})$.

3.8.4 Colour rearrangement

HERWIG version 6 contains a colour rearrangement model based on the space-time structure of an event at the end of the parton shower. This is illustrated in the simple example shown below where showering results in a colour-neutral $qg\bar{q}$ final state. In the conventional HERWIG hadronization model (corresponding to the default value of the reconnection parameter, `CLRECO = .FALSE.`), after a non-perturbative splitting of the final-state gluons, colour singlet clusters are formed from neighbouring $q\bar{q}$ pairs: $(ij)(pq)(kl)$. However when `CLRECO = .TRUE.` the program first creates colour singlet clusters as normal but then checks all (non-neighbouring) pairs of clusters to test if a colour rearrangement lowers the sum of the clusters' spatial sizes added

in quadrature. A cluster's size d_{ij} is defined to be the Lorentz-invariant space-time distance between the production points of its constituent quark q_i and antiquark \bar{q}_j . If an allowed alternative is found, that is, $(ij)(kl) \rightarrow (il)(jk)$ such that $|d_{ij}|^2 + |d_{kl}|^2 > |d_{il}|^2 + |d_{jk}|^2$, then it is accepted with a probability given by the parameter `PRECO` (default value 1/9).



Note that not all colour rearrangements are allowed, for instance in the example shown $(ij)(pq) \rightarrow (iq)(jp)$ is forbidden since the cluster (jp) is a colour octet — it contains both products from a non-perturbative gluon splitting.

Multiple colour rearrangements are considered by the program, as are those between clusters in jets arising from a single, colour neutral source, for example Z^0 decay (as shown above), or due to more than one source, for example $e^+e^- \rightarrow W^+W^- \rightarrow 4$ jets. In the latter case a new parameter, `EXAG`, is available to exaggerate the lifetime of the W^\pm or any other weak boson, so that any dependence of rearrangement effects on source separation can be investigated.

The `CLRECO` option can be used for all the processes available in `HERWIG`. Note, however, that before using the program with `CLRECO = .TRUE.` for detailed physics analyses the default parameters should be retuned to LEP data with this option switched on.

3.8.5 B- \bar{B} mixing

When `MIXING = .TRUE.`, particle-antiparticle mixing for $B_{d,s}^0$ mesons is implemented. The probability that a meson is mixed when it decays is given in terms of its lab-frame decay time t by:

$$P_{\text{mix}}(t) = \frac{1}{2} - \frac{\cos(Xtm/c\tau E)}{2 \cosh(Ytm/c\tau E)},$$

where $X = \Delta M/\Gamma$, $Y = \Delta\Gamma/2\Gamma$ and m , τ , E are the B^0 mass, lifetime and energy. The ratios X and Y are stored in `XMIX(I)` and `YMIX(I)`, $I = 1, 2$ for $q = s, d$. Whenever a neutral B meson occurs in an event, a copy of the original entry is always added to the event record, with `ISTHEP = 200`, which gives the particle's flavour at the production (or cluster decay) time. This is in addition to the usual decaying particle entry with `ISTHEP = 199`.

| Name | Description | Default |
|--------|------------------------------|---------|
| PART1 | Type of particle in beam 1 | 'PBAR ' |
| PART2 | Type of particle in beam 2 | 'P ' |
| PBEAM1 | Momentum of beam 1 | 900.0 |
| PBEAM2 | Momentum of beam 2 | 900.0 |
| IPROC | Type of process to generate | 1500 |
| MAXEV | Number of events to generate | 100 |

Table 6: Main program variables.

4. Processes

4.1 Beams

As indicated in table 6, a number of variables must be set in the main program HWIGPR to specify what is to be simulated. The beam particle types PART1, PART2 can take any of the values NAME listed in table 7.

In the case of point-like photon/QCD processes, IPROC = 5000–5999, the first particle must be the photon or a lepton. In addition, beams 'K+' and 'K-' are supported for minimum bias non-diffractive soft hadronic events (IPROC = 8000) only. In the case that the beam momenta PBEAM1 and PBEAM2 are not equal, the default procedure (USECMF = .TRUE.) is to generate events in the beam-beam centre-of-mass frame and boost them back to the laboratory frame afterwards.

| | NAME | | NAME |
|------------|-----------|------------------|-------------|
| e^+ | 'E+ ' | e^- | 'E- ' |
| μ^+ | 'MU+ ' | μ^- | 'MU- ' |
| ν_e | 'NU_E ' | $\bar{\nu}_e$ | 'NU_EBAR ' |
| ν_μ | 'NU_MU ' | $\bar{\nu}_\mu$ | 'NU_MUBAR ' |
| ν_τ | 'NU_TAU ' | $\bar{\nu}_\tau$ | 'NU_TAUBR ' |
| p | 'P ' | \bar{p} | 'PBAR ' |
| n | 'N ' | \bar{n} | 'NBAR ' |
| π^+ | 'PI+ ' | π^- | 'PI- ' |
| γ | 'GAMMA ' | | |

Table 7: Beam particles.

In hadronic processes with lepton beams (e.g. photoproduction in ep), the lepton \rightarrow lepton + photon vertex uses the full transverse-momentum dependent splitting function, with exact light-cone kinematics, i.e the Equivalent Photon Approximation (EPA). This means that the photon-hadron collision has a transverse momentum in the lepton-hadron frame and must be boosted to a frame where it has no transverse momentum. Thus the c.m.f. boost described above is always used in these processes, regardless of the value of USECMF. The correct lower energy cutoff appropriate to the hadronic process is applied to the photon. The Q^2 of the photon is generated within the kinematically allowed limits, or the user-defined limits Q2WWMN and Q2WWMX (defaults 0 and 4) whichever is more restrictive.⁸ Similarly for the photon's light-cone momentum fraction, with user-defined limits YWWMIN and YWWMAX (default 0 and 1).

⁸The WW in parameter names is a relic from earlier versions that used the less accurate Weizsacker-Williams approximation.

Together with the Bjorken y -variable limits Y_{MIN} and Y_{MAX} , this allows different ranges for the tagged and untagged photons in two-photon DIS.

4.1.1 Parton distributions

The parton momentum fraction distributions of the beam particles are used in the generation of initial-state parton showers and also in the non-perturbative process of linking the shower with the beam hadron and its remnant. Since the parton showering is done in leading-logarithmic order, there is no strong motivation to use next-to-leading order parton distributions, although this has become customary since the most up-to-date distributions are deduced from next-to-leading order fits to (inclusive) data. Thus the most common option is to use the interface to the **PDFLIB** parton distribution library [50].

The **HERWIG** interface is compatible with **PDFLIB** version 4. **AUTPDF** should be set to the author group as listed in the **PDFLIB** manual, e.g. 'MRS', and **MODPDF** to the set number in the new convention. It is permissible to choose the **PDFLIB** set independently for each of the two beams. For example, to use MRS D- for the proton and Gordon-Storow set 1 for the photon in γ -hadron or lepton-hadron collisions, one sets:

```
AUTPDF(2)='MRS'
MODPDF(2)=28
AUTPDF(1)='GS'
MODPDF(1)=2
```

If the **PDFLIB** interface is not used, the parton distributions are chosen from the **HERWIG** internal sets according to the value of the parameter **NSTRU**. The default parton distributions in **HERWIG** versions prior to 6.3 were very old and did not include fits to any of the HERA data. Therefore several new PDFs have been included in versions 6.3 and higher. These are shown in table 8.

It should be noted that we have only added leading-order fits because the evolution algorithms in **HERWIG**, in particular the backward-evolution algorithm for initial-state parton showering, are only leading-order and therefore inconsistencies could occur with next-to-leading-order distributions.

The new default structure function set **NSTRU=8** is the average of two of the published fits [51], because this has been found [52] to be closer to the central value of more recent next-to-leading-order fits. The other fits can then be used to assess the effects of varying the high- x gluon.

These new **HERWIG** parton distributions are only available for nucleons. For pion beams, either the old **NSTRU=1,2** pion sets or **PDFLIB** should be used.

For photons, the default is to use the Drees-Grassie parton distributions [53]. The heavy quark content of the photon uses the corrections to the Drees-Grassie distribution functions for light quarks, calculated by Drees and Kim [54]. There is also an interface to the Schuler-Sjöstrand [55] parton distribution functions for the

| NSTRU | Description |
|-------|--|
| 6 | Central α_S and gluon leading-order fit of [51] |
| 7 | Higher gluon leading-order fit of [51] |
| 8 | Average of central and higher gluon leading-order fits of [51] |

Table 8: New internal MRST parton distributions.

photon, version 2. These appear as PDFLIB sets with author group ‘SaSph’, but are actually implemented via a call to their SASGAM code. The value in MODPDF specifies the set (1-4 for 1D [recommended set], 1M, 2D, 2M), whether the Bethe-Heitler process is used for heavy flavours (add 10), whether the P^2 -dependence is included (add 20), and which of their P^2 models is used (add 100 times their IP2 parameter).

An option to damp the parton distributions of off mass-shell photons relative to on-shell photons, according to the scheme of Drees and Godbole [56] has been introduced. The adjustable parameter PHOMAS defines the crossover from the non-suppressed to suppressed regimes. Recommended values lie in the range from QC DLAM to 1 GeV. The default value PHOMAS = 0 corresponds to no suppression, as in previous versions.

4.2 Summary of subprocesses

We give in table 9 a list of the currently available hard subprocesses IPROC. More detailed descriptions are given in sections 4.3–4.12, and then in section 4.13 there are instructions to users on how to add a new process.

| IPROC | Process |
|----------|---|
| 100 | $\ell^+\ell^- \rightarrow q\bar{q}(g)$ (all q flavours) |
| 100+IQ | $\ell^+\ell^- \rightarrow q\bar{q}(g)$ (IQ = 1, 2, 3, 4, 5, 6 for $q = d, u, s, c, b, t$) |
| 107 | $\ell^+\ell^- \rightarrow gg(g)$ (fictitious process) |
| 110 | $\ell^+\ell^- \rightarrow q\bar{q}g$ (all flavours) |
| 110+IQ | $\ell^+\ell^- \rightarrow q\bar{q}g$ (IQ as above) |
| 120 | $\ell^+\ell^- \rightarrow q\bar{q}$ (all flavours, no hard gluon correction) |
| 120+IQ | $\ell^+\ell^- \rightarrow q\bar{q}$ (IQ as above, no hard gluon correction) |
| 127 | $\ell^+\ell^- \rightarrow gg$ (fictitious process, no hard gluon correction) |
| 150+IL | $\ell^+\ell^- \rightarrow \ell'\bar{\ell}'$ (IL = 1, 2, 3 for $\ell' = e, \mu, \tau$, N.B. $\ell \neq \ell'$) |
| 200 | $\ell^+\ell^- \rightarrow W^+W^-$ (see sect. 4.3.2 on control of W/Z decays) |
| 250 | $\ell^+\ell^- \rightarrow Z^0Z^0$ (see sect. 4.3.2 on control of W/Z decays) |
| 300 | $\ell^+\ell^- \rightarrow Z^0H_{\text{SM}}^0 \rightarrow Z^0q\bar{q}$ (all flavours) |
| 300+IQ | $\ell^+\ell^- \rightarrow Z^0H_{\text{SM}}^0 \rightarrow Z^0q\bar{q}$ (IQ as above) |
| 306+IL | $\ell^+\ell^- \rightarrow Z^0H_{\text{SM}}^0 \rightarrow Z^0\ell\bar{\ell}$ (IL as above) |
| 310, 311 | $\ell^+\ell^- \rightarrow Z^0H_{\text{SM}}^0 \rightarrow Z^0W^+W^-, Z^0Z^0Z^0$ |

Table 9: Process codes. (Continues)

| IPROC | Process |
|--------------|--|
| 312 | $l^+l^- \rightarrow Z^0 H_{\text{SM}}^0 \rightarrow Z^0 \gamma \gamma$ |
| 399 | $l^+l^- \rightarrow Z^0 H_{\text{SM}}^0 \rightarrow Z^0 \text{ anything}$ |
| 400+ID | $l^+l^- \rightarrow \nu \bar{\nu} H_{\text{SM}}^0 + l^+l^- H_{\text{SM}}^0$ (ID as in IPROC = 300 + ID) |
| 500+ID | $l^+l^- \rightarrow l^+l^- \gamma \gamma \rightarrow l^+l^- q \bar{q} / \ell \bar{\ell} / W^+ W^-$ (ID=0-10 as in IPROC = 300 + ID) |
| 550+ID | $l^+l^- \rightarrow l \nu_e \gamma W \rightarrow l \nu_e q \bar{q}' / \ell \bar{\ell}'$ (ID=0-9 as in IPROC = 300 + ID) |
| 600 | $l^+l^- \rightarrow q \bar{q} g g, q \bar{q} q' \bar{q}'$ (all q flavours) |
| 600+IQ | $l^+l^- \rightarrow q \bar{q} g g, q \bar{q} q' \bar{q}'$ (IQ as above) After generation, IHPR0 is subprocess (see sect. 4.3.5) |
| 700-99 | Minimal Supersymmetric Standard Model (MSSM) processes |
| 700 | $l^+l^- \rightarrow$ 2-particle processes (sum of 710, 730, 740 and 760) |
| 710 | $l^+l^- \rightarrow$ neutralino pairs (all neutralinos) |
| 706+4IN1+IN2 | $l^+l^- \rightarrow \tilde{\chi}_{\text{IN}1}^0 \tilde{\chi}_{\text{IN}2}^0$ (IN1, 2=neutralino mass eigenstate) |
| 730 | $l^+l^- \rightarrow$ chargino pairs (all charginos) |
| 728+2IC1+IC2 | $l^+l^- \rightarrow \tilde{\chi}_{\text{IC}1}^+ \tilde{\chi}_{\text{IC}2}^-$ (IC1, 2=chargino mass eigenstate) |
| 740 | $l^+l^- \rightarrow$ slepton pairs (all flavours) |
| 736+5IL | $l^+l^- \rightarrow \tilde{\ell}_{L,R} \tilde{\ell}_{L,R}^*$ (IL = 1, 2, 3 for $\tilde{\ell} = \tilde{e}, \tilde{\mu}, \tilde{\tau}$) |
| 737+5IL | $l^+l^- \rightarrow \tilde{\ell}_L \tilde{\ell}_L^*$ (IL as above) |
| 738+5IL | $l^+l^- \rightarrow \tilde{\ell}_L \tilde{\ell}_R^*$ (IL as above) |
| 739+5IL | $l^+l^- \rightarrow \tilde{\ell}_R \tilde{\ell}_R^*$ (IL as above) |
| 740+5IL | $l^+l^- \rightarrow \tilde{\nu}_L \tilde{\nu}_L^*$ (IL = 1, 2, 3 for $\tilde{\nu}_e, \tilde{\nu}_\mu, \tilde{\nu}_\tau$) |
| 760 | $l^+l^- \rightarrow$ squark pairs (all flavours) |
| 757+4IQ | $l^+l^- \rightarrow \tilde{q}_{L,R} \tilde{q}_{L,R}^*$ (IQ = 1, 2, 3, 4, 5, 6 for $\tilde{q} = \tilde{d}, \tilde{u}, \tilde{s}, \tilde{c}, \tilde{b}, \tilde{t}$) |
| 758+4IQ | $l^+l^- \rightarrow \tilde{q}_L \tilde{q}_L^*$ (IQ as above) |
| 759+4IQ | $l^+l^- \rightarrow \tilde{q}_L \tilde{q}_R^*$ (IQ as above) |
| 760+4IQ | $l^+l^- \rightarrow \tilde{q}_R \tilde{q}_R^*$ (IQ as above) |
| 800-99 | R-parity violating supersymmetric processes |
| 800 | Single sparticle production, sum of 810-840 |
| 810 | $l^+l^- \rightarrow \tilde{\chi}^0 \nu_i$, (all neutralinos) |
| 810+IN | $l^+l^- \rightarrow \tilde{\chi}_{\text{IN}}^0 \nu_i$, (IN=neutralino mass state) |
| 820 | $l^+l^- \rightarrow \tilde{\chi}^- e_i^+$ (all charginos) |
| 820+IC | $l^+l^- \rightarrow \tilde{\chi}_{\text{IC}}^- e_i^+$, (IC=chargino mass state) |
| 830 | $l^+l^- \rightarrow \tilde{\nu}_i Z^0$ and $l^+l^- \rightarrow \tilde{\ell}_i^+ W^-$ |
| 840 | $l^+l^- \rightarrow \tilde{\nu}_i h^0 / H^0 / A^0$ and $l^+l^- \rightarrow \tilde{\ell}_i^+ H^-$ |
| 850 | $l^+l^- \rightarrow \tilde{\nu}_i \gamma$ |
| 860 | Sum of 870 and 880 |
| 870 | $l^+l^- \rightarrow l^+l^-$, via LLE only |
| 867+3IL1+IL2 | $l^+l^- \rightarrow \ell_{\text{IL}1}^+ \ell_{\text{IL}2}^-$ (IL1, 2=1, 2, 3 for e, μ, τ) |

Table 9: Process codes. (Continues)

| IPROC | Process |
|--------------|---|
| 880 | $\ell^+\ell^- \rightarrow \bar{d}d$, via LLE and LQD |
| 877+3IQ1+IQ2 | $\ell^+\ell^- \rightarrow d_{\text{IL1}}\bar{d}_{\text{IL2}}$ (IQ1, 2=1,2,3 for d, s, b) |
| 910 | $\ell^+\ell^- \rightarrow \nu_e\bar{\nu}_e h^0 + e^+e^- h^0$ |
| 920 | $\ell^+\ell^- \rightarrow \nu_e\bar{\nu}_e H^0 + e^+e^- H^0$ |
| 960 | $\ell^+\ell^- \rightarrow Z^0 h^0$ |
| 970 | $\ell^+\ell^- \rightarrow Z^0 H^0$ |
| 955 | $\ell^+\ell^- \rightarrow H^+H^-$ |
| 965 | $\ell^+\ell^- \rightarrow A^0 h^0$ |
| 965 | $\ell^+\ell^- \rightarrow A^0 H^0$ |
| 1000+ID | $\ell^+\ell^- \rightarrow t\bar{t} H_{\text{SM}}^0$ (ID as in IPROC=300+ID) |
| 1110+IQ | $\ell^+\ell^- \rightarrow q\bar{q} h^0$ (IQ as in IPROC=100+IQ) |
| 1116+IL | $\ell^+\ell^- \rightarrow \ell^+\ell^- h^0$ (IL=1,2,3 for e, μ, τ) |
| 1120+IQ | $\ell^+\ell^- \rightarrow q\bar{q} H^0$ (IQ as in IPROC=100+IQ) |
| 1126+IL | $\ell^+\ell^- \rightarrow \ell^+\ell^- H^0$ (IL=1,2,3 for e, μ, τ) |
| 1130+IQ | $\ell^+\ell^- \rightarrow q\bar{q} A^0$ (IQ as in IPROC=100+IQ) |
| 1136+IL | $\ell^+\ell^- \rightarrow \ell^+\ell^- A^0$ (IL=1,2,3 for e, μ, τ) |
| 1140 | $\ell^+\ell^- \rightarrow d\bar{u} H^+ + \text{ch. conj.}$ |
| 1141 | $\ell^+\ell^- \rightarrow s\bar{c} H^+ + \text{ch. conj.}$ |
| 1142 | $\ell^+\ell^- \rightarrow b\bar{t} H^+ + \text{ch. conj.}$ |
| 1143 | $\ell^+\ell^- \rightarrow e\bar{\nu}_e H^+ + \text{ch. conj.}$ |
| 1144 | $\ell^+\ell^- \rightarrow \mu\bar{\nu}_\mu H^+ + \text{ch. conj.}$ |
| 1145 | $\ell^+\ell^- \rightarrow \tau\bar{\nu}_\tau H^+ + \text{ch. conj.}$ |
| 1200-99 | Reserved for other $\ell^+\ell^-$ processes |
| 1300 | $q\bar{q} \rightarrow Z^0/\gamma \rightarrow q'\bar{q}'$ (all flavours) |
| 1300+IQ | $q\bar{q} \rightarrow Z^0/\gamma \rightarrow q'\bar{q}'$ (IQ = 1, 2, 3, 4, 5, 6 for $q = d, u, s, c, b, t$) |
| 1350 | $q\bar{q} \rightarrow Z^0/\gamma \rightarrow \ell\bar{\ell}$ (all lepton species) |
| 1350+IL | $q\bar{q} \rightarrow Z^0/\gamma \rightarrow \ell\bar{\ell}$ (IL = 1 - 6 for $\ell = e, \nu_e, \mu, \nu_\mu, \text{etc.}$) |
| 1399 | $q\bar{q} \rightarrow Z^0/\gamma \rightarrow \text{anything}$ |
| 1400 | $q\bar{q} \rightarrow W^\pm \rightarrow q'\bar{q}''$ (all flavours) |
| 1400+IQ | $q\bar{q} \rightarrow W^\pm \rightarrow q'\bar{q}''$ (q' or q'' as above) |
| 1450 | $q\bar{q} \rightarrow W^\pm \rightarrow \ell\nu_\ell$ (all lepton species) |
| 1450+IL | $q\bar{q} \rightarrow W^\pm \rightarrow \ell\nu_\ell$ (IL = 1, 2, 3 for $\ell = e, \mu, \tau$) |
| 1499 | $q\bar{q} \rightarrow W^\pm \rightarrow \text{anything}$ |
| 1500 | QCD $2 \rightarrow 2$ hard parton scattering After generation, IHPR0 is subprocess (see sect. 4.6.2) |
| 1600+ID | $gg/q\bar{q} \rightarrow H_{\text{SM}}^0$ (ID as in IPROC = 300 + ID) |
| 1700+IQ | QCD heavy quark production (IQ as above) After generation, IHPR0 is subprocess (see sect. 4.6.2) |
| 1800 | QCD direct photon + jet production |

Table 9: Process codes. (Continues)

| IPROC | Process |
|-----------|--|
| | After generation, IHPR0 is subprocess (see sect. 4.6.5) |
| 1900+ID | $q\bar{q} \rightarrow q'\bar{q}'W^+W^-/Z^0Z^0 \rightarrow q'\bar{q}'H_{\text{SM}}^0$ (ID as in IPROC = 300 + ID) |
| 2000 | t production via W^\pm exchange (sum of 2001–2008) |
| 2001–4 | $\bar{u}\bar{b} \rightarrow \bar{d}\bar{t}, \quad \bar{d}\bar{b} \rightarrow \bar{u}\bar{t}, \quad \bar{d}\bar{b} \rightarrow \bar{u}\bar{t}, \quad ub \rightarrow dt$ |
| 2005–8 | $\bar{c}\bar{b} \rightarrow \bar{s}\bar{t}, \quad \bar{s}\bar{b} \rightarrow \bar{c}\bar{t}, \quad \bar{s}\bar{b} \rightarrow \bar{c}\bar{t}, \quad cb \rightarrow st$ |
| 2100 | W^\pm + jet production |
| 2110 | W^\pm + jet production (Compton only: $gq \rightarrow Wq$) |
| 2120 | W^\pm + jet production (annihilation only: $q\bar{q} \rightarrow Wg$) |
| 2150 | Z^0 + jet production |
| 2160 | Z^0 + jet production (Compton only: $gq \rightarrow Zq$) |
| 2170 | Z^0 + jet production (annihilation only: $q\bar{q} \rightarrow Zg$) |
| 2200 | QCD direct photon pair production After generation, IHPR0 is subprocess (see sect. 4.6.5) |
| 2300+ID | QCD SM Higgs + jet production (ID as in IPROC=300+ID) After generation, IHPR0 is subprocess (see sect. 4.6.10) |
| 2400 | Mueller-Tang colour singlet exchange |
| 2450 | Quark scattering via photon exchange |
| 2500+ID | $gg/q\bar{q} \rightarrow t\bar{t}H_{\text{SM}}^0$ (ID as in IPROC=300+ID) |
| 2600+ID | $q\bar{q}' \rightarrow W^\pm H_{\text{SM}}^0$ (ID as in IPROC=300+ID) |
| 2700+ID | $q\bar{q} \rightarrow Z^0 H_{\text{SM}}^0$ (ID as in IPROC=300+ID) |
| 2800 | W^+W^- production in hadron-hadron collisions |
| 2810 | Z^0Z^0 production in hadron-hadron collisions (including photon terms) |
| 2815 | Z^0Z^0 production in hadron-hadron collisions (Z^0 only) |
| 2820 | $W^\pm Z^0$ production in hadron-hadron collisions (including photon terms) |
| 2825 | $W^\pm Z^0$ production in hadron-hadron collisions (Z^0 only) |
| 2850 | hadron-hadron $\rightarrow W^+W^-X$ using MC@NLO |
| 2860 | hadron-hadron $\rightarrow Z^0Z^0X$ using MC@NLO |
| 2870 | hadron-hadron $\rightarrow W^+Z^0X$ using MC@NLO |
| 2880 | hadron-hadron $\rightarrow W^-Z^0X$ using MC@NLO |
| 2900+IQ | $gg + q\bar{q} \rightarrow Q\bar{Q}Z^0$ for massless Q and \bar{Q} (IQ=1...6 for $Q = d...t$) |
| 2910+IQ | $gg + q\bar{q} \rightarrow Q\bar{Q}Z^0$, for massive Q and \bar{Q} (IQ=1...6 for $Q = d...t$) |
| 3000-3999 | Minimal Supersymmetric Standard Model (MSSM) processes |
| 3000 | 2-parton \rightarrow 2-sparticle processes (sum of those below) |
| 3010 | 2-parton \rightarrow 2-sparton processes |
| 3020 | 2-parton \rightarrow 2-gaugino processes |
| 3030 | 2-parton \rightarrow 2-slepton processes |
| 3100+ISQ | $gg/q\bar{q} \rightarrow \tilde{q}\tilde{q}'^*H^\pm$ (ISQ=IPROC–3100 as from table 15) |
| 3200+ISQ | $gg/q\bar{q} \rightarrow \tilde{q}\tilde{q}'^*h, H, A$ (ISQ=IPROC–3200 as from table 16) |

Table 9: Process codes. (Continues)

| IPROC | Process |
|-----------|--|
| 3310,3315 | $q\bar{q}' \rightarrow W^\pm h^0, H^\pm h^0$ (all q, q' flavours – gauge bosons mediated only) |
| 3320,3325 | $q\bar{q}' \rightarrow W^\pm H^0, H^\pm H^0$ (") |
| 3335 | $q\bar{q}' \rightarrow H^\pm A^0$ (") |
| 3350 | $q\bar{q} \rightarrow W^\pm H^\mp$ (Higgstrahlung and Higgs mediated) |
| 3355 | $q\bar{q} \rightarrow H^\pm H^\mp$ (all q flavours — gauge boson mediated only) |
| 3360,3365 | $q\bar{q} \rightarrow Z^0 h^0, A^0 h^0$ (") |
| 3370,3375 | $q\bar{q} \rightarrow Z^0 H^0, A^0 H^0$ (") |
| 3410 | $bg \rightarrow b h^0 + \text{ch. conj.}$ |
| 3420 | $bg \rightarrow b H^0 + \text{ch. conj.}$ |
| 3430 | $bg \rightarrow b A^0 + \text{ch. conj.}$ |
| 3450 | $bg \rightarrow t H^- + \text{ch. conj.}$ |
| 3500 | $bq \rightarrow bq' H^\pm + \text{ch. conj.}$ |
| 3610 | $q\bar{q}/gg \rightarrow h^0$ (light scalar Higgs) |
| 3620 | $q\bar{q}/gg \rightarrow H^0$ (heavy scalar Higgs) |
| 3630 | $q\bar{q}/gg \rightarrow A^0$ (pseudoscalar Higgs) |
| 3710 | $q\bar{q} \rightarrow q'\bar{q}'W^+W^-/Z^0Z^0 \rightarrow q'\bar{q}'h^0$ |
| 3720 | $q\bar{q} \rightarrow q'\bar{q}'W^+W^-/Z^0Z^0 \rightarrow q'\bar{q}'H^0$ |
| 3810+IQ | $gg + q\bar{q} \rightarrow Q\bar{Q}h^0$ (all q flavours in s -channel, IQ as usual for Q flavour) |
| 3820+IQ | $gg + q\bar{q} \rightarrow Q\bar{Q}H^0$ (") |
| 3830+IQ | $gg + q\bar{q} \rightarrow Q\bar{Q}A^0$ (") |
| 3839 | $gg + q\bar{q} \rightarrow b\bar{t}H^+ + \text{ch. conjg.}$ (all q flavours in s -channel) |
| 3840+IQ | $gg \rightarrow Q\bar{Q}h^0$ (IQ as above) |
| 3850+IQ | $gg \rightarrow Q\bar{Q}H^0$ (") |
| 3860+IQ | $gg \rightarrow Q\bar{Q}A^0$ (") |
| 3869 | $gg \rightarrow b\bar{t}H^+ + \text{ch. conjg.}$ |
| 3870+IQ | $q\bar{q} \rightarrow Q\bar{Q}h^0$ (all q flavours in s -channel, IQ as above) |
| 3880+IQ | $q\bar{q} \rightarrow Q\bar{Q}H^0$ (") |
| 3890+IQ | $q\bar{q} \rightarrow Q\bar{Q}A^0$ (") |
| 3899 | $q\bar{q} \rightarrow b\bar{t}H^+ + \text{ch. conjg.}$ (all q flavours in s -channel) |
| 3900–99 | Reserved for other hadron-hadron MSSM processes |
| 4000–99 | R-parity violating supersymmetric processes via LQD |
| 4000 | single sparticle production, sum of 4010–4050 |
| 4010 | $\bar{u}_j d_k \rightarrow \tilde{\chi}^0 l_i^-, \bar{d}_j d_k \rightarrow \tilde{\chi}^0 \nu_i$ (all neutralinos) |
| 4010+IN | $\bar{u}_j d_k \rightarrow \tilde{\chi}_{\text{IN}}^0 l_i^-, \bar{d}_j d_k \rightarrow \tilde{\chi}_{\text{IN}}^0 \nu_i$ (IN=neutralino mass state) |
| 4020 | $\bar{u}_j d_k \rightarrow \tilde{\chi}^- \nu_i, \bar{d}_j d_k \rightarrow \tilde{\chi}^- e_i^+$ (all charginos) |
| 4020+IC | $\bar{u}_j d_k \rightarrow \tilde{\chi}_{\text{IC}}^- \nu_i, \bar{d}_j d_k \rightarrow \tilde{\chi}_{\text{IC}}^- e_i^+$ (IC=chargino mass state) |
| 4040 | $u_j \bar{d}_k \rightarrow \tilde{\tau}_i^+ Z^0, u_j \bar{d}_k \rightarrow \tilde{\nu}_i W^+$ and $d_j \bar{d}_k \rightarrow \tilde{\ell}_i^+ W^-$ |
| 4050 | $u_j \bar{d}_k \rightarrow \tilde{\ell}_i^+ h^0/H^0/A^0, u_j \bar{d}_k \rightarrow \tilde{\nu}_i H^+$ and $d_j \bar{d}_k \rightarrow \tilde{\ell}_i^+ H^-$ |

Table 9: Process codes. (Continues)

| IPROC | Process |
|----------|--|
| 4060 | Sum of 4070 and 4080 |
| 4070 | $\bar{u}_j d_k \rightarrow \bar{u}_l d_m$ and $\bar{d}_j d_k \rightarrow \bar{d}_l d_m$, via LQD only |
| 4080 | $\bar{u}_j d_k \rightarrow \nu_j l_k^-$ and $\bar{d}_j d_k \rightarrow l_j^+ l_k^-$, via LQD and LLE |
| 4100-99 | R-parity violating supersymmetric processes via UDD |
| 4100 | single sparticle production, sum of 4110–4150 |
| 4110 | $u_i d_j \rightarrow \tilde{\chi}^0 \bar{d}_k$, $d_j d_k \rightarrow \tilde{\chi}^0 \bar{u}_i$ (all neutralinos) |
| 4110 +IN | $u_i d_j \rightarrow \tilde{\chi}_{\text{IN}}^0 \bar{d}_k$, $d_j d_k \rightarrow \tilde{\chi}_{\text{IN}}^0 \bar{u}_i$ (IN as above) |
| 4120 | $u_i d_j \rightarrow \tilde{\chi}^+ \bar{u}_k$, $d_j d_k \rightarrow \tilde{\chi}^- \bar{d}_i$ (all charginos) |
| 4120 +IC | $u_i d_j \rightarrow \tilde{\chi}_{\text{IC}}^+ \bar{u}_k$, $d_j d_k \rightarrow \tilde{\chi}_{\text{IC}}^- \bar{d}_i$ (IC as above) |
| 4130 | $u_i d_j \rightarrow \tilde{g} \bar{d}_k$, $d_j d_k \rightarrow \tilde{g} \bar{u}_i$ |
| 4140 | $u_i d_j \rightarrow \tilde{b}_1^* Z^0$, $d_j d_k \rightarrow \tilde{t}_1^* Z^0$, $u_i d_j \rightarrow \tilde{t}_i^* W^+$ and $d_j d_k \rightarrow \tilde{b}_i^* W^-$ |
| 4150 | $u_i d_j \rightarrow \tilde{d}_{k1}^* h^0/H^0/A^0$, $d_j d_k \rightarrow \tilde{u}_{i1}^* h^0/H^0/A^0$, $u_i d_j \rightarrow \tilde{u}_{k\alpha}^* H^+$, $d_j d_k \rightarrow \tilde{d}_{i\alpha}^* H^-$ |
| 4160 | $u_i d_j \rightarrow u_l d_m$, $d_j d_k \rightarrow d_l d_m$ via UDD. |
| 4200-99 | Graviton resonance production |
| 4200 | Sum of 4210, 4250 and 4270 |
| 4210 | $gg/q\bar{q} \rightarrow G \rightarrow gg/q\bar{q}$ (all partons) |
| 4210+IQ | $gg/q\bar{q} \rightarrow G \rightarrow q\bar{q}$ (IQ as above) |
| 4220 | $gg/q\bar{q} \rightarrow G \rightarrow gg$ |
| 4250 | $gg/q\bar{q} \rightarrow G \rightarrow \ell\bar{\ell}$ (all leptons) |
| 4250+IL | $gg/q\bar{q} \rightarrow G \rightarrow \ell\bar{\ell}$ (IL = 1 – 6 for $\ell = e, \nu_e, \mu, \nu_\mu$, etc.) |
| 4260 | $gg/q\bar{q} \rightarrow G \rightarrow \gamma\gamma$ |
| 4270 | $gg/q\bar{q} \rightarrow G \rightarrow W^+W^-/Z^0Z^0/H_{\text{SM}}^0H_{\text{SM}}^0$ |
| 4271 | $gg/q\bar{q} \rightarrow G \rightarrow W^+W^-$ |
| 4272 | $gg/q\bar{q} \rightarrow G \rightarrow Z^0Z^0$ |
| 4273 | $gg/q\bar{q} \rightarrow G \rightarrow H_{\text{SM}}^0H_{\text{SM}}^0$ |
| 5000 | Pointlike photon-hadron jet production (all flavours) |
| 5100+IQ | Pointlike photon heavy flavour pair production (IQ as above) |
| 5200+IQ | Pointlike photon heavy flavour single excitation (IQ as above) |
| | After generation, IHPRO is subprocess (see sect. 4.6.5) |
| 5300 | Quark-photon Compton scattering |
| 5500 | Pointlike photon production of light (u, d, s) L=0 mesons |
| 5510,20 | S=0 mesons only, S=1 mesons only |
| | After generation, IHPRO is subprocess (see sect. 4.6.5) |
| 6000 | $\gamma\gamma \rightarrow q\bar{q}$ (all flavours) |
| 6000+IQ | $\gamma\gamma \rightarrow q\bar{q}$ (IQ as above) |
| 6006+IL | $\gamma\gamma \rightarrow \ell\bar{\ell}$ (IL = 1, 2, 3 for $\ell = e, \mu, \tau$) |
| 6010 | $\gamma\gamma \rightarrow W^+W^-$ |
| 7000 – | Baryon-number violating and other multi- W^\pm processes |

Table 9: Process codes. (Continues)

| IPROC | Process |
|----------|---|
| 7999 | generated by HERBVI package |
| 8000 | Minimum bias soft hadron-hadron event |
| 9000 | Deep inelastic lepton scattering (all neutral current) |
| 9000+IQ | Deep inelastic lepton scattering (NC on flavour IQ) |
| 9010 | Deep inelastic lepton scattering (all charged current) |
| 9010+IQ | Deep inelastic lepton scattering (CC on flavour IQ) |
| 9100 | Boson-gluon fusion in neutral current DIS (all flavours) |
| 9100+IQ | Boson-gluon fusion in neutral current DIS (IQ as above) |
| 9107 | J/ψ + gluon production by boson-gluon fusion |
| 9110 | QCD Compton process in neutral current DIS (all flavours) |
| 9110+IP | QCD Compton process in NC DIS (IP=1–12 for $d - t, \bar{d} - \bar{t}$) |
| 9130 | All $\mathcal{O}(\alpha_S)$ NC processes (i.e. 9100+9110) |
| 9140+IP | Heavy quark production by charged-current boson-gluon fusion IP: 1 = $s\bar{c}$, 2 = $b\bar{c}$, 3 = $s\bar{t}$, 4 = $b\bar{t}$ (+ ch. conj.) |
| 9500+ID | $W^+W^-/Z^0Z^0 \rightarrow H_{\text{SM}}^0$ in DIS (ID as in IPROC = 300 + ID) |
| 10000+IP | as IPROC = IP but with soft underlying event (soft remnant fragmentation in lepton-hadron) suppressed |

Table 9: Process codes.

4.2.1 Treatment of quark masses

The extent to which quark mass effects are included in the hard process cross section is different in different processes. In many processes, they are always treated as massless: IPROC = 1300, 1800, 1900, 2100, 2300, 2400, 5300, 9000. In two processes they are all treated as massless except the top quark, for which the mass is correctly incorporated: 1400, 2000. In the case of massless pair production, only quark flavours that are kinematically allowed are produced. In all cases the event kinematics incorporate the quark mass, even when it is not used to calculate the cross section. In two processes, quarks are always treated as massive: 500, 9100. Finally, in several processes, the behaviour is different depending on whether a specific quark flavour is requested, in which case its mass is included, or not, in which case all quarks are treated as massless. These are: IPROC = 100, 110, 120, QCD $2 \rightarrow 2$ scattering (1500 vs. 1700+IQ), jets in direct photoproduction (5000 vs. 5100+IQ and 5200+IQ). In the case of IPROC = 2900,2910 one has the option of using the massless or massive matrix element.

These differences can cause inconsistencies between different ways of generating the same process. The most noticeable example is in direct photoproduction, where one can use process 9130, which uses the exact $2 \rightarrow 3$ matrix element $e + g \rightarrow e + q + \bar{q}$, or process 5000, which uses the Equivalent Photon Approximation (EPA) for $e \rightarrow e + \gamma$ and the $2 \rightarrow 2$ matrix element for $\gamma + g \rightarrow q + \bar{q}$. For typical HERA

kinematics, the EPA is valid to a few per cent, but the difference between the two processes is much larger, about 20% for $\text{PTMIN} = 2 \text{ GeV}$. This is entirely due to the difference in quark mass treatments, as can be checked by comparing process 9130 with processes 5100+IQ and 5200+IQ summed over IQ.

4.2.2 Couplings

The two-loop QCD coupling at scale Q is given by subroutine `HWUALF` with arguments `IOPT = 1` and `SCALE = Q`. Threshold matching is performed at the quark mass scales $Q = \text{RMASS}(i)$. Setting `IOPT = 0` initialises the coupling using the 5-flavour value $\Lambda_{\overline{\text{MS}}} = \text{QC DLAM}$. Other values of `IOPT` are for internal use only.

The electromagnetic coupling is given by `HWUAEM(Q2) = e2/(4π)`; it runs according to the prescription in ref. [57] with the hadronic term as given in ref. [58]. The parameter `ALPHEM` \equiv `HWUAEM(0)`, default value 0.0072993, provides the normalization at the Thomson limit; it is used for all processes involving real photons. Photon emission in parton showers and in the ‘dead-zone’ in e^+e^- processes can be enhanced by a factor of `ALPFAC` (default = 1). The normalised electric charges of the fundamental fermions are stored in the array `QFCH(I)`, where $I = 1\text{--}6$ for the quarks d, u, s, c, b, t (e.g. `QFCH(4) = 2./3.`) and 11–16 for the leptons $e, \nu_e, \mu, \nu_\mu, \tau, \nu_\tau$.

The weak neutral current is taken to be of the form $e(v_f + a_f \gamma_5) \gamma_\mu$, where the electric charge is evaluated at a scale appropriate to the process. The arrays `VFCH(I, J)` and `AFCH(I, J)` store the couplings: I as before, $J = 1$ for the minimal Standard Model and 2 for possible Z' couplings (only used if `ZPRIME=.TRUE.`). Note that universality is not assumed — couplings can be arbitrarily set separately for each fermion species. The default couplings are given in terms of `SWEIN = sin2 θW`, default value 0.2319, as:

$$v_f = (T_3/2 - Q \sin^2 \theta_W) / (\cos \theta_W \sin \theta_W), \quad a_f = T_3 / (2 \cos \theta_W \sin \theta_W).$$

The weak charged current is given in terms of $g = e / \sin \theta_W$ and the Cabbibo-Kobayashi-Maskawa mixing matrix, the elements squared of which are stored in `VCKM(K, L)`, $K = 1, 2, 3$ for u, c, t , $L = 1, 2, 3$ for d, s, b . The variable `SCABI = sin2 θCabibbo` is however also retained for the present. Note the Fermi constant G_{Fermi} is eliminated from all cross sections.

The overall scale for all cross sections, given in nanobarns, is set by `GEV2NB = (ħc/e)2`, default value 389379.

We now give more detailed descriptions of the various subprocesses, concentrating again on the new features since ref. [1].

4.3 Lepton-antilepton Standard Model processes

Lepton beam polarization effects are included in $e^+e^- \rightarrow 2/3$ jet production and the Bjorken process (ZH production). Incoming lepton and antilepton beam polariza-

tions are specified by setting the two 3-vectors EPOLN and PPOLN: component 3 is longitudinal and 1,2 transverse.

Photon initial-state radiation (ISR) in e^+e^- annihilation events is allowed. The parameter TMNISR sets the minimum \hat{s}/s value (default = 10^{-4}), ZMXISR sets the (arbitrary) separation between unresolved and resolved emission (default = $1-10^{-6}$). Setting ZMXISR = 0 switches off photon ISR.

Where processes are listed for $\ell^+\ell^-$ they are available for e^+e^- and $\mu^+\mu^-$ annihilation. Many of the processes listed for e^+e^- will also work for $\mu^+\mu^-$, but we have not been systematic in ensuring this.

4.3.1 IPROC=100–127: hadron production

A correction to hard gluon emission in e^+e^- events has been added and is now the default process for IPROC=100+IQ. The $\mathcal{O}(\alpha_S)$ matrix element is used to add events in the ‘dead zone’ of phase-space corresponding to a quark-antiquark pair recoiling from a hard gluon [16]. Although this is asymptotically negligible, and cannot be produced within the shower itself, it has a significant effect at LEP1 energies. As a result, the default parameters have been retuned, and show a marked improvement in agreement with e^+e^- data for event shapes sensitive to three-jet configurations.

The routine HWBDED implements this hard correction while HWBRAN has been modified to include the soft matrix-element corrections described in section 3.2.3.

When IPROC=100+IQ, hard gluons emitted into the dead zone are assigned to the quark or antiquark shower and do not appear explicitly in the event record.

The $q\bar{q}g$ process alone, generated according to the $\mathcal{O}(\alpha_S)$ $q\bar{q}g$ matrix element with a maximum thrust cutoff THMAX (default 0.9), is given by IPROC=110+IQ.

The uncorrected $q\bar{q}$ process has been retained for comparative purposes and is available as IPROC=120+IQ.

The fictional e^+e^- processes $e^+e^- \rightarrow g + g(+g)$, IPROC=107 and 127, is treated just like $e^+e^- \rightarrow q\bar{q}$, summed over light quark flavours, for direct comparisons between quark and gluon jets.

4.3.2 IPROC=150–250: lepton and electroweak boson production

In IPROC=150, only the s -channel process, mediated by a virtual photon or Z^0 , is included, so the final-state leptons must be different from the initial ones.

The processes of W^+W^- and Z^0Z^0 pair production, IPROC=200 and 250, are based on a program kindly supplied by Zoltan Kunszt, which fully includes decay correlations. The QCD $\mathcal{O}(\alpha_S)$ matrix element correction for hard gluon emission in hadronic W and Z decays has also been implemented in these processes, according to the method described in section 3.2.3. In contrast to IPROC=100+IQ, any hard gluons emitted into the dead zone are shown explicitly in the event record.

4.3.3 IPROC=300–499: Higgs boson production

HERWIG generates SM Higgs bosons in lepton-antilepton collisions through the Bjorken process $Z^{(*)} \rightarrow Z^{(*)}H_{\text{SM}}^0$ with one or both Z^0 's off-shell (IPROC = 300 + ID) and W^+W^-/Z^0Z^0 fusion (IPROC = 400 + ID). See section 3.4 for explanation of how the Higgs decay is controlled by the value of ID.

4.3.4 IPROC=500–559: two-photon/photon-boson processes

In the e^+e^- two-photon processes, IPROC = 500 + ID, ID = 0 – 10 is the same as in Higgs processes for $q\bar{q}$, $\ell\bar{\ell}$ and W^+W^- . The Equivalent Photon Approximation (EPA) is used for the $e \rightarrow e\gamma$ vertices. The phase space is controlled by EMMIN and EMMAX for the two-photon centre-of-mass frame (CMF) mass, PTMIN and PTMAX for the transverse momentum of the CMF in the lab, and CTMAX for the c.m. angle of the outgoing particles. The additional phase-space variable WHMIN sets the minimum allowed hadronic mass and affects photoproduction reactions (γ -hadron and γ - γ) and DIS.

In photon- W^\pm fusion, IPROC = 550 + ID, ID = 0 – 9 is also the same as in Higgs processes, except that ID=1 or 2 both give the sum of $d\bar{u}$ and $u\bar{d}$ etc. The EPA is used for the $e \rightarrow e\gamma$ vertex. The phase space is controlled by EMMIN and EMMAX only. The full 2 \rightarrow 3 matrix elements for $\gamma e \rightarrow f\bar{f}'\nu$ are used, so the cross section for real W^\pm production is correctly included. In the case of $\gamma\gamma \rightarrow WW$ the decay correlations are not yet correctly included: the W 's currently decay isotropically.

4.3.5 IPROC=600–656: four jet production

Electron-positron annihilation to four jets is provided by IPROC=600+IQ, where a non-zero value for IQ guarantees production of quark flavour IQ whilst IQ=0 corresponds to the natural flavour mix. IPROC=650+IQ is as above but without those terms in the matrix element which orient the event w.r.t. the lepton beam direction. The matrix elements are based on those of Ellis, Ross and Terrano [59] with orientation terms from Catani and Seymour [60]. The soft and collinear divergences are avoided by imposing a minimum y_{cut} , Y4JT (default 0.01), on the initial four partons. The interjet distance y_{cut} is calculated using either the Durham or JADE metrics, as selected by the logical variable DURHAM (default .TRUE.). In order to improve efficiency parameterizations of the volume of four-body phase space are used: these are accurate up to a few percent for y_{cut} values less than 0.14. Note also that the phase space is for massless partons, as are the matrix elements, though a mass threshold cut is applied.

The argument of the strong coupling is set equal to EMSCA, the scale for the parton showers. This is taken to be the smallest of the y_{cut} values times the c.m. energy squared if FIX4JT=.FALSE. (default); otherwise the argument is fixed at Y4JT times the c.m. energy squared.

The matrix elements for the $q\bar{q}gg$ and $q\bar{q}q\bar{q}$ (same flavour quark) final states receive contributions from two colour flows each. The actual process and colour flow generated is indicated by `IHPRO` as shown in table 10. The meaning of ‘c/f conn.’ is discussed in section 4.6.2 below. The treatment of the interference terms between the two colour flows is controlled by the array `IOP4JT(1)` for $q\bar{q}gg$ and `IOP4JT(2)` for $q\bar{q}q\bar{q}$ (identical quark flavour):

| IHPRO | $\gamma^* \rightarrow 1+2+3+4$ | c/f conn. |
|-------|--------------------------------|-----------|
| 91 | $q + \bar{q} + g + g$ | 3 1 4 2 |
| 92 | $q + \bar{q} + g + g$ | 4 1 2 3 |
| 93 | $q + \bar{q} + q + \bar{q}$ | 4 1 2 3 |
| 94 | $q + \bar{q} + q + \bar{q}$ | 2 1 4 3 |
| 95 | $q + \bar{q} + q' + \bar{q}'$ | 4 1 2 3 |

Table 10: Four jet subprocesses.

$$\text{IOP4JT}(1) = \begin{cases} 0 & \text{neglect} \\ 1 & \text{extreme 3142} \\ 2 & \text{extreme 4123} \end{cases} \quad \text{IOP4JT}(2) = \begin{cases} 0 & \text{neglect} \\ 1 & \text{extreme 4123} \\ 2 & \text{extreme 2143} \end{cases}$$

In both instances the default value is 0.

See ref. [61] for some applications and discussions of the new four-jet implementation in e^+e^- annihilations.

4.4 Lepton-antilepton supersymmetric processes (MSSM)

The R-parity conserving lepton-antilepton SUSY processes have `IPROC` = 700 – 799 and \mathcal{R}_p processes have `IPROC` = 800 – 899. Lepton beam polarization effects are included for all of the SUSY production processes. The processes have all been implemented in such a way as to allow either e^+e^- or $\mu^+\mu^-$ as the initial state. As with the SM lepton-antilepton processes, ISR is allowed for the SUSY production processes.

As, by probing the individual thresholds, it may be possible to study the production of a given sparticle pair in lepton-antilepton collisions, we have provided more control over the sparticles produced than for the hadron-hadron SUSY production processes described in section 4.7.

We remind the reader here that all SUSY particle data have to be read from an input file before event generation (see section 3.5.1).

4.4.1 `IPROC=700–799`: gaugino, slepton and/or squark production

With `IPROC` = 700 one obtains the four processes `IPROC` = 710, 730, 740, 760 in the correct proportions. The matrix elements have been derived independently and the cross sections are in good agreement with those from `SUSYGEN` [62]. For all these processes the hard process scale `EMSCA` has been set to the centre-of-mass energy.

The gaugino and sfermion mixing conventions of Haber and Kane [40] are adopted in all cases. In addition, the neutralino mixing matrix `ZMIXSS` is defined internally

in terms of the photino, zino and current eigenstate neutral higgsino components, instead of the bino, W_3 -ino and higgsino components adopted for ZMXNSS, equivalent to N_{ij} in [40].

IPROC = 710 gives lepton-antilepton \rightarrow neutralino pair production. A number of additional IPROC codes have been provided to enable the user to produce given neutralino mass eigenstates. It should be noted that in order to provide a compact code for these processes there is more than one possible IPROC number for some processes. For example the final state $\tilde{\chi}_1^0\tilde{\chi}_3^0$ can be produced using either the IPROC codes 713 or 721.

IPROC = 730 gives lepton-antilepton \rightarrow chargino pair production. As with the neutralino production there are codes to allow a given pair of charginos to be produced.

IPROC = 740 gives lepton-antilepton \rightarrow slepton pair production. In these processes for the first two generations the left/right eigenstates are produced, while for the third generation the mass eigenstates are produced. In the processes producing given slepton pairs for $\tilde{\tau}$ production processes the left eigenstate is replaced by the lighter mass eigenstate and the right eigenstate by the heavier mass eigenstate.

IPROC = 760 gives lepton-antilepton \rightarrow squark pair production. As with the other processes additional codes are provided to allow the production of given $\tilde{q}\tilde{q}^*$ pairs. For stop and sbottom production the mass eigenstates are produced, while for the first two generations the left/right eigenstates are generated. As with the slepton production for the third generation when a given squark pair is requested the left eigenstate is replaced by the lighter mass eigenstate and the right eigenstate by the heavier mass eigenstate.

4.5 Other lepton-antilepton non-Standard-Model processes

4.5.1 IPROC=800–899: R-parity violating SUSY processes

A range of possible \mathcal{R}_p production processes in lepton-antilepton collisions is included. Unlike the case of \mathcal{R}_p production in hadron-hadron collisions, section 4.8.1, we have included processes for which there is either no s -channel resonance or the resonance is not kinematically accessible.

All the possible single sparticle production mechanisms which occur via the first term in the superpotential given in [42] are included. This includes the process $\ell^+\ell^- \rightarrow \gamma\tilde{\nu}$ for which there is no s -channel resonance. As the cross section for this process diverges in the limit that the photon is collinear with the incoming lepton beams a cut on the p_T of the outgoing particles $p_T > \text{PTMIN}$ has been imposed for this process (IPROC=850). The ISR is switched off for this process as including it would lead to a double counting of the photon radiation. For this reason this process

is not included in the code `IPROC=800` which generates all the other single sparticle production mechanisms.

We have also included some processes for the production of SM particles via s -channel sneutrino exchange. In addition to the s -channel sneutrino diagrams the t -channel sparticle exchanges, SM diagrams and all the interference terms are included. This uses a generalization of the formulae of [63]. A cut $p_T > \text{PTMIN}$ is used in the process $\ell^+\ell^- \rightarrow \ell^+\ell^-$ (`IPROC=870`) to avoid the divergence as $t \rightarrow 0$ in the Bhabha scattering cross section.

Except where stated explicitly above, no `PTMIN` cut is applied.

4.5.2 `IPROC=900–999`: MSSM Higgs production processes

For MSSM Higgs pair production (`IPROC=955–965`) a new subroutine has been introduced, `HWHIHH`, whereas for the other processes we make use of the implementation of their SM counterparts, which are based on the subroutines `HWHIGW` and `HWHIGZ`.

4.5.3 `IPROC=1000–1199`: SM and MSSM Higgs associated production

SM and MSSM Higgs production in association with fermion pairs in lepton-lepton collisions is available in version 6.5. These processes were introduced in [64] and their phenomenological relevance was discussed in [65].

Fermion masses are retained in the final state according to the `HERWIG` defaults. The same values appear in the Yukawa couplings. Notice that in the case of charged Higgs boson production the Cabibbo-Kobayashi-Maskawa mixing matrix has been assumed to be diagonal. Furthermore, due to the rather different phase space distribution of the final state products, all processes can only be produced separately, not collectively. Initial- and final-state radiation (both QED and QCD) and beamsstrahlung are included via the usual `HERWIG` algorithms. Finally notice that the use of the `IPROC` series 1000 and 1100 for $\ell^+\ell^-$ processes required some internal modification to `HERWIG`, which was originally designed to generate leptonic processes only for `IPROC < 1000`. Now we assume an $\ell^+\ell^-$ process whenever `IPROC < 1300`. These modifications have no implications for the traditional user, but may affect more knowledgeable ones who have edited previous versions of the main `HERWIG` code.

4.6 Hadron-hadron Standard Model processes

4.6.1 `IPROC=1300–1499`: Drell-Yan processes

The Drell-Yan code is extended to the production of all fermion pairs; `1300` gives all quark flavours; `1300+IQ` a specific quark flavour, `1350` all leptons (including neutrinos) `1350+IL` a specific lepton flavour. The s -channel component of the interference with like-flavour $q\bar{q}$ scattering is included here.

| IHPRO | $1 + 2 \rightarrow 3 + 4$ | c/f conn. |
|-------|---|-----------|
| 1 | $q + q \rightarrow q + q$ | 3 4 2 1 |
| 2 | $q + q \rightarrow q + q$ | 4 3 1 2 |
| 3 | $q + q' \rightarrow q + q'$ | 3 4 2 1 |
| 4 | $q + \bar{q} \rightarrow q' + \bar{q}'$ | 2 4 1 3 |
| 5 | $q + \bar{q} \rightarrow q + \bar{q}$ | 3 1 4 2 |
| 6 | $q + \bar{q} \rightarrow q + \bar{q}$ | 2 4 1 3 |
| 7 | $q + \bar{q} \rightarrow g + g$ | 2 4 1 3 |
| 8 | $q + \bar{q} \rightarrow g + g$ | 2 3 4 1 |
| 9 | $q + \bar{q}' \rightarrow q + \bar{q}'$ | 3 1 4 2 |
| 10 | $q + g \rightarrow q + g$ | 3 1 4 2 |
| 11 | $q + g \rightarrow q + g$ | 3 4 2 1 |
| 12 | $\bar{q} + q \rightarrow \bar{q}' + q'$ | 3 1 4 2 |
| 13 | $\bar{q} + q \rightarrow \bar{q} + q$ | 2 4 1 3 |
| 14 | $\bar{q} + q \rightarrow \bar{q} + q$ | 3 1 4 2 |
| 15 | $\bar{q} + q \rightarrow g + g$ | 3 1 4 2 |
| 16 | $\bar{q} + q \rightarrow g + g$ | 4 1 2 3 |
| 17 | $\bar{q} + q' \rightarrow \bar{q} + q'$ | 2 4 1 3 |
| 18 | $\bar{q} + \bar{q} \rightarrow \bar{q} + \bar{q}$ | 4 3 1 2 |
| 19 | $\bar{q} + \bar{q} \rightarrow \bar{q} + \bar{q}$ | 3 4 2 1 |
| 20 | $\bar{q} + \bar{q}' \rightarrow \bar{q} + \bar{q}'$ | 4 3 1 2 |
| 21 | $\bar{q} + g \rightarrow \bar{q} + g$ | 2 4 1 3 |
| 22 | $\bar{q} + g \rightarrow \bar{q} + g$ | 4 3 1 2 |
| 23 | $g + q \rightarrow g + q$ | 2 4 1 3 |
| 24 | $g + q \rightarrow g + q$ | 3 4 2 1 |
| 25 | $g + \bar{q} \rightarrow g + \bar{q}$ | 3 1 4 2 |
| 26 | $g + \bar{q} \rightarrow g + \bar{q}$ | 4 3 1 2 |
| 27 | $g + g \rightarrow q + \bar{q}$ | 2 4 1 3 |
| 28 | $g + g \rightarrow q + \bar{q}$ | 4 1 2 3 |
| 29 | $g + g \rightarrow g + g$ | 4 1 2 3 |
| 30 | $g + g \rightarrow g + g$ | 4 3 1 2 |
| 31 | $g + g \rightarrow g + g$ | 2 4 1 3 |

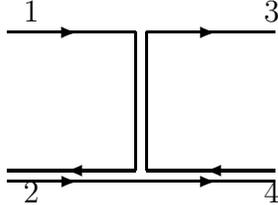
Table 11: QCD subprocesses.

The initial-state parton showers in Drell-Yan processes are matched to the exact $\mathcal{O}(\alpha_S)$ matrix-element result as discussed in section 3.2.3. The routine `HWBDYP` implements the hard corrections whilst `HWSBRN` includes the soft corrections to the initial-state radiation. For further details see ref. [20].

4.6.2 IPROC=1500: QCD $2 \rightarrow 2$ processes

At present only $2 \rightarrow 2$ subprocesses are implemented. They are classified in ta-

ble 11. Here and in other subprocess tables, ‘c/f conn.’ refers to the colour/flavour connections between the partons: ‘ $i j k l$ ’ means that the colour of parton 1 comes from parton i , that of 2 from j , etc. For antiquarks, which have no colour (only anticolour), the label shows instead to which parton the flavour is connected. For this colour/flavour labelling all partons are defined as outgoing. Thus, for example, process 10 has colour connections 3 1 4 2, corresponding to the colour flow diagram:



When different colour flows are possible, they are listed as separate subprocesses. This separation is not exact but is normally a good approximation [6, 7]. The separation is now performed using the improved method proposed in [31], as outlined in section 3.1. The sum of the colour flows is the exact lowest-order cross section.

4.6.3 IPROC=1600–1699: Higgs boson production by parton fusion

IPROC = 1600 + ID gives the sum of gg and $q\bar{q}$ fusion. The lowest-order formulae that we have used can be found in [41]. The hard processes are implemented in the subroutine HWHIGS.

4.6.4 IPROC=1700–1706: heavy quark production

The separation of colour flows is now performed using the improved method proposed in [31], as outlined in section 3.1. The classification of subprocesses according to IHPR0 is as for IPROC=1500.

4.6.5 IPROC=1800: QCD direct photon plus jet production

The relevant IHPR0 codes are 41–47 in table 12. For future reference we also collect here the codes for other processes that involve outgoing direct photons or incoming pointlike photons (IPROC=2200, 5000–5520). Note that the photon is colour/flavour-connected to itself. In the cases IHPR0=71–76, M represents an $L = 0$ meson (see IPROC=5500).

4.6.6 IPROC=1900–1999: Higgs boson production by weak boson fusion

The $q\bar{q} \rightarrow q^{(\prime)}\bar{q}^{(\prime)}VV \rightarrow q^{(\prime)}\bar{q}^{(\prime)}H_{\text{SM}}^0$ subprocesses, for $VV = W^+W^-, Z^0Z^0$, summed over initial- and final-state quarks can be invoked by setting IPROC=1900+ID, with ID used to identify the Higgs decay.

The formulae used are well known in the literature and can be found e.g. in [22]. This process is administered by the subroutine HWHIGW, which also handles the similar cases initiated by e^+e^- and $e^\pm p$ collisions.

4.6.7 IPROC=2000–2008: single top production

The process of single top quark production by W -boson exchange includes so far only those processes initiated by a b -quark (or antiquark) and a first- or second-generation quark or antiquark. Note that this requires b -quarks to be available in the parton distribution functions.

4.6.8 IPROC=2100–2170: electro-weak boson plus jet production

The electroweak boson decay correlations and width are now correctly included in these processes.

4.6.9 IPROC=2200: direct photon pair production

See section 4.6.5 for IHPRO codes (61–63).

| IHPRO | $1 + 2 \rightarrow 3 + 4$ | c/f conn. |
|-------|--|-----------|
| 41 | $q + \bar{q} \rightarrow g + \gamma$ | 2 3 1 4 |
| 42 | $q + g \rightarrow q + \gamma$ | 3 1 2 4 |
| 43 | $\bar{q} + q \rightarrow g + \gamma$ | 3 1 2 4 |
| 44 | $\bar{q} + g \rightarrow \bar{q} + \gamma$ | 2 3 1 4 |
| 45 | $g + q \rightarrow q + \gamma$ | 2 3 1 4 |
| 46 | $g + \bar{q} \rightarrow \bar{q} + \gamma$ | 3 1 2 4 |
| 47 | $g + g \rightarrow g + \gamma$ | 2 3 1 4 |
| 51 | $\gamma + q \rightarrow g + q$ | 1 4 2 3 |
| 52 | $\gamma + \bar{q} \rightarrow g + \bar{q}$ | 1 3 4 2 |
| 53 | $\gamma + g \rightarrow q + \bar{q}$ | 1 4 2 3 |
| 61 | $q + \bar{q} \rightarrow \gamma + \gamma$ | 2 1 3 4 |
| 62 | $\bar{q} + q \rightarrow \gamma + \gamma$ | 2 1 3 4 |
| 63 | $g + g \rightarrow \gamma + \gamma$ | 2 1 3 4 |
| 71 | $\gamma + q \rightarrow M(S = 0) + q'$ | 1 4 3 2 |
| 72 | $\gamma + q \rightarrow M(S = 1)_L + q'$ | 1 4 3 2 |
| 73 | $\gamma + q \rightarrow M(S = 1)_T + q'$ | 1 4 3 2 |
| 74 | $\gamma + \bar{q} \rightarrow M(S = 0) + \bar{q}'$ | 1 4 3 2 |
| 75 | $\gamma + \bar{q} \rightarrow M(S = 1)_L + \bar{q}'$ | 1 4 3 2 |
| 76 | $\gamma + \bar{q} \rightarrow M(S = 1)_T + \bar{q}'$ | 1 4 3 2 |

Table 12: Direct photon subprocesses.

4.6.10 IPROC=2300–2399: Higgs boson plus jet production

High transverse momentum, scalar Higgs production via one-loop diagrams, in association with a jet, is available as IPROC=2300, within the SM. Only the top quark is included in the loops with IAPHIG controlling the approximation used: IAPHIG=0 gives the zero top mass limit, 1 (default) the exact result, 2 the infinite top mass limit. The various subprocesses are illustrated in table 13.

Note that the Higgs boson is colour/flavour connected to itself.

The relevant routines HWHGJ1, HWHGJA/B/C/D, HWUCI2 and HWULI2 use (non-standard Fortran 77) DOUBLE COMPLEX variables which may not be accepted by some compilers and are called COMPLEX*16 by others. Users can change to COMPLEX variables, but this involves a risk of rounding errors spoiling numerical cancellations.

| IHPRO | $1 + 2 \rightarrow 3 + 4$ | c/f conn. |
|-------|--|-----------|
| 81 | $q + \bar{q} \rightarrow g + H_{SM}^0$ | 2 3 1 4 |
| 82 | $q + g \rightarrow q + H_{SM}^0$ | 3 1 2 4 |
| 83 | $\bar{q} + q \rightarrow g + H_{SM}^0$ | 3 1 2 4 |
| 84 | $\bar{q} + g \rightarrow \bar{q} + H_{SM}^0$ | 2 3 1 4 |
| 85 | $g + q \rightarrow q + H_{SM}^0$ | 2 3 1 4 |
| 86 | $g + \bar{q} \rightarrow \bar{q} + H_{SM}^0$ | 3 1 2 4 |
| 87 | $g + g \rightarrow g + H_{SM}^0$ | 2 3 1 4 |

Table 13: Higgs plus jet subprocesses.

4.6.11 IPROC=2400–2450: colour singlet exchange

IPROC=2400: Two-to-two parton scattering via exchange of a colour singlet, Mueller-Tang pomeron [66]. The fixed α_S and ω_0 are given by ASFIXD (default 0.25) and OMEGA0 (0.3) respectively.

IPROC=2450: Photon exchange, for like-flavour $q\bar{q}$ pairs including the t -channel component of the interference with $q\bar{q} \rightarrow q\bar{q}$ via an s -channel photon or Z^0 .

4.6.12 IPROC=2500–2599: Higgs boson plus top quark pair production

The SM $2 \rightarrow 3$ Higgs production subprocesses of the type $gg \rightarrow t\bar{t}H_{\text{SM}}^0$ and $q\bar{q} \rightarrow t\bar{t}H_{\text{SM}}^0$, for any flavour of initial state quarks q , are new to HERWIG version 6 and are handled by the subroutines HWHIGQ and HWH2QH. They are invoked by setting IPROC=2500+ID (both gg and $q\bar{q}$), with ID administering the Higgs decay channels as in IPROC=300+ID. The initial state quark flavours q are always summed over. Notice that, given the size of the Yukawa couplings of the Higgs boson to quarks, in practice only the associated production with top quarks is of phenomenological relevance in the SM. The matrix elements used in the implementation can be found in ref. [22]. The treatment of the Higgs width here is as described in section 3.4.

4.6.13 IPROC=2600–2799: Higgs plus weak boson production

The associated production of SM Higgs scalars with W^\pm (IPROC=2600-2699) and Z^0 (IPROC=2700-2799) gauge bosons initiated by quark-antiquark fusion via the $2 \rightarrow 2$ processes $q\bar{q} \rightarrow W^\pm H_{\text{SM}}^0$ and $q\bar{q} \rightarrow Z^0 H_{\text{SM}}^0$ is now available. A summation is as usual intended on the incoming quarks. The formulae given in [22] are used. The production processes are generated by the two new subroutines HWHIGV and HWH2VH whereas the Higgs decays are administered through the ID increment, as in IPROC=300+ID. Again, the treatment of the Higgs boson width here is as discussed in section 3.4.

4.6.14 IPROC=2800–2825: Gauge boson pair production

In version 6.3, the code already included in HERWIG for $e^+e^- \rightarrow WW/ZZ$ [67] was adapted for hadron-hadron collisions, including photons and the photon/Z interference for the resonant diagrams.

All of these processes use a cut EMMIN (default value 20 GeV) on the mass of the gauge bosons produced. The cut PTMIN (default 10 GeV) on the transverse momentum of the bosons is also used. Both these cuts should not be taken to zero simultaneously if photon terms are included. The phase space for these processes contains a number of peaks and it was therefore necessary to use an adaptive multi-channel phase-space integration method which is described below.

In versions 6.4 and above, the hard process scale EMSCA for this process has been changed to the parton-parton centre-of-mass energy from the average of the produced boson masses, which was used previously.

4.6.15 IPROC=2850–2880: Gauge boson pairs using MC@NLO

These codes activate the interface to the program MC@NLO for diboson production at next-to-leading order (see sect. 9.6).

4.6.16 IPROC=2900–2916: $Q\bar{Q}Z$ production

The matrix elements of [68] were used for the massless case and an independent calculation, using the approach of [69], which was checked both for gauge invariance and against the massless case for the massive result.

In both cases the decay of the Z is fully included and is selected using MODBOS. PTMIN controls the minimum transverse momentum of the outgoing quarks. As with gauge boson pair production it was necessary to use an optimized multi-channel phase-space integrator which is described below.

The phase space for both gauge boson pair production and $Q\bar{Q}Z$ is complicated, as these processes are both treated as $2 \rightarrow 4$ processes. In order to obtain a reasonable efficiency it was necessary to adopt a multi-channel approach based on that described in [70, 71].

In each case a number of different channels are included which attempt to map the phase space for the different processes. The default weights for these different channels have been chosen to optimize the efficiency for the Tevatron and LHC; a choice of which to use is made based on the beam energy. However, the choice is affected by the phase space cuts applied. Therefore if these are significantly altered the weights for the different channels need re-optimizing.

This is controlled by the new variable OPTM (default `.FALSE.`). If `OPTM=.TRUE.`, before performing the initial search for the maximum weight HERWIG will attempt to optimize the efficiency using the procedure suggested in [71].

This is done by generating IOPSTP (default 10) iterations of IOPSH (default 1000) events. The choice of IOPSTP and IOPSH is a compromise between run time and accuracy. The value of IOPSH should not be significantly reduced because the procedure attempts to minimize the error on the Monte Carlo evaluation of the cross section and if IOPSH is small the error on the error can be significant. If you need to re-optimize the weights we would recommend a long run just to optimize the weights which can then be used in all the runs to generate events. The new subroutine HWIPHS was added to initialise the phase space.

4.7 Hadron-hadron supersymmetric processes (MSSM)

The R-parity conserving SUSY processes occupy the IPROC entries of the series 3000 (sparticle processes) and 3300–3600 (Higgs boson production), while \mathcal{R}_p processes have `IPROC = 4000 – 4199`.

As with the lepton-antilepton SUSY processes the SUSY particle data must be read in from an input file before event generation as described in section 3.5.1. In

particular, unlike those of the SM Higgs boson H_{SM}^0 , the widths and decay modes of the SUSY Higgs bosons are not computed by HERWIG.

A large number of final states involving the production of both neutral and charged Higgs bosons of the Minimal Supersymmetric Standard Model (MSSM) have been made available in version 6.3. They all proceed via $2 \rightarrow 3$ body hard scattering subprocesses. They are listed below, with corresponding process numbers (IQ and ISQ are as detailed in the following subsections). Further details of their implementation can be found in [22]

The new subroutines introduced to administer the following processes are HWHIBQ and HWH2BH for IPROC=3500, plus HWHISQ and HWH2SH for IPROC=3100, 3200. In addition, HWHIGQ has been modified to accommodate the IPROC=3800 series.

4.7.1 IPROC=3000–3030: sparton, gaugino and/or slepton production

With IPROC=3000 one obtains the three following processes, IPROC=3010, 3020, 3030, in the correct proportions. The variable IHPR0 gives the subprocess actually generated (table 14).

The matrix elements have been derived independently and the cross sections are in good agreement with those from ISAJET [39].

The hard process scale EMSCA has to be chosen globally for all sparton processes, e.g. for the argument of the QCD coupling. This is done using the kinematics appropriate to production of the lightest supersymmetric particle (LSP) and

$$\text{EMSCA} = \sqrt{\frac{2 \hat{s} \hat{t}' \hat{u}'}{\hat{s}^2 + \hat{t}'^2 + \hat{u}'^2}}.$$

with $\hat{t}' = \hat{t} - m^2$, $\hat{u}' = \hat{u} - m^2$ where m is the LSP mass.

IPROC = 3010 gives 2-parton \rightarrow 2-sparton processes. All QCD sparton, i.e. squark and gluino, pair production processes are implemented. The matrix elements and the scheme for separating different colour flow parts are as given in [31].

IPROC = 3020 gives 2-parton \rightarrow 2-gaugino or gaugino+sparton processes. All gaugino, i.e. chargino and neutralino, pair production processes and gaugino-sparton associated production processes are implemented.

The gaugino and sfermion mixing conventions of Haber and Kane [40] are used as described in section 4.4.

The various subprocesses, which include the $1 \leftrightarrow 2$ and charge conjugate reactions omitted below for brevity, are shown in table 14.

Note that the gauginos connect to themselves. The indices a, b, i, j label gauginos in the order of increasing mass and take values $a, b = 1 - 2$ and $i, j = 1 - 4$.

Gaugino mixing matrices are implemented in all subprocesses. The associated production subprocesses IHPR0=3026, 3027 include stop and sbottom left-right mixings. CKM mixing is implemented in subprocesses IHPR0=3023, 3025, 3027 but neglected in subprocess IHPR0=3021.

IPROC = 3030 gives 2-parton \rightarrow 2-slepton processes. All Drell-Yan slepton production processes are implemented. The formulae agree with those of refs. [72, 73] in the limit of no stau left-right mixing.

4.7.2 IPROC=3110–3178: charged Higgs plus squark pair production

| IHPRO | 1 + 2 \rightarrow 3 + 4 | c/f conn. |
|-------|---|-----------|
| 3021 | $q + \bar{q} \rightarrow \tilde{\chi}_a^\pm + \tilde{\chi}_b^\mp$ | 2 1 3 4 |
| 3022 | $q + \bar{q} \rightarrow \tilde{\chi}_i^0 + \tilde{\chi}_j^0$ | 2 1 3 4 |
| 3023 | $q + \bar{q}' \rightarrow \tilde{\chi}_a^\pm + \tilde{\chi}_i^0$ | 2 1 3 4 |
| 3024 | $q + \bar{q} \rightarrow \tilde{\chi}_i^0 + \tilde{g}$ | 2 4 3 1 |
| 3025 | $q + \bar{q}' \rightarrow \tilde{\chi}_a^\pm + \tilde{g}$ | 2 4 3 1 |
| 3026 | $g + q \rightarrow \tilde{\chi}_i^0 + \tilde{q}$ | 2 4 3 1 |
| 3027 | $g + q \rightarrow \tilde{\chi}_a^\pm + \tilde{q}'$ | 2 4 3 1 |

Table 14: SUSY subprocesses.

The production of charged Higgs bosons of the MSSM in association with squark pairs, of bottom and top flavours only, is implemented via the 3100 series of IPROC numbers (table 15). Their phenomenological relevance has been discussed in [74].

One should add 30(60) to IPROC for $gg(q\bar{q})$ -only initiated processes.

4.7.3 IPROC=3210–3298: neutral Higgs plus squark pair production

| IPROC | partons \rightarrow spartons | Higgs |
|-------|---|---------|
| 3110 | $gg + q\bar{q} \rightarrow \tilde{q}_i \tilde{q}_j^*$ | H^\pm |
| 3111 | $gg + q\bar{q} \rightarrow \tilde{b}_1 \tilde{t}_1^*$ | H^+ |
| 3112 | $gg + q\bar{q} \rightarrow \tilde{b}_1 \tilde{t}_2^*$ | H^+ |
| 3113 | $gg + q\bar{q} \rightarrow \tilde{b}_2 \tilde{t}_1^*$ | H^+ |
| 3114 | $gg + q\bar{q} \rightarrow \tilde{b}_2 \tilde{t}_2^*$ | H^+ |
| 3115 | $gg + q\bar{q} \rightarrow \tilde{t}_1 \tilde{b}_1^*$ | H^- |
| 3116 | $gg + q\bar{q} \rightarrow \tilde{t}_1 \tilde{b}_2^*$ | H^- |
| 3117 | $gg + q\bar{q} \rightarrow \tilde{t}_2 \tilde{b}_1^*$ | H^- |
| 3118 | $gg + q\bar{q} \rightarrow \tilde{t}_2 \tilde{b}_2^*$ | H^- |

Table 15: Processes for IPROC=3110–3178.

The production of neutral Higgs bosons of the MSSM in association with squark pairs, of bottom and top flavours only, is implemented via the 3200 series of IPROC numbers (table 16). Their phenomenological relevance has been discussed in [74, 75].

One should add 30(60) to IPROC for $gg(q\bar{q})$ -only initiated processes.

4.7.4 IPROC=3310–3375: Higgs-Higgs and Higgs-gauge boson pair production

The production of Higgs-Higgs and Higgs-gauge boson pairs of the MSSM is implemented at tree level. We include gauge boson mediated contributions but not Higgstrahlung from the initial state, the only exception being $W^\pm H^\mp$ production (IPROC=3350), which does include diagrams where the Higgs boson couples to the initial partons as well as those mediated by neutral Higgs states [76]. Some of these processes are the MSSM equivalent of IPROC=2600 and 2700 described earlier for the case of the SM. Here, the cases IPROC=3310(3320) correspond to $W^\pm h^0 (W^\pm H^0)$ and IPROC=3360(3370) to $Z^0 h^0 (Z^0 H^0)$ final states. (No similar A^0 production can occur at leading order.) The array ENHANC is used to implement the MSSM couplings of Higgs scalars to gauge bosons.

| IPROC | partons \rightarrow spartons | Higgs |
|------------------|--|-----------|
| 3210(3220)[3230] | $gg + q\bar{q} \rightarrow \tilde{q}_i\tilde{q}_j^*$ | $h(H)[A]$ |
| 3211(3221)[3231] | $gg + q\bar{q} \rightarrow \tilde{b}_1\tilde{b}_1^*$ | $h(H)[A]$ |
| 3212(3222)[3232] | $gg + q\bar{q} \rightarrow \tilde{b}_1\tilde{b}_2^*$ | $h(H)[A]$ |
| 3213(3223)[3233] | $gg + q\bar{q} \rightarrow \tilde{b}_2\tilde{b}_1^*$ | $h(H)[A]$ |
| 3214(3224)[3234] | $gg + q\bar{q} \rightarrow \tilde{b}_2\tilde{b}_2^*$ | $h(H)[A]$ |
| 3215(3225)[3235] | $gg + q\bar{q} \rightarrow \tilde{t}_1\tilde{t}_1^*$ | $h(H)[A]$ |
| 3216(3226)[3236] | $gg + q\bar{q} \rightarrow \tilde{t}_1\tilde{t}_2^*$ | $h(H)[A]$ |
| 3217(3227)[3237] | $gg + q\bar{q} \rightarrow \tilde{t}_2\tilde{t}_1^*$ | $h(H)[A]$ |
| 3218(3228)[3238] | $gg + q\bar{q} \rightarrow \tilde{t}_2\tilde{t}_2^*$ | $h(H)[A]$ |

Table 16: Processes for IPROC=3210–3298.

4.7.5 IPROC=3410–3450: Higgs boson plus heavy quark production

We have included so far only those processes initiated by a b -quark (or antiquark) and a gluon. Note that this requires b -quarks to be available in the parton distribution functions.

4.7.6 IPROC=3500: charged Higgs boson from bq -initiated processes

This process is relevant for charged Higgs scalar production at large $\tan\beta$ values, see [77].

4.7.7 IPROC=3610–3630: neutral Higgs production by parton fusion

These processes are the MSSM analogues of the SM processes 1600 etc. Recall however that the MSSM Higgs decay modes are controlled by the SUSY input data (see section 3.5.1) and not by the value of IPROC. The subroutines HWHIGS and HWHIGT have been modified to take account of squark loop contributions and parity-violating Higgs-fermion couplings in the MSSM case.

4.7.8 IPROC=3710–3720: neutral Higgs production via weak boson fusion

These processes are the MSSM counterparts of the SM process of weak vector-vector fusion in hadronic collisions (IPROC=1900). They are computed using the same subroutines and setting the $\Phi^0 VV$ couplings to $\sin(\beta - \alpha)$ for $\Phi^0 = h^0$ (IPROC=3710) and to $\cos(\beta - \alpha)$ for $\Phi^0 = H^0$ (IPROC=3720), respectively, where $V = W^\pm, Z^0$. (There is no $A^0 VV$ coupling at tree level.)

These reactions are two of the major direct production channels of neutral CP-even Higgs bosons of the MSSM at hadron colliders, such as the LHC (see e.g. [78]).

4.7.9 IPROC=3811–3899: Higgs boson plus heavy quark pair production

For the case of neutral Higgs states, IPROC=3810+IQ corresponds to h^0 production, IPROC=3820+IQ to H^0 and IPROC=3830+IQ to A^0 . (For the last case, the vari-

able PARITY is set to -1 .) Note also the production of charged Higgs states, via IPROC=3839, 3869 and 3899, in association with pairs of top-bottom quarks.

In the usage of the IPROC numbers corresponding to neutral Higgs states, when b -quarks are involved in gg -fusion modes (IPROC(+30)=3845, 3855 or 3865), the user should take care to avoid double-counting the chosen process with the corresponding $2 \rightarrow 1$ and $2 \rightarrow 2$ cases of IPROC=3610–3630 and IPROC=3410–3430 initiated by quark-antiquark annihilation, i.e. $b\bar{b} \rightarrow$ Higgs, and (anti)quark-gluon scattering, i.e. $bg \rightarrow b$ Higgs, respectively: see [79]. Similar arguments hold for the charged Higgs states, as the gg -induced process (IPROC(+30)=3869) is an alternative implementation of IPROC=3450 [80].

The associate production of neutral Higgs bosons (both CP-even and CP-odd) of the MSSM with heavy $Q\bar{Q}$ pairs ($Q = b$ and t) is of extreme phenomenological relevance as a discovery mode of Higgs scalars, both at the Tevatron (Run 2) and the LHC (see e.g. [78,81]), as is the case of the charged Higgs channel [80,82].

4.8 Other hadron-hadron non-Standard-Model processes

4.8.1 IPROC=4000–4199: R-parity violating SUSY processes

We include all the possible production processes of resonant sleptons and squarks in hadron-hadron collisions, for arbitrary numbers of non-zero \mathcal{R}_p couplings. These processes are implemented as two-to-two processes, i.e. with the decay of the resonant particle included. This allows us to include the t -channel diagrams where these occur. However we have not implemented those processes which can only occur via a t -channel diagram, or where the resonance will never be accessible. So for example while we include the process $u_i d_j \rightarrow \tilde{b}_1^* Z^0$, which can occur via a resonant \tilde{b}_2^* , we do not include the process $u_i d_j \rightarrow \tilde{b}_2^* Z^0$, which cannot occur via a resonant diagram. In all cases both the processes listed and their charge conjugates are included.

The scale choice is $\sqrt{\hat{s}}$ rather than the conventional transverse mass, due to the large number of different processes which must be calculated. The colour connection structure of these processes and their matrix elements can be found in ref. [42].

4.8.2 IPROC=4200–4299 : graviton resonance production

In some models with extra dimensions, Kaluza-Klein excitations of the graviton can be produced with significant cross sections at TeV-scale colliders. When the scale of the extra dimensions is not large, the excitations are manifest as discrete resonances.

The production of a resonant excitation of the graviton is implemented as a $2 \rightarrow 2$ process including the decay of the resonance. The process is treated in a model-independent way, assuming only that there is a universal coupling of the graviton resonance to the SM fields. The effective lagrangian is given by

$$\mathcal{L}_I = -\frac{1}{\Lambda_\pi} h^{\mu\nu} T_{\mu\nu},$$

where $h^{\mu\nu}$ is the spin-2 field and $T_{\mu\nu}$ is the energy-momentum tensor of the SM fields. Although in these models there are usually many resonances, we have implemented only one. Others can be studied by making appropriate changes in the parameters. Graviton resonance production is described in more detail in [83].

The process is controlled by the coupling `GRVLAM` = Λ_π , with dimensions of mass and default value 10 TeV, and by the mass `EMGRV` (default 1 TeV) and width `GAMGRV` of the resonance. If the width is set to zero (the default), the subroutine `HWHGRV` which calculates the cross section also calculates the width.

The parton-level cross section for this process is non-unitary and is proportional to \hat{s}/EMGRV^4 at high energies. The fall-off of the parton distribution functions is not sufficient to suppress this bad high energy behaviour. Hence the parameters `EMMIN` and `EMMAX` controlling the minimum and maximum values of $\sqrt{\hat{s}}$ must be set. The default is to set these to 90% and 110% of the graviton resonance mass respectively. If the width of the resonance is more than a few percent of its mass then these limits should be reset.

After event generation, `IHPRO` is set to 50 for $q\bar{q}$ initiated subprocesses and to 51 for gg initiated subprocesses.

4.9 Photon-hadron and photon-photon processes

4.9.1 `IPROC=5000–5520`: pointlike photon-hadron processes

Pointlike photon-hadron scattering to produce QCD jets is available as `IPROC` = 5000 – 5206. This is suitable for fixed-target photoproduction, provided events are generated in a frame in which the target has high momentum, and then boosted back to the lab. This is done if `USECMF` = `.TRUE.`, the default, in which case the frame for event generation is the beam-target c.m. frame. `IPROC` = 5100 + `IQ` gives flavour `IQ` pair production, $\gamma + g \rightarrow Q\bar{Q}$, and `IPROC` = 5200 + `IQ` gives flavour `IQ` single excitation, $\gamma + Q \rightarrow g + Q$, both including quark masses. `IPROC` = 5000 gives a sum over all processes and flavours, 5100 and 5200, with massless quark kinematics. In all cases, after event generation the code `IHPRO` is set to 51, 52 or 53 according to the hard subprocess, as specified in section 4.6.5. `IPROC` = 5300 gives Compton scattering, $\gamma + q \rightarrow \gamma + q$.

The direct, higher twist, production of light (u, d, s) $L=0$ mesons by point-like photons is also available: `IPROC` = 5500 for all spin =0 and 1 mesons; 5510 for only $S=0$ mesons; and 5520 for only $S=1$ mesons. The vector mesons are produced with transverse or longitudinal polarization and decayed accordingly. The corresponding `IHPRO` codes (71–76) are also listed in section 4.6.5.

All these processes are available with lepton as well as hadron beams, using the Equivalent Photon Approximation. The phase-space variable `WHMIN` sets the minimum allowed hadronic mass and affects photoproduction reactions (γ -hadron and γ - γ) and DIS. In lepton-hadron DIS it is largely irrelevant since there is already

a cut on Bjorken y which at fixed s is almost the same, but for lepton-gamma DIS it makes a big difference. Direct $\gamma + \gamma^* \rightarrow q + \bar{q}$ is included in the hard correction for lepton-gamma DIS.

4.9.2 IPROC=6000–6010: pointlike photon-photon processes

Direct $\gamma\gamma \rightarrow$ charged particle pairs has been implemented with $\text{IPROC} = 6000 + \text{IQ}$: if $\text{IQ} = 1 - 6$ then only quark flavour IQ is produced, if $\text{IQ} = 7, 8$ or 9 then only lepton flavour e, μ or τ is produced and if $\text{IQ} = 10$ then only W pairs are produced: in these cases particle mass effects are included. If $\text{IQ} = 0$, the natural mix of quark pairs is produced using massless matrix elements but including a mass threshold cut. The range of allowed transverse momenta is controlled by PTMIN and PTMAX as usual.

4.10 Baryon number violating processes

4.10.1 IPROC=7000–7999: generated by the HERBVI package

See section 9.8 for details.

4.11 Minimum bias soft hadron-hadron collisions

4.11.1 IPROC=8000: minimum bias soft hadron-hadron event

Non-diffractive, soft hadronic, minimum bias events ($\text{IPROC}=8000$) can be generated for the following combinations of beam and target: $p, \bar{p}, \pi^\pm, K^\pm, e^\pm, \mu^\pm, \gamma$ on target p (or vice versa); p, \bar{p} on target n (or vice versa); or γ on γ . The event weight is the estimated cross section based on the parameterizations of Donnachie and Landshoff [84]. The non-diffractive cross section is assumed to be 70% of the total. For lepton beams a photon is first generated using the Effective Photon Approximation (see section 4.1) and then the on-shell photon cross section is used. See section 3.7.3 for discussion of the model used and the relevant parameters.

4.12 Deep inelastic lepton scattering

Deep inelastic (DIS) processes are broadly divided into those that start at $\mathcal{O}(\alpha_S^0)$ ($\text{IPROC}=90^{**}$) and those like heavy quark and dijet production which start at $\mathcal{O}(\alpha_S^1)$ ($\text{IPROC}=91^{**}$). Note that the DIS $\mathcal{O}(\alpha_S)$ jet production processes, $\text{IPROC}=92^{**}$, have been withdrawn since they are subsumed within $\text{IPROC}=91^{**}$.

The default limits on Q^2 in DIS processes ($\text{Q2MIN}, \text{Q2MAX}$) have been set very small/large ($0, 10^{10}$ GeV) and are reset to the kinematic limits unless changed by the user. This means the default Q2MIN is not suitable for simple neutral current DIS ($\text{IPROC}=9000$ etc), but is appropriate for jet and heavy quark photoproduction. The range of the Bjorken- y variable ($y = Q^2/xs$) can be limited by YBMIN and YBMAX .

The kinematic reconstruction of DIS processes can now take place in the Breit frame, if $\text{BREIT}=.TRUE.$ (the default value). Previous versions used the lab frame.

Although the reconstruction is fully invariant under Lorentz boosts along the incoming hadron's direction, it is not under transverse boosts, so there should be some difference between the two frames. The boost is not performed for very small $Q^2 (< 10^{-4})$ to avoid numerical instabilities, but the two frames are in any case equivalent for such small values.

The phase space for boson-gluon fusion is controlled by the parameters **EMMIN**, **EMMAX** (see section 4.3.4). The default values $(0, \sqrt{s})$ correspond to the behaviour of version 5.1.

Lepton beam polarization effects are included in all DIS processes apart from J/ψ production. The polarization is specified as in lepton-antilepton processes, i.e. by setting the 3-vectors **EPOLN** and **PPOLN**: component 3 is longitudinal and 1,2 transverse. Transverse only occurs in e^+e^- routines; recall that two transverse 'measurements' are needed to see an effect so it should not arise elsewhere. Note that in DIS processes one has to set either **EPOLN** if it is a lepton or (exclusive) **PPOLN** if an antilepton.

All the DIS processes **IPROC=9000–9599** are available in e^+e^- as well as lepton-hadron collisions. The program generates a photon from the second beam (only) in the Equivalent Photon Approximation and the default is to use Drees-Grassie [53,54] structure functions for DIS on the photon.

The parameter **WHMIN** sets the minimum allowed hadronic mass in DIS. In lepton-hadron DIS it is largely irrelevant since there is already a cut on Bjorken y which at fixed s is almost the same but for lepton-gamma DIS it makes a big difference.

In addition to the processes listed here, a full simulation of QCD instanton-induced processes in DIS [85] is available through an interface to the program **QCDINS** [86]. For details, see the web page <http://www.desy.de/~t00fri/qcdins/qcdins.html>

4.12.1 IPROC=9000–9006: neutral current

Matrix-element corrections to DIS are available, following the general method described in section 3.2.3. The hard correction is implemented in **HWBDIS** and the soft correction is included in routines **HWBRAN** and **HWSBRN** for the final- and initial-state radiation respectively.

4.12.2 IPROC=9010–9016: charged current

These are the charged current processes corresponding to those above, with the same treatment of hard and soft matrix element corrections.

4.12.3 IPROC=9100–9130: $\mathcal{O}(\alpha_s)$ neutral current processes

The photoproduction processes have been extended from the original heavy quark production program, to include all quark pair production (**IPROC=9100-9106**) and QCD Compton (**IPROC=9110–9122**), as well as the sum of the two (**IPROC=9130**). The possible flavours for processes 9100, 9110 and 9130 are limited by the input parameters **IFLMIN** and **IFLMAX** (defaults are 1 and 3, i.e. only u, d, s flavours).

A sign error has been corrected that led to the incorrect sign for the lepton-jet azimuthal correlation in QCD Compton processes in versions before 5.7.

J/ψ production (IPROC=9107) now uses the Equivalent Photon Approximation instead of Weizsacker-Williams, with the same phase-space cuts as hadronic processes with lepton beams (see section 4.1).

The argument of the running coupling is controlled by the parameter BGSAT — see section 6.

4.12.4 IPROC=9140–9144: charged-current heavy quark production

At present only $W^\pm g$ fusion processes are implemented.

4.12.5 IPROC=9500–9599: Higgs production by weak boson fusion

The process of W^+W^-/Z^0Z^0 fusion into the SM Higgs boson is also available in $e^\pm p$ collisions, as IPROC = 9500+ID. For details of the implementation, see section 3.4 and the corresponding processes initiated by lepton-lepton and hadron-hadron collisions, IPROC=400+ID and IPROC=1900+ID, respectively.

4.13 Including new subprocesses

The procedure for including further subprocesses remains substantially as described in ref. [1] but is repeated here for completeness. However, we now recommend that users make use of the Les Houches interface, see Section 9.1.

The parton and hard subprocess 4-momenta, masses and identity codes need to be entered in COMMON/HEPEVT/ with the appropriate status codes ISTHEP(I) = 110–114 to tell the program which is which (see the table in section 8.3.1). The colour/flavour structure should be specified by the second mother and daughter pointers as explained in section 4.6.2.

The HERWIG identity codes IDHW(I) in COMMON/HWEVNT/ also need to be set correctly. The IDHW codes can be listed in a run with IPRINT = 2: the most important are the quarks 1–6 (as IDHEP), antiquarks 7–12, gluon 13, overall centre-of-mass 14, hard centre-of-mass 15, soft centre-of-mass 16, photon 59, leptons 121–126, antileptons 127–132.

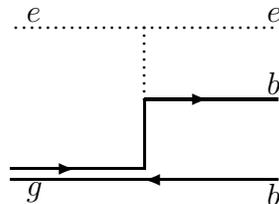
The utility subroutine HWUIDT(IOPT,IPDG,IHWG,NAME) is provided to translate between Particle Data Group code IPDG, HERWIG code IHWG, and HERWIG CHARACTER*8 NAME, with IOPT = 1, 2, 3 depending on which of IPDG, IHWG and NAME is the input argument.

Consider for example the process of virtual photon-gluon fusion to make $b + \bar{b}$ in proton-electron collisions (in fact this process is included as IPROC = 9105). We assume the user provides a subroutine to generate the momenta PHEP for the hard

| IHEP | Entry | ISTHEP | IDHEP | JMOHEP | JDAHEP | IDHW |
|------|-----------|--------|-------|--------|--------|------|
| 1 | e beam | 101 | 11 | 0 0 | 0 0 | 121 |
| 2 | p beam | 102 | 2212 | 0 0 | 0 0 | 73 |
| 3 | ep c.m. | 103 | 0 | 0 0 | 0 0 | 14 |
| 4 | e in | 111 | 11 | 6 7 | 0 7 | 121 |
| 5 | gluon | 112 | 21 | 6 9 | 0 8 | 13 |
| 6 | hard cm | 110 | 0 | 4 5 | 7 9 | 15 |
| 7 | e out | 113 | 11 | 6 4 | 0 4 | 121 |
| 8 | b | 114 | 5 | 6 5 | 0 9 | 5 |
| 9 | \bar{b} | 114 | -5 | 6 8 | 0 5 | 11 |

Table 17: Event record entries for $eg \rightarrow ebb\bar{b}$.

subprocess $e + g \rightarrow ebb\bar{b}$. The colour structure is



Thus the momenta generated, together with those of the initial beams and the overall centre of mass, could be entered in the sequence shown in table 17.

Note that if there are more than two outgoing partons, the first has status 113 and all the others 114. Each parton has $JMOHEP(1, I) = 6$ to indicate the location of the hard c.m. for this subprocess, while $JMOHEP(2, I)$ gives the location of the colour mother (treating the incoming gluon as outgoing) or the connected electron. $JDAHEP(1, I)$ will be set by the jet generator `HWBGEN`, while $JDAHEP(2, I)$ points to the anticolour mother (or connected electron). Finally the `HERWIG` identifiers $IDHW(I)$ could be set to the indicated values by means of the translation subroutine `HWUIDT` as follows:

```

CHARACTER*8 NAME
.....
NHEP=9
IDHEP(1)=11
IDHEP(2)=2212
.....
IDHEP(9)=-5
DO 10 I=1,NHEP
10 CALL HWUIDT(1, IDHEP(I), IDHW(I), NAME)
IDHW(6)=15

```

The last statement is needed because $IDPDG(I) = 0$ returns $IDHW(I) = 14$. If subroutine `HWBGEN` is now called, it will find the coloured partons and generate QCD jets from them. Subsequent calls to `HWCFOR` etc. can then be used to form clusters and hadronize them.

If the hard subprocess routine is called from `HWEPRO`, like those already provided, it must have two options controlled by the logical variable `GENEV` in `COMMON/HWHARD/`. For `GENEV = .FALSE.`, an event weight (normally the cross section in nanobarns) is generated and stored as `EVWGT` in `COMMON/HWEVNT/`. If this weight is accepted by `HWEPRO`, the subroutine is called a second time with `GENEV = .TRUE.` and the corresponding event data should then be generated and stored as explained above. On certain computers it will be necessary to `SAVE` those variables that determine event characteristics between the two subroutine calls.

The parameter `NMXJET` sets the maximum number of outgoing partons in a hard subprocess (default 200).

5. Parameters

The quantities that may be regarded as adjustable parameters are indicated in table 18. Notes on parameters are given below.

| Name | Description | Default |
|------------------------|---|-----------------------|
| <code>QC DLAM</code> | Λ_{QCD} (see below) | 0.18 |
| <code>RMASS(1)</code> | Down quark mass | 0.32 |
| <code>RMASS(2)</code> | Up quark mass | 0.32 |
| <code>RMASS(3)</code> | Strange quark mass | 0.50 |
| <code>RMASS(4)</code> | Charmed quark mass | 1.55 |
| <code>RMASS(5)</code> | Bottom quark mass | 4.95 |
| <code>RMASS(6)</code> | Top quark mass | 174.3 |
| <code>RMASS(13)</code> | Gluon effective mass | 0.75 |
| <code>VQCUT</code> | Quark virtuality cutoff (added to quark masses in parton showers) | 0.48 |
| <code>VGCUT</code> | Gluon virtuality cutoff (added to effective mass in parton showers) | 0.10 |
| <code>VPCUT</code> | Photon virtuality cutoff | 0.40 |
| <code>CLMAX</code> | Maximum cluster mass parameter | 3.35 |
| <code>CLPOW</code> | Power in maximum cluster mass | 2.00 |
| <code>PSPLT(1)</code> | Split cluster spectrum parameter | 1.00 |
| <code>PSPLT(2)</code> | 1: light cluster, 2 heavy b -cluster | <code>PSPLT(1)</code> |
| <code>QDIQK</code> | Maximum scale for gluon \rightarrow diquarks | 0.00 |
| <code>PDIQK</code> | Gluon \rightarrow diquarks rate parameter | 5.00 |
| <code>QSPAC</code> | Cutoff for spacelike evolution | 2.50 |
| <code>PTRMS</code> | Intrinsic p_T in incoming hadrons | 0.00 |

Table 18: Adjustable parameters.

- QCDLAM can be identified at high momentum fractions (x or z) with the fundamental 5-flavour QCD scale $\Lambda_{\overline{\text{MS}}}^{(5)}$. However, this relation does not necessarily hold in other regions of phase space, since higher order corrections are not treated precisely enough to remove renormalisation scheme ambiguities [13].
- RMASS(1, 2, 3, 13) are effective light quark and gluon masses used in the hadronization phase of the program. They can be set to zero provided the parton shower cutoffs VQCUT and VGCUT are large enough to prevent divergences (see below).
- For cluster hadronization, it must be possible to split gluons into $q\bar{q}$, i.e. RMASS(13) must be at least twice the lightest quark mass. Similarly it may be impossible for heavy-flavoured clusters to decay if RMASS(4, 5) are too low.
- VQCUT and VGCUT are needed if the quark and gluon effective masses become small. The condition to avoid divergences in parton showers is

$$\frac{1}{Q_i} + \frac{1}{Q_j} < \frac{1}{\text{QCDL3}}$$

for either i or j or both gluons, where $Q_i = \text{RMASS}(i) + \text{VQCUT}$ for quarks, $\text{RMASS}(13) + \text{VGCUT}$ for gluons, and QCDL3 is the three-flavour QCD scale used internally by HERWIG. QCDL3 is obtained by matching at the b - and c -quark mass scales from the internal five-flavour scale

$$\text{QCDL5} = \text{QCDLAM} \times \exp\left(\frac{151 - 9\pi^2}{138}\right) / \sqrt{2} = 1.109 \times \text{QCDLAM}.$$

Note that, in the notation of ref. [13] and section 3.2, $\text{QCDL5} = \Lambda_{\text{phys}} / \sqrt{2}$ for five flavours.

- VPCUT is the analogous quantity for photon emission. It now defaults to 0.4 GeV. Previous versions defaulted to \sqrt{s} , switching off such emission. Results after experimental cuts are insensitive to its exact value in the range 0.1 to 1.0 GeV.
- CLMAX and CLPOW determine the maximum allowed mass of a cluster made from quarks i and j as follows

$$M^{\text{CLPOW}} < \text{CLMAX}^{\text{CLPOW}} + (\text{RMASS}(i) + \text{RMASS}(j))^{\text{CLPOW}}.$$

Since the cluster mass spectrum falls rapidly at high mass, results become insensitive to CLMAX and CLPOW at large values of CLMAX. Smaller values of CLPOW will increase the yield of heavier clusters (and hence of baryons) for heavy quarks, without affecting light quarks much. For example, the default value gives no b -baryons whereas CLPOW = 1.0 makes b -baryons/ b -hadrons about 1/4.

- PSPLT determines the mass distribution in the cluster splitting $\mathcal{C}_1 \rightarrow \mathcal{C}_2 + \mathcal{C}_3$ when \mathcal{C}_1 is above the maximum allowed mass. The masses of \mathcal{C}_2 and \mathcal{C}_3 are generated uniformly in M^{PSPLT} . As long as the number of split clusters is small, dependence on PSPLT is weak.
- QDIQK greater than twice the lightest diquark mass enables non-perturbative gluon splitting into diquarks as well as quarks. The probability of this is $\text{PDIQK} \times dQ/Q$ for scales Q below QDIQK. The diquark masses are taken to be the sum of constituent quark masses. Thus the default value $\text{QDIQK} = 0$ suppresses gluon \rightarrow diquark splitting.
- QSPAC is the scale below which the structure functions of incoming hadrons are frozen and non-valence constituent partons are forced to evolve to valence partons, if $\text{ISPAC} = 0$. For $\text{ISPAC} = 2$, structure functions are frozen at scale QSPAC, but evolution continues down to the infrared cutoff.
- PTRMS is the width of the (gaussian) intrinsic transverse momentum distribution of valence partons in incoming hadrons at scale QSPAC.

In practice, the parameters that have been found most effective in fitting data are QC DLAM, the gluon effective mass $\text{RMASS}(13)$, and the cluster mass parameter CLMAX. Note that QSPAC, PTRMS and ENSOF do not affect lepton-lepton collisions.

The default parameter values are based on those that were found to give good agreement when comparing earlier versions with event shape distributions at LEP. However, the substantial changes in this version mean that a re-tuning of parameters would be very worthwhile.

Up-to-date details of HERWIG parameter tunes can be found via the official web page cited in section 2.

6. Control switches, constants and options

A number of quantities can be reset to control the program and various options:

| Name | Description | Default |
|--------|--|---------|
| NEVHEP | Current number of events | 0 |
| NHEP | Current number of entries in /HEPEVT/ | 0 |
| IPRINT | Information to include in print out | 1 |
| MAXPR | Number of events to print out | 1 |
| PRVTX | Include vertex information in print out | .TRUE. |
| NPRFMT | Controls number of sig. figs. in print out | 1 |
| PRNDEC | Use decimal/hexadecimal in print out | .TRUE. |
| PRNDEF | Produce ASCII (stout) version of print out | .TRUE. |
| PRNTEX | Produce L ^A T _E X version of print out | .FALSE. |

Table 19: Control switches, constants and options. (Continues)

| Name | Description | Default |
|-----------|---|---------|
| PRNWEB | Produce html version of print out | .FALSE. |
| MAXER | Maximum number of errors to tolerate | 10 |
| LWEVT | Unit for writing output events | 0 |
| LRSUD | Unit for reading Sudakov table | 0 |
| LWSUD | Unit for writing Sudakov table | 77 |
| SUDORD | α_S order in Sudakov table | 1 |
| INTER | Order of interpolation in Sudakov tables | 3 |
| NRN(1) | Random number seed 1 | 17673 |
| NRN(2) | Random number seed 2 | 63565 |
| WGTMAX | Max. weight (0 to search for it) | 0.0 |
| NOWGT | Generate unweighted events with EVWGT=AVWGT | .TRUE. |
| AVWGT | Mean event weight | 1.0 |
| EFFMIN | Min. acceptable Monte Carlo efficiency | 0.001 |
| NEGWTS | Whether or not to allow negative weight events | .FALSE. |
| AZSOFT | Include soft gluon azimuthal correlations | .TRUE. |
| AZSPIN | Include gluon spin azimuthal correlations | .TRUE. |
| HARDME | Use hard matrix-element corrections | .TRUE. |
| SOFTME | Use soft matrix-element corrections | .TRUE. |
| GCUTME | Gluon energy cut in top M.E. correction | 2.0 |
| NCOLO | Number of colours | 3 |
| NFLAV | Number of (producible) flavours | 6 |
| MODPDF(I) | PDFLIB parton set and author group for beam | -1 |
| AUTPDF(I) | I (=1,2) (if MODPDF < 0 do not use PDFLIB) | 'MRS' |
| NSTRU | Input parton set (1,2 = Duke-Owens sets 1,2; 3,4 = EHLQ sets 1,2; 5 = Owens set 1.1, 6,7,8 = MRST, see table 8) | 8 |
| PRSOFT | Probability of soft underlying event | 1.0 |
| ENSOF | Multiplicity enhancement for SUE: $n = \langle n_{p\bar{p}} \rangle (\text{ENSOF} \sqrt{s})$ | 1.0 |
| PMBN1 | Mean multiplicity in SUE/Min. bias event | +9.110 |
| PMBN2 | $\langle n_{p\bar{p}} \rangle (\sqrt{s}) = \text{PMBN1} s^{\text{PMBN2}} + \text{PMBN3}$ | +0.115 |
| PMBN3 | | -9.500 |
| PMBK1 | Negative binomial param. $k^{-1} = \text{PMBK1} \log_e(s) + \text{PMBK2}$ | +0.029 |
| PMBK2 | | -0.014 |
| PMBM1 | Soft cluster mass spectrum: $(M - M_1 - M_2 - \text{PMBM1}) e^{-\text{PMBM2}M}$ | 0.2 |
| PMBM2 | | 2.0 |

Table 19: Control switches, constants and options. (Continues)

| Name | Description | Default |
|----------------|--|-------------------------|
| PMBP1 | Soft cluster P_T spectrum: $p_T e^{-\text{PMBPi} \sqrt{p_T^2 + M^2}}$, | |
| | d, u quarks | 5.2 |
| PMBP2 | s, c quarks | 3.0 |
| PMBP3 | diquarks | 5.2 |
| IOPREM | Options for treatment of remnant clusters | 1 |
| BTCLM | Mass parameter in remnant fragmentation | 1.0 |
| VMIN2 | Min. parton virtuality ² in distance calcs. | 0.1 |
| CLRECO | Include colour rearrangement | .FALSE. |
| PRECO | Probability for rearrangement | 1/9 |
| EXAG | Lifetime scaling for weak bosons | 1.0 |
| ETAMIX | η/η' mixing angle in degrees | -23 |
| PHIMIX | ϕ/ω mixing angle in degrees | +36 |
| H1MIX | $h_1(1380)/h_1(1170)$ mixing angle in degrees | $\tan^{-1}(1/\sqrt{2})$ |
| F0MIX | $-/f_0(1370)$ mixing angle in degrees | $\tan^{-1}(1/\sqrt{2})$ |
| F1MIX | $f_1(1420)/f_1(1285)$ mixing angle in degrees | $\tan^{-1}(1/\sqrt{2})$ |
| F2MIX | f_2'/f_2 mixing angle in degrees | +26 |
| ET2MIX | $\eta_2(1645)/\eta_2(1870)$ mixing angle in degrees | $\tan^{-1}(1/\sqrt{2})$ |
| OMHMIX | $-/\omega(1600)$ mixing angle in degrees | $\tan^{-1}(1/\sqrt{2})$ |
| PH3MIX | ϕ_3/ω_3 mixing angle in degrees | +28 |
| B1LIM | B cluster \rightarrow 1 hadron parameter | 0.0 |
| CLDIR(I) | Decay orientation of perturbative clusters, 0: isotropic, 1: along quark direction | 1,1 |
| CLSMR(I) | Width of gaussian angle smearing, (I=1: light cluster, I=2: heavy b -cluster) | 0.0,0.0 |
| PWT(I) | A priori weights for $f\bar{f}$ -pairs in cluster decay, I=1-6: $f = d, u, s, c, b, t$ I=7: $f = qq'$ | 1.0 |
| REPWT(L, J, N) | A priori weight for $n^{(2S+1)}L_J$ mesons | 1.0 |
| SNGWT | A priori weight for singlet baryons | 1.0 |
| DECWT | A priori weight for decuplet baryons | 1.0 |
| PLTCUT | Minimum lifetime for particle to be set stable | 1.0×10^{-8} |
| VTOCDK(I) | Veto decay of clusters to hadron I | .FALSE. |
| VTOCDK(I) | Veto decay of resonances to hadron I I=290-293, $f_0(980), a_0(980)$ | .FALSE. .TRUE. |
| PIPSMR | Smear the primary vertex | .FALSE. |
| VIPWID(1) | x width (mm) | 0.25 |
| VIPWID(2) | y width (mm) | 0.015 |
| VIPWID(3) | z width (mm) | 1.8 |
| MAXDKL | Veto decays outside given volume | .FALSE. |

Table 19: Control switches, constants and options. (Continues)

| Name | Description | Default |
|------------|---|---|
| IOPDKL | Option for volume: 1=cylinder, 2=sphere | 1 |
| DXRCYL | Radius for cylindrical option (mm) | 20 |
| DXZMAX | Length for cylindrical option (mm) | 500 |
| DXRSPH | Radius for spherical option (mm) | 100 |
| BDECAY | Controls which B Decay package is used. Allowed values are: 'HERW', 'EURO' or 'CLEO' | 'HERW' |
| MIXING | Include neutral B meson mixing | .TRUE. |
| XMIX(1) | $\Delta M/\Gamma$ for B_s^0 | 10.0 |
| XMIX(2) | $\Delta M/\Gamma$ for B_d^0 | 0.7 |
| YMIX(1) | $\Delta\Gamma/2\Gamma$ for B_s^0 | 0.2 |
| YMIX(2) | $\Delta\Gamma/2\Gamma$ for B_d^0 | 0.0 |
| RMASS(198) | W^+ mass | 80.42 |
| RMASS(199) | W^- mass | RMASS(198) |
| GAMW | W^\pm width | 2.12 |
| RMASS(200) | Z^0 mass | 91.188 |
| GAMZ | Z^0 width | 2.495 |
| WZRFR | Use W/Z rest frame for decay parton showers | .TRUE. |
| MODBOS(I) | Force decay modes for weak bosons, see sect. 3.4 | 0 |
| RMASS(201) | SM Higgs mass | 115 |
| IOPHIG | Options for large Higgs mass distribution | 3 |
| GAMMAX | Limit on range of Higgs mass distribution | 10. |
| ENHANC(I) | Enhancement factor for SM Higgs decay mode I | 1.0 |
| RMASS(209) | Hypothetical 4th generation 'bottom' quark mass | 200. |
| RMASS(215) | corresponding antiquark mass | RMASS(209) |
| ALPHEM | Thompson limit value of $\alpha_{em}(0)$ | 0.0072993 |
| SWEIN | Value of $\sin^2 \theta_W$ | 0.2319 |
| QFCH(I) | Fermion electric charge I=1-6: d, \dots, t | |
| AFCH(I, J) | Fermion weak axial charge I=10-16: e, \dots, ν_τ | see sect. 4.2.2 |
| VFCH(I, J) | Fermion weak vector charge J=1: Z , J=2: Z' | |
| ZPRIME | Include a Z' in γ^*/Z^0 processes | .FALSE |
| RMASS(202) | Mass of the Z' | 500. |
| GAMZP | Width of the Z' | 5.0 |
| VCKM(I, J) | Cabibbo-Kobayashi-Maskawa matrix elements: $V_{KL}^2, K=1-3: u, c, t$ L=1-3: d, s, b | $\begin{pmatrix} 0.9512 & 0.0488 & 0 \\ 0.0488 & 0.9492 & 0.002 \\ 0 & 0.002 & 0.998 \end{pmatrix}$ |
| SCABI | Value of $\sin^2 \theta_{\text{Cabibbo}}$ | 0.0488 |
| EPOLN(1) | Electron and positron beam | 0.0 |
| EPOLN(2) | polarizations in DIS and e^+e^- | 0.0 |
| EPOLN(3) | annihilation. First two cmpts are | 0.0 |

Table 19: Control switches, constants and options. (Continues)

| Name | Description | Default |
|-----------|---|---------------|
| PPOLN(1) | transverse and only used in e^+e^- , | 0.0 |
| PPOLN(2) | 3rd cmpt is longitudinal, and is | 0.0 |
| PPOLN(3) | +/- 1 for fully rh/lh polarized | 0.0 |
| QLIM | Upper limit on hard process scale | 10^8 |
| THMAX | Max. value of thrust in IPROC=110–116 | 0.9 |
| Y4JT | Min. jet separation in IPROC=600–656 | 0.01 |
| DURHAM | Use Durham/JADE algorithm in IPROC=600–656 | .TRUE. |
| | Colour interferences in IPROC=600–656: | |
| IOP4JT(1) | $q\bar{q}gg$ 0: neglect, 1: extreme 3142, 2: extreme 4123 | 0 |
| IOP4JT(2) | $q\bar{q}q\bar{q}$ 0: neglect, 1: extreme 4123, 2: extreme 2143 | 0 |
| BGSHAT | Boson-gluon fusion scale (see below) | .TRUE. |
| BREIT | Use Breit frame for DIS kinematics | .TRUE. |
| USECMF | Use hadron-hadron c.m., | .TRUE. |
| NOSPAC | Switch off spacelike showers | .FALSE. |
| ISPAC | Changes meaning of QSPAC (see the earlier notes on QSPAC) | 0 |
| TMNISR | Min. value of \hat{s}/S for photon ISR | 10^{-4} |
| ZMXISR | Max. momentum fraction for photon ISR | $1 - 10^{-6}$ |
| ASFIXD | Values of fixed α_s and $\omega = 12 \log_e(2)\alpha_s/\pi$ | 0.25 |
| OMEGA | for Mueller-Tang cross section | 0.3 |
| IAPHIG | Approx. used in Higgs+jet production IPROC=2300-2312 | 1 |
| PHOMAS | Damp structure functions for off mass-shell photons (0 for no damping) | 0.0 |
| PRESPL | Preserve longitudinal momentum of hard c.m. | .TRUE. |
| PTMIN | Min. p_T in hadronic jet production | 10.0 |
| PTMAX | Max. p_T in hadronic jet production | 10^8 |
| PTPOW | $1/p_T^{\text{PTPOW}}$ for jet sampling | 4.0 |
| YJMIN | Min. jet rapidity | -8.0 |
| YJMAX | Max. jet rapidity | +8.0 |
| EMMIN | Min. dilepton mass in Drell-Yan | 10.0 |
| EMMAX | Max. dilepton mass in Drell-Yan | 10^8 |
| EMPOW | $1/m^{\text{EMPOW}}$ for Drell-Yan sampling | 4.0 |
| Q2MIN | Min. Q^2 in deep inelastic scattering | 0 |
| Q2MAX | Max. Q^2 in deep inelastic scattering | 10^{10} |
| Q2POW | $1/Q^{2\text{Q2POW}}$ for DIS sampling | 2.5 |
| YBMIN | Min. and max. Bjorken- y in DIS | 0.0 |
| YBMAX | | 1.0 |

Table 19: Control switches, constants and options. (Continues)

| Name | Description | Default |
|---------|--|--------------------------|
| WHMIN | Min. hadronic mass in γ -induced processes (inc. DIS) | 0.0 |
| ZJMAX | Max. z in J/ψ production | 0.9 |
| Q2WWMN | Min. and max. Q^2 in | 0.0 |
| Q2WWMX | Equivalent Photon Approximation | 4.0 |
| YWWMIN | Min. and max. photon light-cone fraction | 0.0 |
| YWWMAX | in Equiv. Photon Approx. | 1.0 |
| CSPEED | Speed of light in vacuum (mm/s) | 2.99792×10^{11} |
| GEV2NB | Value of $(\hbar c/e)^2$ | 389 379 |
| IBSH | Number of shots for initial max. weight search | 10 000 |
| IBRN(1) | 1st random number seed for max. weight search | 1246579 |
| IBRN(2) | 2nd random number seed for max. weight search | 8447766 |
| NQEV | Number of entries in Sudakov FF look-up table | 1024 |
| ZBINM | Max. bin size for z in spacelike branching | 0.05 |
| NZBIN | Max. number of z bins in spacelike branching | 100 |
| NBTRY | Max. number of attempts to branch a parton | 200 |
| NCTRY | Max. number of attempts to decay a cluster | 200 |
| NETRY | Max. number of attempts to generate a mass | 200 |
| NSTRY | Max. number of attempts at soft subprocess | 200 |
| ACCUR | Precision for soft gaussian integration | 10^{-6} |
| RPARTY | R-parity conservation in SUSY | .TRUE. |
| SUSYIN | Check to see if SUSY data are already loaded | .FALSE. |
| LRSUSY | Unit for reading SUSY data (if needed) | 66 |
| SYSPIN | Spin correlations in decays | .TRUE. |
| THREEB | SUSY three body decays | .TRUE. |
| FOURB | SUSY four body decays | .FALSE. |
| TAUDEC | Tau decay package (HERWIG or TAUOLA) | HERWIG |
| LHSOFT | Generation of soft event for Les Houches interface | .TRUE. |
| LHGLSF | Self-connected gluons for Les Houches interface | .FALSE. |
| OPTM | Optimisation of phase space | .FALSE. |
| IOPSTP | Number of steps for phase space optimisation | 10 |
| IOPSH | Number of weights for phase space optimisation | 1000 |

Table 19: Control switches, constants and options.

Printout options are listed in table 20.

The contents of /HEPEVT/ can be printed by calling HWUEPR, those of /HWPART/ (the last parton shower) by calling HWUBPR. The logical variable PRNDEC (default .TRUE. unless $NMXHEP > 9999$) causes track numbers in event listings to be printed

| | |
|------------|--|
| IPRINT = 0 | Print program title only |
| 1 | Print selected input parameters |
| 2 | 1 + table of particle codes and properties |
| 3 | 2 + tables of Sudakov form factors |

Table 20: Printout options.

in decimal, or hexadecimal if false. The latter is necessary for very large events such as those generated by the HERBVI package (see above).

The maximum number of errors `MAXER` refers to errors from which the program cannot recover without killing an event and starting a new one. Such errors are not necessarily a cause for grave concern because the phase space for backward evolution of initial-state showers is complicated and the program may occasionally step outside it (in which case the event weight should be zero anyway). When generating large numbers of events, it is advisable to increase `MAXER` in proportion, e.g. to `MAXEV/100`.

See section 8.2 on form factors for details of `LRSUD`, `LWSUD` and `SUDORD`.

The parameter `EFFMIN` sets the minimum allowed efficiency for the generation of unweighted events. A warning is printed once in every $10/\text{EFFMIN}$ weights if the efficiency is below $10 \times \text{EFFMIN}$, and running is stopped if the efficiency is below `EFFMIN`. See sect. 6.1 for details of `NEGWTS`.

Variables `HARDME` and `SOFTME` invoke hard and soft matrix-element corrections respectively, as described in subsection 3.2.3.

If `BGSHAT` is `.TRUE.`, the scale used for heavy quark production via boson-gluon fusion in lepton-hadron collisions will be the hard subprocess c.m. energy \hat{s} . If it is `.FALSE.`, the scale used will be

$$\frac{2 \hat{s} \hat{t} \hat{u}}{\hat{s}^2 + \hat{t}^2 + \hat{u}^2},$$

except in the case of $J/\psi + g$ production, where \hat{u} is used.

If `BREIT` is true, the kinematic reconstruction of deep inelastic events takes place in the Breit frame (i.e. the frame where the exchanged boson is purely spacelike, and collinear with the incoming hadron). In fact the reconstruction procedure is invariant under longitudinal boosts, so any frame in which the boson and hadron are collinear would be equivalent, and it is only the transverse part of the boost that has an effect. The `BREIT` frame option becomes very inaccurate for very small Q^2 . It is therefore only used if $Q^2 > 10^{-4}$ (the lab and Breit frames are anyway equivalent for such small Q^2). If `BREIT` is false, reconstruction takes place in the lab frame.

If `USECMF` is true, the entire event record is boosted to the hadron-hadron c.m. frame before event processing, and boosted back afterwards. This means that fixed-target simulation can be done in the lab frame, i.e. with `PBEAM2 = 0`. For hadronic processes with lepton beams, this boosting is always done, regardless of the value of `USECMF`.

In version 6.5, a new logical input variable, `PRESPL [.TRUE.]`, has been introduced to control whether the longitudinal momentum (`PRESPL = .TRUE.`), or rapidity (`PRESPL = .FALSE.`), of the hard process centre-of-mass is preserved in hadron collisions after initial-state parton showering. At present the only function of this variable is to allow users to study the effects of momentum reshuffling, which is necessary after showering to compensate for jet masses. In future, it is anticipated that setting `PRESPL=.FALSE.` will simplify the treatment of other processes in `MC@NLO` (see sect. 9.6).

The quantities from `PTMIN` to `ZJMAX` control the region of phase space in which events are generated and importance sampling inside those regions. See section 8.3.2 on event weights for further details on these quantities and the use of `WGTMAX` and `NOWGT`.

If hadronic processes with lepton beams are requested, the photon emission vertex includes the full transverse-momentum-dependent kinematics (the Equivalent Photon Approximation). The variables `Q2WWMN` and `Q2WWMX` set the minimum and maximum virtualities generated respectively. For normal simulation, `Q2WWMN` should be zero, and `Q2WWMX` should be the largest Q^2 through which the lepton can be scattered without being detected. The variables `YWWMIN` and `YWWMAX` control the range of lightcone momentum fraction generated.

In addition there are options to give different weights to the various flavours of quarks and diquarks, and to resonances of different spins. So far, these options have not been used. See the comments in the initialisation routine `HWIGIN` for details.

6.1 Negative weights option

In a number of new applications such as `MC@NLO` (see sect. 9.6), parton configurations with negative weight are used to produce more accurate predictions, and therefore the possibility of negative event weights has to be considered. In general, a Monte Carlo program generates N_w weights $\{w_i\}$ such that the estimated cross section is

$$\sigma = \frac{1}{N_w} \sum_{i=1}^{N_w} w_i \equiv \bar{w} . \quad (6.1)$$

The corresponding error depends on the width of the weight distribution:

$$\frac{\delta\sigma}{\sigma} = \frac{1}{\sqrt{N_w}} \frac{\delta w_{\text{rms}}}{\bar{w}} . \quad (6.2)$$

If only *positive weights* are generated, and there exists a maximum weight w_{max} , then *unweighted* events can be generated by ‘hit and miss’: $w'_i = 0$ or 1 with probability $P(w'_i = 1) = w_i/w_{\text{max}}$. Then

$$\frac{\delta\sigma}{\sigma} = \sqrt{\frac{w_{\text{max}} - \bar{w}}{N_w \bar{w}}} = \sqrt{\frac{w_{\text{max}} - \bar{w}}{N_e w_{\text{max}}}} \sim \frac{1}{\sqrt{N_e}} \quad (6.3)$$

where $N_e = N_w \overline{w} / w_{\max}$ is the number of *events* generated. The time needed (especially for detector simulation) depends mainly on the number of events. Hence the inefficiency of ‘hit and miss’ is not necessarily a disaster. This is the usual approach adopted in Monte Carlo event generators.

Negative weights can be generated by subtraction procedures for matrix element corrections. These are not a problem of principle but prevent naive ‘hit and miss’. To generalize ‘hit and miss’, one can generate unweighted events ($w'_i = 1$) and ‘antievnts’ ($w'_i = -1$) with

$$\text{sign}(w'_i) = \text{sign}(w_i) , \quad (6.4)$$

$$P(w'_i = \pm 1) = |w_i| / |w|_{\max} . \quad (6.5)$$

Then

$$\frac{\delta\sigma}{\sigma} = \sqrt{\frac{|\overline{w}| |w|_{\max} - \overline{w}^2}{N_w \overline{w}^2}} \sim \frac{1}{\sqrt{N_e}} \frac{|\overline{w}|}{\overline{w}} \quad (6.6)$$

where $N_e = N_w |\overline{w}| / |w|_{\max}$ is now the total number of *events+antievnts* generated. Again, the time needed is almost proportional to N_e , so this is tolerable as long as $|\overline{w}| \sim \overline{w}$. The cross section after any cuts that may be applied is

$$\sigma_c = \frac{|\overline{w}|}{N_e} (N_+ - N_-) \quad (6.7)$$

where N_+ events and N_- antievnts pass the cuts.

To allow for the possibility of negative weights, a new logical parameter `NEGWTS` has been introduced. The default (`NEGWTS=.FALSE.`) is as before: negative weights are forbidden. If one is detected, a non-fatal warning is issued and the event weight is set to zero.

If `NEGWTS=.TRUE.`, negative weights are allowed. Statistics are computed and printed accordingly. If unweighted events are requested (`NOWGT=.TRUE.`), the initial search stores the maximum and mean absolute weights, $|w|_{\max}$ and $|\overline{w}|$. Events and antievnts are selected according to Eqs. (6.4,6.5) and `EVWGT` is reset to $|\overline{w}| \text{sign}(w_i)$, so that the numerator in Eq. (6.7) is the sum of `EVWGTs` for contributing (anti)events.

7. Particle data

From `HERWIG` version 5.9 onwards, new 8-character particle names have been introduced and the revised 7 digit PDG numbering scheme, as advocated in the LEP2 report [26], has been adopted. All hadron and lepton masses are given to five significant figures whenever possible.

Unstable hadrons from clusters produced in both the hard and soft components of the event decay according to simplified decay schemes, which can be tabulated by specifying the print option `IPRINT = 2`. Decays modes are ‘invented’ where

| IDHW | RNAME | IDPDG | IDHW | RNAME | IDPDG |
|------|----------|-------|------|----------|-------|
| 395 | OMEGA_3 | 227 | 396 | PHI_3 | 337 |
| 397 | ETA_2(L) | 10225 | 398 | ETA_2(H) | 10335 |
| 399 | OMEGA(H) | 30223 | | | |

Table 21: New isoscalar states.

| IDHW | RNAME | IDPDG | IDHW | RNAME | IDPDG |
|------|---------|---------|------|-------|----------|
| 57 | FH_1 | 20333 | | | |
| 293 | FOP0 | 9010221 | 294 | FH_00 | 10221 |
| 62 | A_0(H)0 | 10111 | 290 | A_00 | 9000111 |
| 63 | A_0(H)+ | 10211 | 291 | A_0+ | 9000211 |
| 64 | A_0(H)- | -10211 | 292 | A_0- | -9000211 |

Table 22: Re-identified/replaced states.

necessary to make the branching ratios add up to 100%. Phase space distributions are assumed except where stated otherwise. See section 3.3 for the treatment of heavy quark decays. After a t , partonic b or quarkonium decay, secondary parton showers are produced by outgoing partons as discussed in ref. [11]; these are hadronized in the same way as primary jets.

There have been a number of additions/changes to the default hadrons included via HWUDAT. Here the identification of hadrons follows the PDG [38, table 13.2], numbered according to their section 30.

All S and P wave mesons are present including the 1P_0 and 3P_1 states and many new, excited B^{**} , B_c and quarkonium states. Also all D wave kaons and some ‘light’ $I=3$ states [π_2 , $\rho(1700)$ and ρ_3]. All the baryons (singlet/octet/decuplet) containing up to one heavy (c, b) quark are included.

New isoscalars states have been added to try to complete the 1^3D_3 , 1^1D_2 and 1^3D_1 multiplets (table 21).

Also the states in table 22 have been redefined. The $f_1(1420)$ state completely replaces the $f_1(1520)$ in the 1^3P_0 multiplet, taking over 57. The $f_0(1370)$ (294) replaces the $f_0(980)$ (293) in the 1^3P_0 multiplet; the latter is retained as it appears in the decays of several other states. The new $a_0(1450)$ states (62–64) replace the three old $a_0(980)$ states (290–292) in the 1^3P_0 multiplet; the latter are kept as they appear in $f_1(1285)$ decays.

| | |
|--------|-------------------------|
| ETAMIX | η/η' , |
| PHIMIX | ω/ϕ , |
| H1MIX | $h_1(1170)/h_1(1380)$, |
| F0MIX | $f_0(1300)/f_0(980)$, |
| F1MIX | $f_1(1285)/f_1(1510)$, |
| F2MIX | f_2/f_2' . |

Table 23: Mixing angles.

By default production of the $f_0(980)$ and $a_0(980)$ states in cluster decays is vetoed.

The mixing angles (in degrees) of all the light, $I=0$ mesons can now be set using table 23.

There were previously some inconsistencies and ambiguities in our conventions for the mixing of flavour ‘octet’ and ‘singlet’ mesons. They are now as in table 24.

| Multiplet | Octet | Singlet | Mixing Angle |
|-----------|----------------|----------------|-----------------|
| 1^1S_0 | η | η' | ETAMIX= -23 . |
| 1^3S_1 | ϕ | ω | PHIMIX= $+36$. |
| 1^1P_1 | $h_1(1380)$ | $h_1(1170)$ | H1MIX=ANGLE |
| 1^3P_0 | missing | $f_0(1370)$ | F0MIX=ANGLE |
| 1^3P_1 | $f_1(1420)$ | $f_1(1285)$ | F1MIX=ANGLE |
| 1^3P_2 | f_2' | f_2 | F2MIX= $+26$. |
| 1^1D_2 | $\eta_2(1645)$ | $\eta_2(1870)$ | ET2MIX=ANGLE |
| 1^3D_1 | missing | $\omega(1600)$ | OMHMIX=ANGLE |
| 1^3D_3 | ϕ_3 | ω_3 | PH3MIX= $+28$. |

Table 24: Mixed meson states.

After mixing, the quark content of the physical states is given in terms of the mixing angle, θ , by table 25 where $\tan\theta_0 = \sqrt{2}$.

Hence, using the default value of ANGLE = $\arctan(1/\sqrt{2}) = +35.3$ for θ gives ideal mixing, that is, the ‘octet’ state = $s\bar{s}$ and the ‘singlet’ = $(d\bar{d} + u\bar{u})/\sqrt{2}$. This choice is important to avoid large isospin violations in the 1^3P_0 and 1^3D_1 multiplets in which the octet member is unknown.

| State | $(d\bar{d} + u\bar{u})/\sqrt{2}$ | $s\bar{s}$ |
|---------|----------------------------------|----------------------------|
| Octet | $\cos(\theta + \theta_0)$ | $-\sin(\theta + \theta_0)$ |
| Singlet | $\sin(\theta + \theta_0)$ | $\cos(\theta + \theta_0)$ |

Table 25: Quark content of mixed states.

Since version 6 contains a large number of supersymmetry processes many new hypothetical particles have been added — see section 3.5. These new states do not interfere with the user’s ability to add new particles as described below.

The resonance decay tables supplied in the program have also been largely revised. Measured/expected modes with branching fraction at or above 1 per mille are given, including 4 and 5 body decays. To print the new tables call HWUDPR.

The layout of HWUDAT has been altered to make it easier to identify and modify particle properties. Three new arrays have been introduced RLTIM, RSPIN and IFLAV. These are: the particle’s lifetime (s), spin, and a code which specifies the flavour content of each hadron — used (in HWURES) to create sets of iso-flavour hadrons for cluster decay. Using the standard numbering of quark flavours the convention is:

- Mesons: $n_q n_{\bar{q}}$, e.g. π^+ : 21, π^- : 12;
- Baryons: $\pm n_{q1} n_{q2} n_{q3}$, e.g. Ξ^0 : 332, $\bar{\Xi}^0$: -332 etc. (< 0 for antibaryons; digits in decreasing order);
- Light, neutral mesons are identified as: 11 if isovector (π^0, ρ^0, \dots), 33 if isoscalar (η, η', \dots).

Some parts of the program have been automated so that it is possible for the user to add new particles by specifying their properties via the arrays in /HWPROP/ and /HWUNAM/ and increasing NRES appropriately: this should be done before a call to HWUINC.

As an example, the following lines add an isoscalar, spin-2 state 'STAN' and a (very light) stable toponium state 'BEER' with the decay mode: $STAN \rightarrow BEER + BEER + BEER$.

```

NRES=NRES+1
RNAME(NRES)='STAN      '
IDPDG(NRES)=666
IFLAV(NRES)=11
ICHRG(NRES)=0.
RMASS(NRES)=0.5
RLTIM(NRES)=1.000D-10
RSPIN(NRES)=2.0
NRES=NRES+1
RNAME(NRES)='BEER      '
IDPDG(NRES)=66
IFLAV(NRES)=66
ICHRG(NRES)=0.
RMASS(NRES)=0.1
RLTIM(NRES)=1.000D+30
RSPIN(NRES)=0.0
CALL HWMODK(666,1.D0,0,66,66,66,0,0)

```

Using the logical arrays VTOCDK and VTORDK the production of specified particles can be stopped in both cluster decays and via the decay of other unstable resonances.

A priori weights for the relative production rates in cluster decays of mesons and baryons differing only via their S and L quantum numbers can be supplied using SNGWT and DECWT for singlet (i.e. Λ -like) and decuplet baryons and REPWT for mesons. The old VECWT now corresponds to REPWT(0,1,0) and TENWT to REPWT(0,2,0).

The arrays FBTM, FTOP and FHVY which stored the branching fractions of the bottom, top and heavier quarks' 'partonic' decays are now no longer used. Such decays are specified in the same way as all other decay modes: this permits different decays to be given to individual heavy hadrons. Partonic decays of charm hadrons and quarkonium states are also now supported. As already mentioned, the products' order in a partonic decay mode is significant: see discussion in section 3.3.

The structure of the program has been altered so that the secondary hard sub-process and subsequent fragmentation associated with each partonic heavy hadron decay appears separately. Thus pre-hadronization top quark decays are treated individually, as are any subsequent bottom hadron partonic decays.

Additionally decays of heavy hadrons to exclusive non-partonic final states are supported. No check against double counting from partonic modes is included. However this is not expected to be a major problem for the semi-leptonic and 2-body hadronic modes supplied.

B decays can also be performed by the EURODEC or CLEO Monte Carlo packages. The new variable BDECAY controls which package is used: 'HERW' for HERWIG; 'EURO' for EURODEC; 'CLEO' for CLEO. The EURODEC package can be obtained from the CERN library. The CLEO package is available by kind permission of the CLEO collaboration.

An array NME has been introduced to enable a possible matrix element to be specified for each decay mode.

- NME = 0: Isotropic decay.
- NME = 100: Free particle $(V - A) * (V - A), (p_0 \cdot p_2)(p_1 \cdot p_3)$.
- NME = 101: Bound quark $(V - A) * (V - A), (p_0 \cdot p_2)(p_1 \cdot [p_3 - x_s p_0])$, $x_s = m_Q/M_0 =$ spectator quark momentum fraction.
- NME = 130: Ore and Powell ortho-positronium matrix element for: onium $\rightarrow gg + g/\gamma$.
- NME = 200: Free-particle $t \rightarrow b$ quark decay through a scalar-fermion-fermion current.
- NME = 300: Gaugino and gluino three-body \mathcal{R}_p decays. This also implements the angular ordering procedure in the \mathcal{R}_p gluino decays.

The list of matrix elements currently supported is modest; users are urged to contact an author to have others implemented. It should be noted however that a number of additional matrix elements are now available via the spin correlation algorithm.

A Z' has been introduced with PDG code 32, HERWIG identifier 202, default mass 500 GeV, width GAMZP (default 5 GeV) and name 'ZOPR '. It is invoked by setting ZPRIME=.TRUE. (default .FALSE.).

The decay tables can be written to/read from a file by using HWIODK, adopting the format advocated in the LEP2 report [26]. In addition to the PDG numbering of particles the HERWIG numbers or character names can be used. This permits easy alteration of the decay tables. In HWUINC a call is made to HWUDKS which sets up HERWIG internal pointers and performs some basic checks of the decay tables. Each decay mode must conserve charge and be kinematically allowed and not contain vetoed decay products. The sum of all branching ratios is set to 1 for all particles. Also a warning is printed if an antiparticle does not have all the charge conjugate decays modes of the particle.

HWMODK enables changes to the decay tables to be made by altering or adding single decay modes including on an event-by-event basis. This can be done before calling HWUINC, in which case when altering the branching ratio and/or matrix element code of an existing mode a warning is given of a duplicate second mode which superseeds the first. Branching ratios set below 10^{-6} are eliminated, whilst if one mode is within 10^{-6} of unity all other modes are removed. Note that some forethought is required if the branching ratios of two modes of the same particle are changed since the operation of rescaling the branching ratio sum to unity causes a non-commutativity in the order of the calls.

It is possible to create particle property and event listings in any combination of 3 formats — standard ASCII, L^AT_EX or html. These options are controlled by the logical variables PRNDEF (default .TRUE.) PRNTEX (default .FALSE.) and PRNWEB (default .FALSE.). The ASCII output is directed to stout (screen/log file) as in previous versions. When a listing of particle properties is requested (IPRINT.GE.2 or HWUDPR is called explicitly) then the following files are produced:

```

If (PRNTEX): HW_decays.tex
If (PRNWEB): HW_decays/index.html
              /PART0000001.html etc.

```

The HW_decays.tex file is written to the working directory whilst the many **.html files appear in the sub-directory HW_decays/ which must have been created previously. Paper sizes and offsets for the L^AT_EX output are stored at the top of the block data file HWUDAT: they may need modifying to suit a particular printer. When event listings are requested (NEVHEP.LE.MAXPR or HWUEPR is called explicitly) the following files are created in the current working directory:

```

If (PRNTEX): HWEV_*****.tex
If (PRNWEB): HWEV_*****.html

```

where *****=0000001 etc. is the event number.

Note that the html file automatically makes links to the index.html file of particle properties, assumed to be in the HW_decays sub-directory.

A new integer variable NPRFMT (default 1) has been introduced to control how many significant figures are shown in each of the 3 event outputs. Basically NPRFMT=1 gives short compact outputs whilst NPRFMT=2 gives long formats.

Note that all the L^AT_EX files use the package longtable.sty to format the tables. Also if NPRFMT=2 or PRVTX=.TRUE. then the L^AT_EX files are designed to be printed in landscape mode.

8. Structure and output

8.1 Main program

The main program HWIGPR has the following form:

```
PROGRAM HWIGPR
C---COMMON BLOCKS ARE INCLUDED AS FILE HERWIG65.INC
  INCLUDE 'HERWIG65.INC'
  INTEGER N
  EXTERNAL HWUDAT
C---MAX NUMBER OF EVENTS THIS RUN
  MAXEV=100
C---BEAM PARTICLES
  PART1='P'
  PART2='P'
C---BEAM MOMENTA
  PBEAM1=7000.
  PBEAM2=PBEAM1
C---PROCESS
  IPROC=3000
C---INITIALISE OTHER COMMON BLOCKS
  CALL HWIGIN
C---USER CAN RESET PARAMETERS AT
C THIS POINT, OTHERWISE DEFAULT
C VALUES IN HWIGIN WILL BE USED.
  PRVTX=.FALSE.
  MAXER=MAXEV/100
  MAXPR=0
  PTMIN=100.
C N.B. TO READ SUDAKOV FORM FACTOR FILE ON UNIT 77
C INSERT THE FOLLOWING TWO LINES IN SUBSEQUENT RUNS
C   LRSUD=77
C   LWSUD=0
C---READ IN SUSY INPUT FILE, IN THIS CASE LHC SUGRA POINT 2
  OPEN(UNIT=LRSUSY,FORM='FORMATTED',STATUS='OLD',ERR=999,
&     FILE='sugra_pt2.1200.in')
  CALL HWISSP
  CLOSE(UNIT=LRSUSY)
C---COMPUTE PARAMETER-DEPENDENT CONSTANTS
  CALL HWUINC
C---CALL HWUSTA TO MAKE ANY PARTICLE STABLE
  CALL HWUSTA('PIO  ')
C---USER'S INITIAL CALCULATIONS
  CALL HWABEG
```

```

C---INITIALISE ELEMENTARY PROCESS
      CALL HWEINI
C---LOOP OVER EVENTS
      DO 100 N=1,MAXEV
C---INITIALISE EVENT
      CALL HWUINE
C---GENERATE HARD SUBPROCESS
      CALL HWEPRO
C---GENERATE PARTON CASCADES
      CALL HWBGEN
C---DO HEAVY OBJECT DECAYS
      CALL HWDHOB
C---DO CLUSTER FORMATION
      CALL HWCFOR
C---DO CLUSTER DECAYS
      CALL HWCDEC
C---DO UNSTABLE PARTICLE DECAYS
      CALL HWDHAD
C---DO HEAVY FLAVOUR HADRON DECAYS
      CALL HWDHVV
C---ADD SOFT UNDERLYING EVENT IF NEEDED
      CALL HWMEVT
C---FINISH EVENT
      CALL HWUFNE
C---USER'S EVENT ANALYSIS
      CALL HWANAL
      100 CONTINUE
C---TERMINATE ELEMENTARY PROCESS
      CALL HWEFIN
C---USER'S TERMINAL CALCULATIONS
      CALL HWAEND
      STOP
999  WRITE (6,*)
      WRITE (6,*) 'SUSY input file did not open correctly.'
      WRITE (6,*) 'Please check that it is in the right place.'
      WRITE (6,*) 'Examples can be obtained from the ISAWIG web page.'
      WRITE (6,*)
      END

```

The declaration `EXTERNAL HWUDAT` is recommended to help the linker with finding the block data on some systems.

Various phases of the simulation can be suppressed by deleting the corresponding subroutine calls, or different subroutines may be substituted. For example, in non-

SUSY studies the call to `HWISEP` should be omitted, and in studies at the parton level everything from `CALL HWCFOR` to `CALL HWMEVT` can be omitted.

Note that the functionality of the routine `HWUINE` in earlier versions has now been split between it and a new routine, `HWUFNE`. A call to the latter *must* be made between the calls to `HWMEVT` and `HWANAL`. A check is built in to prevent execution if this is not done.

The analysis routine `HWANAL` should always begin with the line

```
IF (IERROR.NE.0) RETURN
```

since if an event is cancelled, each of the routines is still called in turn until reaching the end of the main loop.

8.2 Form factor file

HERWIG uses look-up tables of Sudakov form factors for the evolution of initial- and final-state parton showers. These can be read from an input file rather than being recomputed each time. The reading, writing and computing of form factor tables is controlled by integer parameters `LRSUD` and `LWSUD` (table 26).

| | |
|-------------------------------|---|
| <code>LRSUD = N > 0</code> | Read form factors for this run from unit N |
| <code>LRSUD = 0</code> | Compute new form factor tables for this run |
| <code>LRSUD < 0</code> | Form factor tables are already loaded |
| <code>LWSUD = N > 0</code> | Write form factors on unit N for future use |
| <code>LWSUD = 0</code> | Do not write new form factor tables |

Table 26: Form factor read/write options.

The option `LRSUD < 0` allows the program to be initialised several times in the same run (e.g. to generate various event types) without recomputing or rereading form factors.

Note that the Sudakov form factors depend on the parameters `QC DLAM`, `VQCUT`, `VGCUT`, `NCOLO`, `NFLAV`, `RMASS(13)` and `RMASS(i)` for $i = 1, \dots, \text{NFLAV}$. Consequently form factor tables *must* be recomputed every time any of these parameters is changed. These parameters are written/read with the form factor tables and checks are performed to ensure consistency.

The parton showering algorithm uses the two-loop running coupling, with matching at each flavour threshold. However, the Sudakov table can be computed with either the one-loop or two-loop form, according to the variable `SUDORD` ($= 1$ or 2 respectively, default= 1). If `SUDORD = 1` the two-loop value is recovered using the veto algorithm in the shower, whereas if `SUDORD = 2` no vetoes are used in the final-state evolution. This means that the relative weight of any shower configuration can be calculated in a closed form, hence that showers can be ‘forced’.

To next-to-leading order the two possibilities should be identical, but they differ at beyond-NLO, so some results may change a little. The most noticeable difference is that the form factor table takes a factor of about five times longer to compute with `SUDORD = 2` than with 1.

When `SUDORD=2`, no veto is needed for gluon splitting to quarks. This means that no vetoes are needed for final state showering, except for the previously-mentioned transverse momentum cut. The removal of vetoes allows preselection of the flavours that a jet will contain, giving a huge increase in the efficiency of rare process simulation [87].

8.3 Event data

`/HEPEVT/` is the LEP standard common block containing current event data (table 27).

| | |
|---------------------------|--|
| <code>NEVHEP</code> | event number |
| <code>NHEP</code> | number of entries for this event |
| <code>ISTHEP(I)</code> | status of entry I (see below) |
| <code>IDHEP(I)</code> | identity of entry I (Particle Data Group code) |
| <code>JMOHEP(1, I)</code> | pointer to first mother of entry I (see below) |
| <code>JMOHEP(2, I)</code> | pointer to second mother of entry I (see below) |
| <code>JDAHEP(1, I)</code> | pointer to first daughter of entry I (see below) |
| <code>JDAHEP(2, I)</code> | pointer to last daughter of entry I (see below) |
| <code>PHEP(*, I)</code> | (p_x, p_y, p_z, E, M) of entry I: $M = \text{sign}(\sqrt{\text{abs}(m^2)}, m^2)$ |
| <code>VHEP(*, I)</code> | (x, y, z, t) of production vertex of entry I (see sect. 3.8) |

Table 27: Current event data.

All momenta are given in GeV/c in the laboratory frame, in which the input beam momenta are `PBEAM1` and `PBEAM2` as specified by the user and point along the $+z$ and $-z$ directions respectively. Final state particles have `ISTHEP(I) = 1`. See section 8.3.1 for a complete list of the special status codes used by `HERWIG`.

The identity codes `IDHEP` are almost as recommended by the LEP Working Group [26], i.e. the revised PDG [38] numbers where defined, `IDHEP = 91` for clusters, 94 for jets, and 0 for objects with no PDG code. The only exception is our use of `IDHEP = 26` for the lightest MSSM Higgs boson, to distinguish it from the SM Higgs boson (PDG code 25). In addition, the ‘generator-specific’ (`IDHEP=81-100`) codes 98 and 99 are used for remnant photons and nucleons, respectively (see section 3.7.2).

`HERWIG` also has its own internal identity codes `IDHW(I)`, stored in `/HWEVNT/`. The utility subroutine `HWUIDT` translates between `HERWIG` and PDG identity codes. See section 4.13 for further details.

The mother and daughter pointers are standard, except that `JMOHEP(2, I)` and `JDAHEP(2, I)` for a *parton* are its *colour mother* and *colour daughter*, i.e. the partons to which its colour and anticolour are connected, respectively. For this purpose the primary partons from a hard subprocess are all regarded as outgoing (see examples in section 4.6.2, 4.13 and 8.5.1). Since a quark has no anticolour, `JDAHEP(2, I)` is used to point to its *flavour* partner. Similarly for `JMOHEP(2, I)` in the case of an antiquark.

In addition to entries representing partons, particles, clusters etc, `/HEPEVT/` contains purely informational entries representing the total centre-of-mass momentum, hard and soft subprocess momenta, etc. See section 8.3.1 for the corresponding status codes.

Information from all stages of event processing is retained in `/HEPEVT/` so the same particle may appear several times with different status codes. For example, an outgoing parton from a hard scattering (entered initially with status 113 or 114) will appear after processing as an on-mass-shell parton before QCD branching (status 123,124), an off-mass-shell entry representing the flavour and momentum of the outgoing jet (status 143,144), and a jet constituent (157). It might also appear again in other contexts, e.g. as a spectator in a heavy flavour decay (status 154,160).

Incoming partons (entered with status 111 or 112, changed to 121 or 122 after branching) give rise to spacelike jets (status 141 or 142) with $m^2 < 0$, indicated by `PHEP(5, IHEP) < 0`, due to the loss of momentum via initial-state bremsstrahlung. The same applies in principle to incoming leptons, but in that case emission of at most a single photon is permitted from each initial-state lepton and the off-shell lepton is given status code 3 (see section 8.3.1).

Each parton jet begins with a status 141–144 jet entry giving the total flavour and momentum of the jet. The first mother pointer of this entry gives the location of the parent hard parton, while the second gives that of the subprocess centre-of-mass momentum. If QCD branching has occurred, this is followed by a lightlike `CONE` entry, which fixes the angular extent of the jet and its azimuthal orientation relative to the parton with which it interferes. The interfering parton is listed as the second mother of the cone. Next come the actual constituents of the jet. If no branching has occurred, there is no cone and the single jet constituent is the same as the jet.

Since version 5.1, the event record has been modified to retain entries for all partons before hadronization (with status `ISTHEP=2`). During hadronization, the gluons are split into quark-antiquark, while other partons are copied to a location (indicated by `JDAHEP(1,*)`) where their momenta may be shifted slightly, to conserve momentum, during heavy cluster splitting. Previously the original momenta were shifted, so momentum appeared not to be conserved at the parton level.

Since version 6.3, to take account of the increased energy and complexity of interactions at LHC and future colliders, the default value of the parameter `NMXHEP`, which sets the array sizes in the standard `/HEPEVT/` common block, has been increased to

4000.

8.3.1 Status codes

A complete list of currently-used **HERWIG** status codes is given below (table 28). Many are used only in intermediate stages of event processing. The most important for users are probably 1 (final-state particle), 101–3 (initial state), 141–4 (jets), and 199 (decayed b -flavoured hadrons).

For technical reasons, some **HERWIG** status codes **ISTHEP** between 153 and 165 have changed their meanings since version 5.1.

The event status **ISTAT** in common `/HWEVNT/` is roughly $\text{ISTHEP} - 100$ where **ISTHEP** is the status of entries being processed. For completed events, $\text{ISTAT} = 100$.

| ISTHEP | Description |
|--------|---|
| 1 | final state particle |
| 2 | parton before hadronization |
| 3 | documentation line |
| 100 | cone limiting jet evolution |
| 101 | ‘beam’ (beam 1) |
| 102 | ‘target’ (beam 2) |
| 103 | overall centre of mass |
| 110 | unprocessed hard process c.m. |
| 111 | unprocessed beam parton |
| 112 | unprocessed target parton |
| 113 | unproc. first outgoing parton |
| 114 | unproc. other outgoing parton |
| 115 | unprocessed spectator parton |
| 120–25 | as 110–15, after processing |
| 130 | lepton in jet (unboosted) |
| 131–34 | as 141–44, unboosted to c.m. |
| 135 | spacelike parton (beam, unboosted) |
| 136 | spacelike parton (target, unboosted) |
| 137 | spectator (beam, unboosted) |
| 138 | spectator (target, unboosted) |
| 139 | parton from branching (unboosted) |
| 140 | parton from gluon splitting (unboosted) |
| 141–44 | jet from parton type 111–14 |
| 145–50 | as 135–40 boosted, unclustered |
| 151 | as 159, not yet clustered |
| 152 | as 160, not yet clustered |
| 153 | spectator from beam |

Table 28: Status codes. (Continues)

| ISTHEP | Description |
|--------|--|
| 154 | spectator from target |
| 155 | heavy quark before decay |
| 156 | spectator before heavy decay |
| 157 | parton from QCD branching |
| 158 | parton from gluon splitting |
| 159 | parton from cluster splitting |
| 160 | spectator after heavy decay |
| 161 | beam spectator after gluon splitting |
| 162 | target spectator after gluon splitting |
| 163 | other cluster before soft process |
| 164 | beam cluster before soft process |
| 165 | target cluster before soft process |
| 167 | unhadronized beam cluster |
| 168 | unhadronized target cluster |
| 170 | soft process centre of mass |
| 171 | soft cluster (beam, unhadronized) |
| 172 | soft cluster (target, unhadronized) |
| 173 | soft cluster (other, unhadronized) |
| 181 | beam cluster (no soft process) |
| 182 | target cluster (no soft process) |
| 183 | hard process cluster (hadronized) |
| 184 | soft cluster (beam, hadronized) |
| 185 | soft cluster (target, hadronized) |
| 186 | soft cluster (other, hadronized) |
| 190–93 | as 195–98, before decays |
| 195 | direct unstable non-hadron |
| 196 | direct unstable hadron (1-body clus.) |
| 197 | direct unstable hadron (2-body clus.) |
| 198 | indirect unstable hadron or lepton |
| 199 | decayed heavy flavour hadron |
| 200 | neutral B meson, flavour at prod'n |

Table 28: Status codes.

8.3.2 Event weights

The default is to generate unweighted events ($EVWGT = AVWGT$). Then event distributions are generated by computing a weight proportional to the cross section and comparing it with a random number times the maximum weight. Set $WGTMAX$ to the maximum weight, or to zero for the program to compute it. If a weight greater than

WGTMAX is generated during execution, a warning is printed and WGTMAX is reset. If this occur too often, output event distributions could be distorted.

To generate weighted events, set NOWGT = .FALSE. in common /HWEVNT/.

In QCD hard scattering and heavy flavour and direct photon production (IPROC=1500–1800) the transverse energy distribution of weighted events (or the efficiency for unweighted events) can be varied using the parameters PTMIN, PTMAX and PTPOW.

Similarly in Drell-Yan processes (IPROC = 1350 etc.) the lepton pair mass distribution is controlled by the parameters EMMIN, EMMAX and EMPow, and in deep inelastic scattering the Q^2 distribution depends on Q2MIN, Q2MAX and Q2POW.

Data on weights generated are output at the end of the run. The mean weight is an estimate of the cross section (in nanobarns) integrated over the region used for event generation. Note that the mean weight is the sum of weights divided by the total number of *weights* generated, not the total number of *events*.

The maximum weight is now always printed in full precision. This is needed to be sure of generating the same events in repeated runs.

In versions 6.3 and higher, the option of generating negative weights has been available. This is controlled by the input parameter NEGWTS [.FALSE.], see sect. 6.1 for details.

8.4 Error conditions

Certain combinations of input parameters may lead to problems in execution. HERWIG tries to detect these and print a warning. Errors during execution are dealt with by HWWARN, which prints the calling subprogram and a code and takes appropriate action. In general, the larger the code the more serious the problem. Refer to the source code to find out why HWWARN was called. It is important to note the subprogram from which the call was issued: many different subprograms use the same error code, but each code is unique within a given subprogram.

Events can be rerun by setting the random number seeds NRN(1) and NRN(2) to the values given in the error message or event dump, and MAXWGT to the maximum weight encountered in the run. The contents of /HEPEVT/ can be printed by calling HWUEPR, those of /HWPART/ (the last parton shower) by calling HWUBPR.

Note that if WGTMAX is increased during event generation, so that this type of message is printed:

```
HWWARN CALLED FROM SUBPROGRAM HWEPRO: CODE = 1
EVENT      21:  SEEDS = 836291635 & 1823648329  WEIGHT = 0.3893E-08
EVENT SURVIVES. EXECUTION CONTINUES
          NEW MAXIMUM WEIGHT = 0.428217360829367E-08
```

then to regenerate any later events, WGTMAX must be set to the printed value, as well as setting NRN to the appropriate seeds.

Examples of error messages are:

```
HWWARN CALLED FROM SUBPROGRAM HWSBRN: CODE = 101
EVENT      31:  SEEDS = 422399901 & 771980111  WEIGHT = 0.3893E-08
EVENT KILLED.  EXECUTION CONTINUES
```

Spacelike (initial-state) parton branching had no phase space. This can happen due to cutoffs which are slightly different in the hard subprocess and the parton shower. Action taken: program throws away this event and starts a new one.

```
HWWARN CALLED FROM SUBPROGRAM HWCHAD: CODE = 102
EVENT      51:  SEEDS = 1033784787 & 1428957533  WEIGHT = 0.3893E-08
EVENT KILLED.  EXECUTION CONTINUES
```

A cluster has been formed with too low a mass to represent any hadron of the correct flavour, and there is no colour-connected cluster from which the necessary additional mass could be transferred.

Action taken: program throws away this event and starts a new one.

```
HWWARN CALLED FROM SUBPROGRAM HWUINE: CODE= 200
EVENT SURVIVES.  RUN ENDS GRACEFULLY
```

CPU time limit liable to be reached before generating MAXEV events.

Action taken: skips to terminal calculations using existing events.

```
HWWARN CALLED FROM SUBPROGRAM HWBSUD: CODE= 500
RUN CANNOT CONTINUE
```

The table of Sudakov form factors read on unit LRSUD does not extend to the maximum momentum scale QLIM specified for this run.

Action taken: run aborted. The user must either reduce QLIM or set LRSUD to zero to make a bigger table (set LWSUD non-zero to write it).

```
HWWARN CALLED FROM SUBPROGRAM HWBSUD: CODE= 515
RUN CANNOT CONTINUE
```

The table of Sudakov form factors read on unit LRSUD is for a different value of a relevant parameter (in this case the b quark mass).

Action taken: run aborted. The user must make a new table (set LWSUD non-zero to write it).

8.5 Sample output

This is the output from the main program listed in section 8.1, with no event printout or user analysis.

```
HERWIG 6.500    16 Oct 2002
```

```
Please reference:  G. Marchesini, B.R. Webber,
```

G.Abbiendi, I.G.Knowles, M.H.Seymour & L.Stanco
Computer Physics Communications 67 (1992) 465

and

G.Corcella, I.G.Knowles, G.Marchesini, S.Moretti,
K.Odagiri, P.Richardson, M.H.Seymour & B.R.Webber,
JHEP 0101 (2001) 010

Since SUSY processes are called,
please also reference: S.Moretti, K.Odagiri,
P.Richardson, M.H.Seymour & B.R.Webber,
JHEP 0204 (2002) 028

Reading in SUSY data from unit 66

INPUT CONDITIONS FOR THIS RUN

BEAM 1 (P) MOM. = 7000.00
BEAM 2 (P) MOM. = 7000.00
PROCESS CODE (IPROC) = 3000
NUMBER OF FLAVOURS = 6
STRUCTURE FUNCTION SET = 8
AZIM SPIN CORRELATIONS = T
AZIM SOFT CORRELATIONS = T
QCD LAMBDA (GEV) = 0.1800
DOWN QUARK MASS = 0.3200
UP QUARK MASS = 0.3200
STRANGE QUARK MASS = 0.5000
CHARMED QUARK MASS = 1.5500
BOTTOM QUARK MASS = 4.9500
TOP QUARK MASS = 175.0000
GLUON EFFECTIVE MASS = 0.7500
EXTRA SHOWER CUTOFF (Q)= 0.4800
EXTRA SHOWER CUTOFF (G)= 0.1000
PHOTON SHOWER CUTOFF = 0.4000
CLUSTER MASS PARAMETER = 3.3500
SPACELIKE EVOLN CUTOFF = 2.5000
INTRINSIC P-TRAN (RMS) = 0.0000
DECAY SPIN CORRELATIONS= T
SUSY THREE BODY ME = T
SUSY FOUR BODY ME = F

NO EVENTS WILL BE WRITTEN TO DISK

B_d: Delt-M/Gam =0.7000 Delt-Gam/2*Gam =0.0000

B_s: Delt-M/Gam = 10.00 Delt-Gam/2*Gam =0.2000

PDFLIB NOT USED FOR BEAM 1

PDFLIB NOT USED FOR BEAM 2

Checking consistency of particle properties

Checking consistency of decay tables

Line 1 is the same as line 2634
Take BR 0.333 and ME code 100 from second entry
Line 2 is the same as line 2635
Take BR 0.333 and ME code 100 from second entry
Line 3 is the same as line 2636
Take BR 0.111 and ME code 100 from second entry
Line 4 is the same as line 2637
Take BR 0.111 and ME code 100 from second entry
Line 5 is the same as line 2638
Take BR 0.111 and ME code 100 from second entry
Line 6 is the same as line 2639
Take BR 0.333 and ME code 100 from second entry
Line 7 is the same as line 2640
Take BR 0.333 and ME code 100 from second entry
Line 8 is the same as line 2641
Take BR 0.111 and ME code 100 from second entry
Line 9 is the same as line 2642
Take BR 0.111 and ME code 100 from second entry
Line 10 is the same as line 2643
Take BR 0.111 and ME code 100 from second entry

WRITING SUDAKOV TABLE ON UNIT 77

WRITING MATRIX ELEMENT TABLE ON UNIT 88

CHECKING SUSY DECAY MATRIX ELEMENTS

PARTICLE TYPE 21=PIO SET STABLE

INITIAL SEARCH FOR MAX WEIGHT

PROCESS CODE IPROC = 3000
RANDOM NO. SEED 1 = 1246579
SEED 2 = 8447766
NUMBER OF SHOTS = 10000
NEW MAXIMUM WEIGHT = 2.4359288434851706E-03
NEW MAXIMUM WEIGHT = 3.7017893759328114E-03
NEW MAXIMUM WEIGHT = 1.9578185739344733E-02

HWWARN CALLED FROM SUBPROGRAM HWSMRS: CODE = 5
EVENT 0: SEEDS = 17673 & 63565 WEIGHT = 0.0000E+00
EVENT SURVIVES. EXECUTION CONTINUES
WARNING: MRST98 CALLED WITH Q OUTSIDE ALLOWED RANGE!
Q VALUE=3.869E+03, MINIMUM=1.118E+00, MAXIMUM=3.162E+03
NO FURTHER WARNINGS WILL BE ISSUED

NEW MAXIMUM WEIGHT = 2.2550328399448680E-02
NEW MAXIMUM WEIGHT = 5.5633613959185035E-02
NEW MAXIMUM WEIGHT = 6.9166986913034176E-02
NEW MAXIMUM WEIGHT = 0.1197405440791255
NEW MAXIMUM WEIGHT = 0.1488818465259009

INITIAL SEARCH FINISHED

OUTPUT ON ELEMENTARY PROCESS

N.B. NEGATIVE WEIGHTS NOT ALLOWED

NUMBER OF EVENTS = 0
NUMBER OF WEIGHTS = 10000
MEAN VALUE OF WGT = 4.1213E-03
RMS SPREAD IN WGT = 1.2862E-02
ACTUAL MAX WEIGHT = 1.3755E-01
ASSUMED MAX WEIGHT = 1.4888E-01

PROCESS CODE IPROC = 3000
CROSS SECTION (PB) = 4.121
ERROR IN C-S (PB) = 0.1286
EFFICIENCY PERCENT = 2.768

SUBROUTINE TIMEL CALLED BUT NOT LINKED.
DUMMY TIMEL WILL BE USED. DELETE DUMMY

AND LINK CERNLIB FOR CPU TIME REMAINING.

OUTPUT ON ELEMENTARY PROCESS

N.B. NEGATIVE WEIGHTS NOT ALLOWED

```
NUMBER OF EVENTS   =          100
NUMBER OF WEIGHTS  =          3699
MEAN VALUE OF WGT  =   3.7473E-03
RMS SPREAD IN WGT  =   1.2205E-02
ACTUAL MAX WEIGHT   =   1.3900E-01
ASSUMED MAX WEIGHT  =   1.4888E-01
```

```
PROCESS CODE IPROC =          3000
CROSS SECTION (PB) =    3.747
ERROR IN C-S (PB)  =    0.2007
EFFICIENCY PERCENT =    2.517
```

8.5.1 Guide to sample output

See ref. [1] for a full discussion of the basic features of HERWIG output, including a listing of a sample event. Here we point out only some new features in comparison to version 5.1.

The beam particles, their energies and the process code `IPROC=3000` indicate the SUSY process of squark and/or gluino production at LHC. The call to `HWISEP` triggers a request for a SUSY particle data file, in the format specified in section 3.5, which is read in from the default unit. In this case the file corresponds to the second LHC SUGRA point discussed in section 3.5.1.

First the program lists the main relevant input parameters, including B_d and B_s mixing parameters. Parton distributions were not requested from the `PDFLIB` library and therefore the default MRST set [51] is used (see sect. 4.1.1.)

Next the program performs some basic checks on the particle data provided. Here it finds that the input file read by `HWISEP` contains top quark decay modes which duplicate the default modes stored in `HWUDAT`. The branching ratios and matrix element codes are accordingly updated to those in the input file.

After an initial search for the maximum weight, the program prints its estimate of the relevant cross section and the expected Monte Carlo efficiency for event generation. During the search for the maximum weight the default parton distributions are called with a parameter, in this case the scale, outside the allowed range and a warning is issued. The maximum or minimum value of the parameter is used instead, depending on whether the value requested is too large or too small.

In the course of event generation a new cross section estimate is generated, which is printed together with the actual Monte Carlo efficiency at the end of the run.

8.6 Subroutine descriptions

We give in table 29 a list of all subroutines with their functions. Note that the third letter of the name usually follows a rough classification scheme.

| Name | Description |
|--------|---|
| | Main program and initialisation |
| HWIGPR | Main program |
| HWIGIN | Default initialisations |
| | Reading/writing/altering decay modes |
| HWIGUP | Initialisation for Les Houches interface |
| HWIMDE | Adds modes for SUSY four body decays |
| HWIODK | Inputs/outputs formatted decay tables |
| HWISPC | Initialisation of couplings for spin correlations and SUSY decays |
| HWISPN | Initialisation for spin correlations and SUSY decays |
| HWISP2 | Initialisation of two body decays for spin correlations and SUSY decays |
| HWISP3 | Initialisation of three body decays for spin correlations and SUSY decays |
| HWISP4 | Initialisation of four body decays for spin correlations and SUSY decays |
| HWIPHS | Initialises optimized phase space |
| HWISSP | Inputs supersymmetric particle data |
| HWMODK | Modifies or adds an individual decay mode |
| | User-provided analysis routines |
| HWABEG | Initialises user's analysis |
| HWAEND | Terminates user's analysis |
| HWANAL | Performs user's analysis on event |
| | Parton branching with interfering gluons |
| HWBAZF | Computes azimuthal correlation functions |
| HWBCON | Makes colour connections between jets |
| HWBDED | Correction to the 'dead zone' in e^+e^- |
| HWBDIS | Correction to the 'dead zone' in DIS |
| HWBDYP | Correction to the 'dead zone' in Drell-Yan |
| HWBFIN | Transfers external lines of jet to /HEPEVT/ |
| HWBGEN | Finds unevolved partons and generates jets |
| HWBGUP | Makes colour and flavour connections for Les Houches events |
| HWBJCO | Combines jets with correct kinematics |
| HWBMAS | Computes masses and trans. momenta in jet |
| HWBRAN | Generates a timelike parton branching |
| HWBRCN | Replaces HWBCON if R-parity is violated |
| HWBRC1 | Finds colour partner in gluino decay |
| HWBRC2 | Finds colour partner in jet |
| HWBSPA | Computes momenta in spacelike jet |

Table 29: Subroutines. (Continues)

| Name | Description |
|--------|--|
| HWBSPN | Computes spin density/decay matrices |
| HWBSU1 | First term in quark Sudakov form factor |
| HWBSU2 | Second term in quark Sudakov form factor |
| HWBSUD | Computes (or reads) Sudakov form factors |
| HWBSUG | Integrand in gluon Sudakov form factor |
| HWBSUL | Logarithmic part of Sudakov form factor |
| HWBTIM | Computes momenta in timelike jet |
| HWBTOP | Correction to the ‘dead zone’ in top decay |
| HWBVMC | Virtual mass cutoff for parton type ID |
| | Cluster hadronization model |
| HWCBCT | Cuts a massive baryon cluster in two |
| HWCBVI | Clusters quarks from a \mathcal{B} interaction |
| HWCBVT | Finds which \mathcal{B} interaction partons came from |
| HWCCCC | Finds colour connections after gluon splitting if \mathcal{B} |
| HWCCUT | Cuts a massive cluster in two |
| HCDEC | Decays clusters into primary hadrons |
| HCFLA | Sets up flavours for HWCHAD |
| HCFOR | Forms clusters |
| HWCOSP | Splits gluons |
| HWCHAD | Decays a cluster into one or two hadrons |
| | Particle and heavy quark decays |
| HWD2ME | Finds maximum weight for a two body decay for spin correlations |
| HWD3ME | SUSY three body decays and spin correlations master routine |
| HWD3M0 | Calculation of SUSY three body matrix element |
| HWD3M1 | Helicity amplitude for $f \rightarrow f f \bar{f}$ via vector boson exchange |
| HWD3M2 | Helicity amplitude for $f \rightarrow f f \bar{f}$ via Higgs exchange |
| HWD3M3 | Helicity amplitude for $f \rightarrow f f \bar{f}$ via antifermion exchange |
| HWD3M4 | Helicity amplitude for $f \rightarrow f f \bar{f}$ via sfermion exchange |
| HWD3M5 | Helicity amplitude for $\bar{f} \rightarrow \bar{f} f f$ via vector boson exchange |
| HWD3M6 | Helicity amplitude for $\phi \rightarrow \phi f \bar{f}$ via vector boson exchange |
| HWD3M7 | Helicity amplitude for $f \rightarrow \tilde{G} f \bar{f}$ via vector boson exchange |
| HWD3M8 | Helicity amplitude for $f \rightarrow \bar{f} \bar{f} f$ via scalar exchange (1st diagram) |
| HWD3M9 | Helicity amplitude for $f \rightarrow \bar{f} \bar{f} f$ via scalar exchange (2nd diagram) |
| HWD3MA | Helicity amplitude for $f \rightarrow \bar{f} \bar{f} f$ via scalar exchange (3rd diagram) |
| HWD3MB | Helicity amplitude for $f \rightarrow f f f$ via scalar exchange (1st diagram) |
| HWD3MC | Helicity amplitude for $f \rightarrow f f f$ via scalar exchange (2nd diagram) |
| HWD3MD | Helicity amplitude for $f \rightarrow f f f$ via scalar exchange (3rd diagram) |
| HWD3MF | Helicity amplitude for $f \rightarrow \bar{f} \bar{f} \bar{f}$ via scalar exchange (1st diagram) |
| HWD3MG | Helicity amplitude for $f \rightarrow \bar{f} \bar{f} \bar{f}$ via scalar exchange (2nd diagram) |

Table 29: Subroutines. (Continues)

| Name | Description |
|---------|--|
| HWD3MH | Helicity amplitude for $f \rightarrow \bar{f}\bar{f}\bar{f}$ via scalar exchange (3rd diagram) |
| HWD3MI | Helicity amplitude for $\bar{f} \rightarrow \bar{f}\bar{f}\bar{f}$ via scalar exchange |
| HWD4ME | Master routine for SUSY four body decays |
| HWD4M0 | Matrix Element for $\phi \rightarrow V^*V^* \rightarrow f\bar{f}f\bar{f}$ |
| HWDBOS | Finds and decays W and Z bosons |
| HWDBOZ | Chooses decay mode of W and Z bosons |
| HWDBZ2 | Copy of HWDBOZ used by hadronic WW, WZ and ZZ production |
| HWDCCHK | Checks given decay mode is self-consistent |
| HWDCLE | Interface to CLEO package for B decays |
| HWDEUR | Interface to EURODEC package for B decays |
| HWDFIV | Generates a five-body decay |
| HWDFOR | Generates a four-body decay |
| HWDHAD | Generates decays of unstable hadrons |
| HWDHGC | Higgs $\rightarrow \gamma\gamma$ decay |
| HWDHGF | Higgs $\rightarrow W^+W^-$ decay |
| HWDHIG | Finds and decays Higgs bosons |
| HWDHOB | Finds and decays heavy objects |
| HWDH01 | Selects decay mode for heavy object |
| HWDH02 | Calculates momenta of heavy object's decay products |
| HWDH03 | Makes colour connects for heavy object decay |
| HWDH04 | Performs parton shower for heavy object decay |
| HWDH05 | Checks for colour disconnections in heavy object decay |
| HWDH06 | Perform \mathcal{R}_p colour connections in heavy object decay |
| HWDHVY | Finds and decays heavy flavours |
| HWDHWT | Subroutine for top decay via a virtual H^\pm |
| HWDRCL | Colour connections for a \mathcal{B} SUSY decay |
| HWDRME | Main \mathcal{R}_p 3-body decay matrix element subroutine |
| HWDRM1 | \mathcal{R}_p 3-body decay matrix element subroutine |
| HWDRM2 | \mathcal{R}_p 3-body decay matrix element subroutine |
| HWDRM3 | \mathcal{R}_p 3-body decay matrix element subroutine |
| HWDRM4 | \mathcal{R}_p 3-body decay matrix element subroutine |
| HWDRM5 | \mathcal{R}_p 3-body decay matrix element subroutine |
| HWDPWT | Phase space three-body decay weight |
| HWDSIN | Performs decays with spin correlations |
| HWDSI1 | Picks next particle to decay for spin correlations |
| HWDSI2 | Pick moment of decay products with spin correlations |
| HWDSI3 | Selects τ polarization and passes it to the decay routine |
| HWDSM2 | Two body decay with spin correlations |
| HWDSM3 | Three body decay with spin correlations |

Table 29: Subroutines. (Continues)

| Name | Description |
|--------|--|
| HWDSM4 | Four body decay with spin correlations |
| HWDTAU | Interface to TAUOLA for τ decays |
| HWDTHR | Generates a three-body decay |
| HWDTOP | Decides whether to decay top quark |
| HWDTWO | Generates a two-body decay |
| HWDWWT | Weak ($V - A$) three-body decay weight |
| HWDXLM | Tests if decay vertex lies in given volume |
| | Elementary subprocess generation |
| HWECIR | Interface to CIRCE |
| HWEFIN | Final calculations on elementary subprocess |
| HWEGAM | Generates incoming photon |
| HWEINI | Initialises elementary subprocess |
| HWEISR | Generates photon emission from e or μ |
| HWEONE | Sets up a $2 \rightarrow 1$ hard subprocess |
| HWEPRO | Generates elementary subprocess |
| HWETWO | Sets up a $2 \rightarrow 2$ hard subprocess |
| | Individual hard subprocesses |
| HWH2BK | Matrix element for $b\bar{b} \rightarrow W^\pm H^\mp$ |
| HWH2BH | Matrix element for H^\pm production via bq -fusion |
| HWH2DD | Function to return the D function of [68] |
| HWH2F1 | Subroutine to return the F function of [69] for a fixed first momentum |
| HWH2F2 | Subroutine to return the F function of [69] for a fixed second momentum |
| HWH2F3 | Subroutine to return the F function of [69] for all first and second momenta |
| HWH2HE | Matrix element for Higgs associated production |
| HWH2M0 | Subroutine to compute the massless matrix element for $Q\bar{Q}Z$ |
| HWH2MQ | Subroutine to compute the massive matrix element for $Q\bar{Q}Z$ |
| HWH2PS | Subroutine to perform the phase-space for Z +two jets |
| HWH2P1 | Subroutine to select quark masses for HWH2PS |
| HWH2P2 | Subroutine to select quark masses for HWH2PS |
| HWH2QH | Matrix element for $q\bar{q}, gg \rightarrow Q\bar{Q}^{(\prime)}$ Higgs |
| HWH2SH | Matrix element for squark pair plus Higgs production |
| HWH2SS | Subroutine to return the S function of [68] |
| HWH2T1 | Function to return the T_1 function of [68] |
| HWH2T2 | Function to return the T_2 function of [68] |
| HWH2T3 | Function to return the T_3 function of [68] |
| HWH2T4 | Function to return the T_4 function of [68] |
| HWH2T5 | Function to return the T_5 function of [68] |
| HWH2T6 | Function to return the T_6 function of [68] |
| HWH2T7 | Function to return the T_7 function of [68] |

Table 29: Subroutines. (Continues)

| Name | Description |
|--------|--|
| HWH2T8 | Function to return the T_8 function of [68] |
| HWH2T9 | Function to return the T_9 function of [68] |
| HWH2T0 | Function to return the T_{10} function of [68] |
| HWH2VH | Matrix element for $q\bar{q}^{(\prime)} \rightarrow V$ Higgs, $V = W^\pm, Z^0$ |
| HWH4JT | Hard subprocess: $e^+e^- \rightarrow 4$ jets |
| HWH4J1 | Matrix element for $e^+e^- \rightarrow 4$ jets |
| HWHBGF | Hard subprocess: boson-gluon fusion (BGF) |
| HWHBKI | Computes kinematics for BGF |
| HWHBRN | Returns a phase-space point for BGF |
| HWHBSG | Computes cross section for BGF |
| HWHDIS | Hard subprocess: deep inelastic e/μ quark |
| HWHDYP | Hard subprocess: Drell-Yan Z^0/γ production |
| HWHDYQ | Subroutine for $Q\bar{Q}Z$ |
| HWHEGG | Hard subprocess: two-photon processes in e^+e^- |
| HWHEGW | Hard subprocess: γW processes in e^+e^- |
| HWHEGX | Calculates cross section for HWHEGW |
| HWHEPA | Hard subprocess: $e^+e^- \rightarrow q\bar{q}$ |
| HWHEPG | Hard subprocess: $e^+e^- \rightarrow q\bar{q}g$ |
| HWHESG | Gaugino pair production in e^+e^- collisions |
| HWHESL | Slepton pair production in e^+e^- collisions |
| HWHESP | Sparticle pair production in e^+e^- collisions |
| HWHESQ | Squark pair production in e^+e^- collisions |
| HWHEW0 | $e^+e^- \rightarrow W^+W^-$ subroutine |
| HWHEW1 | $e^+e^- \rightarrow W^+W^-$ subroutine |
| HWHEW2 | $e^+e^- \rightarrow W^+W^-$ subroutine |
| HWHEW3 | $e^+e^- \rightarrow W^+W^-$ subroutine |
| HWHEW4 | $e^+e^- \rightarrow W^+W^-$ subroutine |
| HWHEW5 | $e^+e^- \rightarrow W^+W^-$ subroutine |
| HWHEWW | Hard subprocess: $e^+e^- \rightarrow W^+W^-$ |
| HWHGBP | Main routine for gauge boson pair production in hadron-hadron |
| HWHGBS | Phase space for gauge boson pair production in hadron-hadron |
| HWHGB1 | Selects gauge boson mass for HWHGBS |
| HWHGB2 | Matrix element for WW in hadron-hadron |
| HWHGB3 | Matrix element for ZZ in hadron-hadron |
| HWHGB4 | Matrix element for WZ in hadron-hadron |
| HWHGB5 | Selects t and u for HWHGBS |
| HWHGRV | Graviton resonance production |
| HWHGUP | External hard process using Les Houches interface |
| HWHHVY | Hard subprocess: heavy quark production |

Table 29: Subroutines. (Continues)

| Name | Description |
|--------|---|
| HWHIBG | Hard subprocess: for $bg \rightarrow Q$ Higgs, with $Q = t, b$ |
| HWHIBK | Hard subprocess: $b\bar{b} \rightarrow W^\pm H^\mp$ |
| HWHIBQ | Subroutine for H^\pm production via bq -fusion |
| HWHIG1 | Matrix elements for Higgs + jet production |
| HWHIGA | Amplitudes squared for Higgs + jet |
| HWHIGB | Loop integrals for Higgs + jet |
| HWHIGE | Hard subprocess: Higgs associated production |
| HWHIGH | Hard subprocess: $q\bar{q} \rightarrow \text{Higgs}_1 + \text{Higgs}_2$ |
| HWHIGJ | QCD Higgs + jet production |
| HWHIGM | Choose any Higgs mass for production routines |
| HWHIGQ | Hard subprocess: $q\bar{q}, gg \rightarrow Q\bar{Q}^{(\prime)}$ Higgs |
| HWHIGS | Hard subprocess: $gg/q\bar{q} \rightarrow \text{Higgs}$ |
| HWHIGT | Computes $gg \rightarrow \text{Higgs}$ cross section |
| HWHIGV | Hard subprocess: $q\bar{q}^{(\prime)} \rightarrow V$ Higgs, $V = W^\pm, Z^0$ |
| HWHIGW | Hard subprocess: $W^+W^-/Z^0Z^0 \rightarrow \text{Higgs}$ |
| HWHIGY | Computes $e^+e^- \rightarrow Z^0 \rightarrow Z^0 H_{\text{SM}}^0$ cross section |
| HWHIGZ | Hard subprocess: $\ell^+\ell^- \rightarrow Z^0 \rightarrow Z^0 H_{\text{SM}}^0$ |
| HWHIHH | Hard subprocess: $\ell^+\ell^-$ SUSY Higgs pair production |
| HWHISQ | Subroutine for squark pair plus Higgs production |
| HWHPH2 | Hard subprocess: direct photon pairs |
| HWHPH0 | Hard subprocess: direct photon production |
| HWHPPB | Box contribution to $gg \rightarrow \gamma\gamma$ |
| HWHPPE | Pointlike photon-parton (fixed flavour) |
| HWHPPH | Pointlike photon-parton (fixed pair flavour) |
| HWHPPM | Pointlike photon-parton direct light meson |
| HWHPPT | Pointlike photon-parton (all flavours) |
| HWHPQS | Pointlike photon-quark (Compton) scattering |
| HWHQCD | QCD $2 \rightarrow 2$ hard subprocesses |
| HWHQCP | Identifies QCD $2 \rightarrow 2$ hard subprocess |
| HWHQCM | Hard subprocess: $\gamma\gamma \rightarrow q\bar{q}, \ell^+\ell^-, W^+W^-$ |
| HWHRBB | \mathcal{R}_p resonant squark to SM particles |
| HWHRBS | \mathcal{R}_p resonant squark to SUSY particles |
| HWHREE | \mathcal{R}_p SM particle production in e^+e^- collisions |
| HWHREM | Treats hard scattering remnants |
| HWHREP | Decides which \mathcal{R}_p subroutine to use in e^+e^- |
| HWHRES | \mathcal{R}_p single sparticle production in e^+e^- collisions |
| HWHRLL | \mathcal{R}_p resonant slepton to SM particles |
| HWHRLS | \mathcal{R}_p resonant slepton to SUSY particles |
| HWHRSP | Decides which \mathcal{R}_p subroutine to use in hadron-hadron |

Table 29: Subroutines. (Continues)

| Name | Description |
|--------|---|
| HWHRSS | Identifies \mathcal{R}_p process |
| HWHSCT | Process extra hard scatterings |
| HWHSNG | Colour singlet parton scattering |
| HWHSNM | Colour singlet parton scattering matrix element |
| HWHSPN | Main routine for spin correlations in the hard process |
| HWHS01 | Helicity amplitude for $f\bar{f} \rightarrow f\bar{f}$ via s -channel vector boson exchange |
| HWHS02 | Helicity amplitude for $f\bar{f} \rightarrow f\bar{f}$ via t -channel scalar exchange |
| HWHS03 | Helicity amplitude for $f\bar{f} \rightarrow f\bar{f}$ via u -channel scalar exchange |
| HWHS04 | Helicity amplitude for $f\bar{f} \rightarrow f\bar{f}$ via s -channel vector boson exchange |
| HWHS05 | Helicity amplitude for $g\bar{g} \rightarrow f\bar{f}$ via t -channel fermion exchange |
| HWHS06 | Helicity amplitude for $g\bar{g} \rightarrow f\bar{f}$ via u -channel fermion exchange |
| HWHS07 | Helicity amplitude for $g\bar{g} \rightarrow f\bar{f}$ via s -channel gluon exchange |
| HWHS08 | Helicity amplitude for $g\bar{f} \rightarrow f\phi$ via t -channel scalar exchange |
| HWHS09 | Helicity amplitude for $g\bar{f} \rightarrow f\phi$ via t -channel scalar exchange |
| HWHS10 | Helicity amplitude for $g\bar{f} \rightarrow f\phi$ via s -channel fermion exchange |
| HWHS11 | Helicity amplitude for $g\bar{f} \rightarrow f\phi$ via s -channel antifermion exchange |
| HWHS12 | Helicity amplitude for $g\bar{f} \rightarrow f\phi$ via u -channel fermion exchange |
| HWHS13 | Helicity amplitude for $g\bar{f} \rightarrow f\phi$ via u -channel fermion exchange |
| HWHS14 | Helicity amplitude for $g\bar{g} \rightarrow f\bar{f}$ via t -channel fermion exchange |
| HWHS15 | Helicity amplitude for $g\bar{g} \rightarrow f\bar{f}$ via u -channel fermion exchange |
| HWHS16 | Helicity amplitude for $g\bar{g} \rightarrow f\bar{f}$ via s -channel gluon exchange |
| HWHS17 | Helicity amplitude for $f\bar{f} \rightarrow f\bar{f}$ via t -channel gauge boson exchange |
| HWHS18 | Helicity amplitude for $f\bar{f} \rightarrow f\bar{f}$ via t -channel gauge boson exchange |
| HWHS19 | Helicity amplitude for $\bar{f}f \rightarrow \bar{f}f$ via t -channel gauge boson exchange |
| HWHS20 | Helicity amplitude for $\bar{f}f \rightarrow \bar{f}f$ via t -channel gauge boson exchange |
| HWHS21 | Helicity amplitude for $f\bar{f} \rightarrow f\bar{f}$ via s -channel scalar exchange |
| HWHS22 | Helicity amplitude for $f\bar{f} \rightarrow f\bar{f}$ via t -channel scalar exchange |
| HWHS23 | Helicity amplitude for $\bar{f}f \rightarrow \bar{f}f$ via u -channel scalar exchange |
| HWHS24 | Helicity amplitude for $\bar{f}f \rightarrow \bar{f}f$ via s -channel scalar exchange |
| HWHS25 | Helicity amplitude for $\bar{f}f \rightarrow \bar{f}f$ via t -channel scalar exchange |
| HWHS26 | Helicity amplitude for $\bar{f}f \rightarrow \bar{f}f$ via u -channel scalar exchange |
| HWHS27 | Helicity amplitude for $f\bar{f} \rightarrow f\bar{f}$ via s -channel scalar exchange |
| HWHS28 | Helicity amplitude for $f\bar{f} \rightarrow f\bar{f}$ via t -channel scalar exchange |
| HWHS29 | Helicity amplitude for $f\bar{f} \rightarrow f\bar{f}$ via u -channel scalar exchange |
| HWHS30 | Helicity amplitude for $\bar{f}f \rightarrow \bar{f}f$ via s -channel scalar exchange |
| HWHS31 | Helicity amplitude for $\bar{f}f \rightarrow \bar{f}f$ via t -channel scalar exchange |
| HWHS32 | Helicity amplitude for $\bar{f}f \rightarrow \bar{f}f$ via u -channel scalar exchange |
| HWHS33 | Helicity amplitude for $f\bar{f} \rightarrow f\bar{f}$ via s -channel scalar exchange |
| HWHS34 | Helicity amplitude for $\bar{f}f \rightarrow \bar{f}f$ via s -channel scalar exchange |

Table 29: Subroutines. (Continues)

| Name | Description |
|---------|--|
| HWHSS1 | Gaugino-gaugino production matrix element |
| HWHSS2 | Gaugino-gaugino production matrix element with polarizations |
| HWHSSG | Gaugino-gaugino/gaugino-sparton production |
| HWHSSL | Slepton pair production |
| HWHSSP | Combines MSSM subprocesses |
| HWHSSQ | SQCD $2 \rightarrow 2$ hard subprocesses |
| HWHSSS | Identifies MSSM hard subprocess |
| HWHV1J | Hard subprocess W/Z + jet production |
| HWHV2J | Master subroutine for all gauge boson + two jet processes |
| HWHVVJ | Dummy WW, WZ, ZZ production subroutine (see sect. 9.6) |
| HWHWEX | Top production by W exchange |
| HWHWPR | Hard subprocess: W production |
| | Soft minimum-bias or underlying event |
| HWMEVT | Generates min bias or soft underlying event |
| HWMLPS | Generates longitudinal phase space |
| HWMNBI | Computes negative binomial probability |
| HWMULT | Chooses min bias charged multiplicity |
| HMMWGT | Calculates weight for minimum bias events |
| | Random number generators |
| HWRAZM | Randomly rotated azimuth |
| HWREXP | Random number: exponential distribution |
| HWREXQ | Random number: exp. dist. with cutoff |
| HWREXT | Random number: exponential transverse mass |
| HWRGAU | Random number: gaussian |
| HWRGEN | Random number generator (l'Ecuyer's method) |
| HWRINT | Random integer |
| HWRLOG | Random logical |
| HWRPIP | Random primary interaction point |
| HWRPOW | Random number: power distribution |
| HWRUNG | Random number: uniform + gaussian tails |
| HWRUNI | Random number: uniform |
| | Spacelike branching of incoming partons |
| HWSBRN | Generates spacelike parton branching |
| HWSDBG | Drees-Grassie gluon distribution in photon |
| HWSDBGQ | Drees-Grassie quark distribution in photon |
| HWSFBR | Chooses a spacelike branching |
| HWSFUN | Hadron structure functions |
| HWSGAM | Gamma function (for structure functions) |
| HWSGEN | Generates x values for spacelike partons |

Table 29: Subroutines. (Continues)

| Name | Description |
|--------|--|
| HWSGQQ | Inserts $g \rightarrow q\bar{q}$ part of gluon form factor |
| HWSMRS | Subroutine for MRST PDFs |
| HWSSPC | Replaces spacelike partons by spectators |
| HWSSUD | Sudakov form factor/structure function |
| HWSTAB | Interpolates in function table (for HWSSUD) |
| HWSVAL | Checks for valence parton |
| | Miscellaneous utilities |
| HWUAEM | Running electromagnetic coupling constant |
| HWUAER | Real part of photon self-energy |
| HWUALF | Two-loop QCD running coupling constant |
| HWUANT | Finds a particle's antiparticle |
| HWUATS | Replaces & with |
| HWUBPR | Prints branching data for last parton shower |
| HWUBST | Boost event record to/from hadron-hadron c.m.f. |
| HWUCFF | Coefficients for e^+e^- and DIS cross sections |
| HWUCI2 | Logarithmic integral Ci_2 |
| HWUDAT | Particle properties (N.B. BLOCK DATA) |
| HWUDKL | Generates decay vertex of unstable particle |
| HWUDKS | Converts decay modes into internal format |
| HWUDPR | Prints particle properties and decay modes |
| HWUECM | Centre-of-mass energy |
| HWUEDT | Insert or delete entries in the event record |
| HWUEEC | Computes coefficients for e^+e^- cross section |
| HWUEMV | Moves entries within the event record |
| HWUEPR | Prints event data |
| HWUFNE | Finishes an event |
| HWUGAU | Adaptive gaussian integration |
| HWUGUP | Run termination for Les Houches Accord |
| HWUIDT | Translates particle identity codes |
| HWUINC | Initial parameter-dependent calculations |
| HWUINE | Initialises an event |
| HWULB4 | Boost: rest frame to lab, no masses assumed |
| HWULDO | Lorentz 4-vector dot product |
| HWULF4 | Boost: lab frame to rest, no masses assumed |
| HWULI2 | Logarithmic integral Li_2 (Spence function) |
| HWULOB | Lorentz transformation: rest frame \rightarrow lab |
| HWULOF | Lorentz transformation: lab \rightarrow rest frame |
| HWULOR | Multiplies by Lorentz matrix |
| HWUMAS | Puts mass in 5th component of vector |

Table 29: Subroutines. (Continues)

| Name | Description |
|--------|--|
| HWUMBW | Generates mass (Breit-Wigner distribution) |
| HWUMPO | Spinor routine |
| HWUMPP | Spinor routine |
| HWUNST | Converts integer to character |
| HWUPCM | Centre-of-mass momentum |
| HWUPUP | Prints contents of Les Houches common block |
| HWURAP | Rapidity |
| HWURES | Computes/prints resonance data |
| HWUROB | Rotation by inverse of matrix R |
| HWUROF | Rotation by matrix R |
| HWUROT | Computes rotation R from vector to z -axis |
| HWUSOR | Sorts an array in ascending order |
| HWUSPR | Print contents of spin correlations common block |
| HWUSQR | Square root with sign retention |
| HWUSTA | Makes a particle type stable |
| HWUTAB | Interpolates in a table |
| HWUTIM | Checks time remaining |
| | Vector manipulation |
| HWVDIF | Vector difference |
| HWVDOT | Vector dot product |
| HWVEQU | Vector equality |
| HWVSCA | Vector times scalar |
| HWVSUM | Vector sum |
| HWVZRI | Vector zero (integer) |
| HWVZRO | Vector zero |
| HWWARN | Issues warnings and deals with errors |

Table 29: Subroutines.

In addition there are the routines for generating the Schuler-Sjöstrand parton distributions of the photon:

SASANO SASBEH SASDIR SASGAM SASVMD

and for putting the output of TAUOLA [88] into the /HEPEVT/ common block:

FILHEP

Finally, there are dummy versions of external routines, which should be deleted if the relevant packages are used:

- CERN Library routine giving TRES= CPU time (in seconds) remaining (dummy returns TRES=10¹⁰):

TIMEL

- CERN PDFLIB structure function package:

PDFSET STRUCTM

- EURODEC B decay package:

EUDINI FRAGMT IEUPDG IPDGEU

- CLEO B decay package:

DECADD QQINIT QQLMAT

- HERBVI baryon number violation package:

HVCBVI HVHBVI

- CIRCE beamstrahlung package (see below):

CIRCEE CIRCES CIRCGG

- TAUOLA τ lepton decay package (see below):

DEXAY INIETC INIMAS INIPHX INITDK PHOINI PHOTOS

- Les Houches interface (see below):

UPINIT UPEVNT

9. Interfaces

9.1 Les Houches

Version 6.5 includes support for the interface between parton level generators and HERWIG using the Les Houches Accord as described in [89]. In general we have tried to code the interface in such a way that from the user point of view it behaves in the same way as that already included in PYTHIA [90].

The interface operates in the following way. If the IPROC code is set negative then HERWIG assumes that the user wants an external hard process using the Les Houches accord.

If this option is used the initialisation will call the routine UPINIT to initialise the external hard process; this name is the same as that used by PYTHIA. This routine should set the values of the run parameters in the Les Houches run common block.

After the initialisation during the event generation phase the routine `UPEVNT` (again this name is the same as that used by `PYTHIA`) is called. This routine should fill the event common block as described in [89].

Dummy copies of both these routines are supplied with `HERWIG` and should be deleted and replaced if you are using this option. Due to the internal structure of `HERWIG` two new parameters are needed to control the interface, in addition to those in the Les Houches common block. The logical input variable `LHSOFT` [`.TRUE`] controls the generation of the soft underlying event; the default is to generate a soft underlying event and so `LHSOFT` must be set `.FALSE.` for lepton-lepton processes. The second variable `LHGLSF` [`.FALSE.`] controls the treatment of colour self-connected gluons, which may occur with some methods of colour decomposition. The default is to kill events with self-connected gluons whereas if `LHGLSF = .TRUE.` an information-only warning is issued instead.

We have not included full support for the interface. In particular

- It is assumed that all events have two particles of status `IDUP=-1`;
- We do not support the status codes `-2` and `-9`;
- The treatment of the code `IDUP=3` is the same as `IDUP=2`, i.e. all intermediate resonances have their masses preserved.

These restrictions are the same as those imposed by `PYTHIA`. If you have any problems with the interface or need the options we have not yet supported please let us know.

It should also be noted that while the interface has been tested with Standard Model processes, for example all the processes in `ALPGEN` [91], it is less well tested for `SUSY` processes.

9.2 CIRCE

Simulation of beamstrahlung is now available, via an interface to the `CIRCE` program [92]. It is implemented as a modification of the standard bremsstrahlung implementation, so is only available for processes for which that is available. The produced radiation is treated in the collinear limit, i.e. `COLISR` and the option `WWA` in routine `HWEGAM` are forcibly set `.TRUE.`.

For both types of distribution function, $f_{e/e}$ and $f_{\gamma/e}$, we use a simplifying approximation: where the correct result should use the convolution of beamstrahlung and bremsstrahlung, we actually use the sum of the two. For the photon distribution this is quite reasonable, but for the electron it is perhaps more questionable. It boils down to the replacement:

$$f_{e/e}(x) = \int_x^1 \frac{dz}{z} f_{e/e,\text{brem}}(z) f_{e/e,\text{beam}}\left(\frac{x}{z}\right) \rightarrow f_{e/e,\text{brem}}(x) + f_{e/e,\text{beam}}(x) - \delta(1-x). \quad (9.1)$$

This is good to the extent that both distributions are dominated by the $x \rightarrow 1$ region. A small utility program can be obtained from the HERWIG web page to test this approximation. For example, for TESLA running at 500 GeV, the integral over $f_{e/e}(x)$ for large x , relevant for threshold shapes, is accurate to 1% for $x > 0.95$ and to 10% for $x > 0.99$, and the value of $f_{e/e}((\frac{90}{500})^2)$, relevant for radiative return to the Z, is accurate to 2%.

In order for the distribution to be probabilistic, the coefficient of the delta function has to remain positive. If it is not, HERWIG will terminate. This can be prevented by adjusting the ZMXISR parameter: the default value, ZMXISR=0.999999 is too large and HERWIG will fail, but reducing it to ZMXISR=0.99999 works fine for all the parameter sets currently available. It is straightforward to check that ZMXISR values in this range do not have an influence on any physical observables, by rerunning with it further reduced.

The interface is controlled by five new variables, which are given in the following table together with their default values:

| | |
|--------|------------|
| CIRCOP | 0 |
| CIRCAC | 2 |
| CIRCVR | 7 |
| CIRCVR | 9999 12 31 |
| CIRCCH | 0 |

CIRCOP is the main control option: CIRCOP=0 switches off beamstrahlung and uses standard HERWIG; CIRCOP=1 switches to collinear kinematics, but still leaves beamstrahlung switched off; CIRCOP=2 uses only beamstrahlung; and CIRCOP=3 uses both beamstrahlung and bremsstrahlung. CIRCOP=0 and CIRCOP=3 should therefore be regarded as ‘off’ and ‘on’, respectively, with the other two options mainly for cross-checking purposes. The variables CIRCAC, CIRCVR, CIRCVR and CIRCCH are simply passed to CIRCE as its input variables `acc`, `ver`, `rev` and `chat`, as described in its documentation. The default values correspond to the most up-to-date revision of version 7 of the TESLA parametrization, with minimal output.

CIRCE can be obtained from

<http://heplix.ikp.physik.tu-darmstadt.de/nlc/beam.html>

9.3 TAUOLA

An interface to the TAUOLA decay package [88] has been added. To use this interface, the dummy subroutines DEXAY, INIETC, INIMAS, INIPHX, INITDK, PHOINI, PHOTOS must be deleted. You should then link to both TAUOLA and PHOTOS. The easiest way to do this is to obtain the TAUOLA/PHOTOS versioning system from

<http://wasm.home.cern.ch/wasm/test.html>

and produce a version with the correct size of the `HEPEVT` common block. This system will provide a `JETSET` demo. If you link `HERWIG` with the code produced by this apart from the `JETSET` interface and main program everything should work.

This interface uses the information from the spin density matrices to select the helicity of the decaying τ leptons if the spin correlation algorithm is being used; otherwise the helicity of the decaying τ is averaged over.

9.4 ISAWIG

`ISAWIG` is an interface which allows `SUSY` spectra and decay tables generated by `ISAJET` [39] to be read into `HERWIG`. The web address is

<http://www.hep.phy.cam.ac.uk/~richardn/HERWIG/ISAWIG/>

To coincide with the release of `HERWIG` 6.5 we have produced a new version of `ISAWIG`. Since the original version of `ISAWIG` there have been a number of new versions of `ISAJET`, often with changes in the sizes of the common blocks from which we extract the information we need. This has necessitated periodical updating of the code to run with the most recent version of `ISAJET`, with the result that the code could no longer be run with older versions. However, the Snowmass points and slopes [93] are defined with `ISAJET` version 7.58 and so we can no longer continue in this way and still be able to generate these points. Therefore, starting with the new `ISAWIG` version 1.2, we are using C preprocessing so that users can define the version of `ISAJET` they are using at compile time. When compiling the main `ISAWIG` code and the modified `SUGRUN` and `SSRUN` programs the following compiler options should be specified:

- `-DISAJET758` to use `ISAJET7.58`,
- `-DISAJET763` to use `ISAJET7.63`.

The default at the moment is to compile code to run with `ISAJET7.64`. In the future this will change so that the most recent version of `ISAJET` becomes the default but we will continue to support the older versions.

9.5 HDECAY

There has also been a new release of the `HDECAY` package [94], version 3. In order to support this version, and the previous version 2.0, we are also using C preprocessing to control the version of `HDECAY` used. In order to achieve this the `HDECAY` interface code has been merged with the main `ISAWIG` program. The following options should be used when compiling `ISAWIG` if you are using `HDECAY`:

- `-DHDECAY2` if you are using version 2 of `HDECAY`
- `-DHDECAY3` if you are using version 3 of `HDECAY`.

As before the default is to compile a dummy routine. If you are using HDECAY you must link with a version of the HDECAY code which has the main HDECAY program removed.

9.6 MC@NLO

The program MC@NLO [95] generates events with

- exclusive rates and distributions accurate to next-to-leading order when expanded in α_s ;
- multiple soft/collinear parton emission generated by HERWIG parton showering;
- hadronization according to the HERWIG cluster model.

At present only the processes of gauge boson pair production in hadron ($h = p$ or \bar{p}) collisions are implemented in MC@NLO, making use of the HERWIG process codes IPROC=2850–2880 (see table 9).

To use these codes, one must delete the dummy HERWIG subroutine HWHVJ and replace it by the one in the MC@NLO package. This will then read and process an input file of parton configurations prepared by MC@NLO. For further details see the MC@NLO web page:

<http://www.hep.phy.cam.ac.uk/theory/webber/MCatNLO/>

Implementation of other processes, such as heavy quark production, in MC@NLO is in progress [96]. These future development will make use of the Les Houches interface discussed in sect. 9.1, rather than special process codes.

9.7 JIMMY

Contrary to our original plans, the JIMMY generator [49] for multiple parton-parton interactions in hadron-hadron, hadron-photon and photon-photon collisions is still not integrated into HERWIG, and is still a separate add-on package. It can be obtained from the JIMMY web page:

<http://jetweb.hep.ucl.ac.uk/JIMMY/index.html>

where references to the relevant papers can also be found.

9.8 HERBVI

An interface is provided to the HERBVI package for electroweak baryon number violation (\mathcal{B}), and other multi- W^\pm production processes [44]. For full details, see

<http://www.hep.phy.cam.ac.uk/~richardn/HERWIG/HERBVI/>

Acknowledgments

We thank G. Abbiendi, J. Chýla and L. Stanco for their collaboration on earlier versions of HERWIG and for their continuing interest. We also thank U. Baur, M.J. Gibbs, E.W.N. Glover, Z. Kunszt and D.R. Ward for contributing code to be incorporated into the program.

We are grateful to the many experimental colleagues who have made valuable criticisms and suggestions over the years, especially K. Hamacher, R. Hemingway and G. Rudolph.

Since this is expected to be the last (Fortran) HERWIG version, we would like to take this opportunity to thank again all those colleagues and users who have contributed to the development of the program, whether by providing code, suggesting improvements or reporting problems. Thanks also to those who worked so hard to establish the Les Houches accord, which should make it possible to expand the application of Fortran HERWIG to new processes without (much) further intervention by the authors. Meanwhile, many of us will be transferring our main efforts to HERWIG++, in preparation for the new era of object-oriented event generation.

References

- [1] G. Marchesini, B.R. Webber, G. Abbiendi, I.G. Knowles, M. H. Seymour and L. Stanco, *HERWIG: a Monte Carlo event generator for simulating hadron emission reactions with interfering gluons. Version 5.1 - april 1991*, *Comput. Phys. Commun.* **67** (1992) 465.
- [2] A. Bassetto, M. Ciafaloni and G. Marchesini, *Jet structure and infrared sensitive quantities in perturbative QCD*, *Phys. Rep.* **100** (1983) 201.
- [3] G. Marchesini and B. R. Webber, *Simulation of QCD jets including soft gluon interference*, *Nucl. Phys.* **B 238** (1984) 1.
- [4] B.R. Webber, *A QCD model for jet fragmentation including soft gluon interference*, *Nucl. Phys.* **B 238** (1984) 492.
- [5] B.R. Webber, *Monte Carlo simulation of hard hadronic processes*, *Ann. Rev. Nucl. Part. Sci.* **36** (1986) 253.
- [6] R.K. Ellis, G. Marchesini and B.R. Webber, *Soft radiation in parton parton scattering*, *Nucl. Phys.* **B 286** (1987) 643.
- [7] G. Marchesini and B.R. Webber, *Monte Carlo simulation of general hard processes with coherent QCD radiation*, *Nucl. Phys.* **B 310** (1988) 461.
- [8] G. Marchesini and B.R. Webber, *Associated transverse energy in hadronic jet production*, *Phys. Rev.* **D 38** (1988) 3419.

- [9] I.G. Knowles, *Spin correlations in parton-parton scattering*, *Nucl. Phys.* **B 310** (1988) 571.
- [10] I.G. Knowles, *A linear algorithm for calculating spin correlations in hadronic collisions*, *Comput. Phys. Commun.* **58** (1990) 271.
- [11] G. Marchesini and B.R. Webber, *Simulation of QCD coherence in heavy quark production and decay*, *Nucl. Phys.* **B 330** (1990) 261.
- [12] G. Marchesini and B.R. Webber, *Simulation of QCD initial state radiation at small x* , *Nucl. Phys.* **B 349** (1991) 617.
- [13] S. Catani, B.R. Webber and G. Marchesini, *QCD coherent branching and semiinclusive processes at large x* , *Nucl. Phys.* **B 349** (1991) 635.
- [14] G. Abbiendi and L. Stanco, *Heavy flavor production at HERA. Simulation with a new Monte Carlo event generator*, *Z. Physik* **C 51** (1991) 81; *A new heavy flavor generator in e-p collisions*, *Comput. Phys. Commun.* **66** (1991) 16.
- [15] M.H. Seymour, *Photon radiation in final state parton showering*, *Z. Physik* **C 56** (1992) 161.
- [16] M.H. Seymour, *Matrix element corrections to parton shower algorithms*, *Comput. Phys. Commun.* **90** (1995) 95.
- [17] M.H. Seymour, *A simple prescription for first order corrections to quark scattering and annihilation processes*, *Nucl. Phys.* **B 436** (1995) 443 [[hep-ph/9410244](#)].
- [18] M.H. Seymour, *Matrix element corrections to parton shower simulation of deep inelastic scattering*, contributed to 27th International Conference on High Energy Physics (ICHEP), Glasgow 1994, Lund preprint LU-TP-94-12, unpublished.
- [19] G. Corcella and M.H. Seymour, *Matrix element corrections to parton shower simulations of heavy quark decay*, *Phys. Lett.* **B 442** (1998) 417 [[hep-ph/9809451](#)].
- [20] G. Corcella, M.H. Seymour, *Initial state radiation in simulations of vector boson production at hadron colliders*, *Nucl. Phys.* **B 565** (2000) 227 [[hep-ph/9908388](#)].
- [21] P. Richardson, *Spin correlations in Monte Carlo simulations*, *J. High Energy Phys.* **0111** (2001) 029 [[hep-ph/0110108](#)].
- [22] S. Moretti, K. Odagiri, P. Richardson, M. H. Seymour and B. R. Webber, *Implementation of supersymmetric processes in the HERWIG event generator*, *J. High Energy Phys.* **0204** (2002) 028 [[hep-ph/0204123](#)].
- [23] D. Amati and G. Veneziano, *Preconfinement as a property of perturbative QCD*, *Phys. Lett.* **B 83** (1979) 87.

- [24] Yu.L. Dokshitzer and S.I. Troyan, *Nonleading perturbative corrections to the dynamics of quark-gluon cascades and soft hadron spectra in e^+e^- annihilation*, Leningrad Nuclear Physics Institute preprint **N 922** (1984);
Y.I. Azimov, Yu.L. Dokshitzer, V.A. Khoze and S.I. Troian, *The string effect and QCD coherence*, *Phys. Lett.* **B 165** (1985) 147; *Similarity of parton and hadron spectra in QCD jets*, *Z. Physik* **C 27** (1985) 65.
- [25] T. Sjöstrand et al., *QCD event generators for LEP*, in *Z Physics at LEP*, G. Altarelli, R. Kleiss and C. Verzegnassi eds., CERN 89-08.
- [26] I.G. Knowles, T. Sjöstrand et al. *Report of QCD Event Generators Working Group*, in *Physics at LEP2*, ed. G. Altarelli, T. Sjöstrand and F. Zwirner, CERN 96-01.
- [27] S. Gieseke, *Event generators – new developments*, to appear in *Proc. 14th Topical Conference on Hadron Collider Physics (Karlsruhe, October 2002)*.
- [28] Yu.L. Dokshitzer, V.A. Khoze, S.I. Troyan and A.H. Müller, *QCD coherence in high-energy reactions*, *Rev. Mod. Phys.* **60** (1988) 373.
- [29] CDF Collaboration, *Evidence for color coherence in $p\bar{p}$ collisions at $\sqrt{s} = 1.8$ TeV*, *Phys. Rev.* **D 50** (1994) 556.
- [30] DØ collaboration, *Color coherent radiation in multijet events from $p\bar{p}$ collisions at $\sqrt{s} = 1.8$ TeV* *Phys. Lett.* **B 414** (1997) 419 [[hep-ex/9706012](#)];
Evidence of color coherence effects in W^+ jets events from $p\bar{p}$ collisions at $\sqrt{s} = 1.8$ TeV, *Phys. Lett.* **B 464** (1999) 145 [[hep-ex/9908017](#)].
- [31] K. Odagiri, *Color connection structure of (supersymmetric) QCD ($2 \rightarrow 2$) processes*, *J. High Energy Phys.* **10** (1998) 006 [[hep-ph/9806531](#)].
- [32] Yu.L. Dokshitzer, V.A. Khoze and S.I. Troian, *New perturbative results in hadron jet physics*, in *Proc. Physics in Collision 6*, Chicago 1986, p.417.
- [33] A. Einstein, B. Podolski and N. Rosen, *Can quantum mechanical description of physical reality be considered complete?*, *Phys. Rev.* **47** (1935) 777.
- [34] G. Marchesini, *QCD coherence in the structure function and associated distributions at small x* , *Nucl. Phys.* **B 445** (1995) 49 [[hep-ph/9412327](#)].
- [35] T. Sjöstrand, *High-energy physics event generation with PYTHIA 5.7 and JETSET 7.4*, *Comput. Phys. Commun.* **82** (1994) 74.
- [36] G. Corcella and S. Moretti, in preparation.
- [37] M.H. Seymour, *The Higgs boson line shape and perturbative unitarity*, *Phys. Lett.* **B 354** (1995) 409 [[hep-ph/9505211](#)].
- [38] D. E. Groom et al., *Review of particle physics*, *Eur. Phys. J.* **C 15** (2000) 1.

- [39] F.E. Paige, S.D. Protopopescu, H. Baer and X. Tata, ISAJET 7.37: *a Monte Carlo event generator for pp , $\bar{p}p$ and e^+e^- reactions*, [hep-ph/9804321]; ISAJET 7.40: *a Monte Carlo event generator for pp , $\bar{p}p$, and e^+e^- reactions* preprint BNL-HET-98/39, FSU-HEP-981016, UH-511-917-98, October 1998, [hep-ph/9810440]. H. Baer, F.E. Paige, S.D. Protopopescu, X. Tata, preprint BNL-HET-99-43, FSU-HEP-991218, UH-511-952-00, [hep-ph/0001086]. Latest version available from <ftp://penguin.phy.bnl.gov:/pub/isajet/>.
- [40] H.E. Haber and G.L. Kane, *The search for supersymmetry: probing physics beyond the Standard Model*, *Phys. Rep.* **117** (1985) 75.
- [41] J.F. Gunion, H. E. Haber, G.L. Kane and S. Dawson, *The Higgs hunter guide*, Addison-Wesley, Reading MA 1990.
- [42] H. Dreiner, P. Richardson and M.H. Seymour, *Parton-shower simulations of R-parity violating supersymmetric models*, *J. High Energy Phys.* **04** (2000) 008 [hep-ph/9912407].
- [43] H. Dreiner, *An introduction to explicit R-parity violation in Perspectives on Supersymmetry*, G.L. Kane ed., World Scientific, pp. 462–479 [hep-ph/9707435].
- [44] M.J. Gibbs, A. Ringwald, B.R. Webber and J.T. Zadrozny, *Monte Carlo simulation of baryon and lepton number violating processes at high-energies*, *Z. Physik C* **66** (1995) 285 [hep-ph/9406266]; M.J. Gibbs, B.R. Webber, HERBVI: *a program for simulation of baryon and lepton number violating processes*, *Comput. Phys. Commun.* **90** (1995) 369 [hep-ph/9504232].
- [45] A. Kupco, *Cluster hadronization in HERWIG 5.9*, in Proc. Workshop on Monte Carlo Generators for HERA Physics, Hamburg 1998, p.292 [hep-ph/9906412].
- [46] B. Andersson, G. Gustafsson, G. Ingelman and T. Sjöstrand, *Parton fragmentation and string dynamics*, *Phys. Rep.* **97** (1983) 33.
- [47] TPC/TWO GAMMA collaboration, H. Aihara et al., *Study of baryon correlations in e^+e^- annihilation at 29 GeV*, *Phys. Rev. Lett.* **57** (1986) 3140.
- [48] UA5 collaboration, G.J. Alner et al., *The UA5 high-energy $\bar{p}p$ simulation program*, *Nucl. Phys. B* **291** (1987) 445.
- [49] J.M. Butterworth and J.R. Forshaw, *Photoproduction of multi-jet events at HERA: a Monte Carlo simulation*, *J. Phys. G* **19** (1993) 1657; J.M. Butterworth, J.R. Forshaw and M.H. Seymour, *Multiparton interactions in photoproduction at HERA*, *Z. Physik C* **72** (1996) 637 [hep-ph/9601371].
- [50] H. Plathow-Besch, PDFLIB: *a library of all available parton density functions of the nucleon, the pion and the photon and the corresponding alpha-s calculations*, *Comput. Phys. Commun.* **75** (1993) 396.

- [51] A.D. Martin, R.G. Roberts, W.J. Stirling and R.S. Thorne, *Scheme dependence, leading order and higher twist studies of MRST partons*, *Phys. Lett.* **B 443** (1998) 301 [[hep-ph/9808371](#)].
- [52] R.S. Thorne, private communication.
- [53] M. Drees and K. Grassie, *Parametrizations of the photon structure and applications to supersymmetric particle production at HERA*, *Z. Physik* **C 28** (1985) 451.
- [54] M. Drees and C.S. Kim, *Associate production of a heavy quark and a gauge boson at e^+p colliders*, *Z. Physik* **C 52** (1991) 503.
- [55] G. A. Schuler and T. Sjostrand, *Parton distributions of the virtual photon*, *Phys. Lett.* **B 376** (1996) 193 [[hep-ph/9601282](#)].
- [56] M. Drees and R.M. Godbole, *Virtual photon structure functions and the parton content of the electron*, *Phys. Rev.* **D 50** (1994) 3124 [[hep-ph/9403229](#)].
- [57] *Z Physics at LEP1*, CERN 89-09, vol. 3, p. 129.
- [58] H. Burkhardt, F. Jegerlehner, G. Penso and C. Verzegnassi, *Uncertainties in the hadronic contribution to the QED vacuum polarization*, *Z. Physik* **C 43** (1989) 497.
- [59] R. K. Ellis, D. A. Ross and A. E. Terrano, *The perturbative calculation of jet structure in e^+e^- annihilation*, *Nucl. Phys.* **B 178** (1981) 421.
- [60] S. Catani and M.H. Seymour, *A general algorithm for calculating jet cross sections in NLO QCD*, *Nucl. Phys.* **B 485** (1997) 291 [[hep-ph/9605323](#)]; erratum *ibid.* **510** (1997) 503.
- [61] S. Moretti and W.J. Stirling, *Spin correlations in $e^+e^- \rightarrow 4jets$* , *Eur. Phys. J.* **C 9** (1999) 81 [[hep-ph/9808429](#)];
S. Moretti, *The implementation of the four-jet matrix elements in HERWIG and elsewhere*, preprint RAL-TR-2000-039, August 2000 [[hep-ph/0008197](#)].
- [62] S. Katsanevas and P. Morawitz, *SUSYGEN 2.2: a Monte Carlo event generator for MSSM sparticle production at e^+e^- colliders*, *Comput. Phys. Commun.* **112** (1998) 227 [[hep-ph/9711417](#)].
- [63] J. Kalinowski, R. Ruckl, H. Spiesberger and P.M. Zerwas, *Supersymmetry with R-parity breaking: contact interactions and resonance formation in leptonic processes at LEP2*, *Phys. Lett.* **B 406** (1997) 314 [[hep-ph/9703436](#)].
- [64] A. Djouadi, J. Kalinowski and P. M. Zerwas, *Higgs radiation off top quarks in high-energy e^+e^- colliders*, *Z. Physik* **C 54** (1992) 255; S. Komamiya, *Searching For Charged Higgs Bosons At $O(1/2\text{-TeV To } 1\text{-TeV})$ e^+e^- Colliders*, *Phys. Rev.* **D 38** (1988) 2158; S. Kanemura, S. Moretti and K. Odagiri, *Single charged Higgs boson production at next generation linear colliders*, *J. High Energy Phys.* **0102** (2001) 011 [[hep-ph/0012030](#)]; *Single production of charged Higgs bosons at linear colliders*, [hep-ph/0101354](#).

- [65] A. Djouadi, J. Kalinowski and P. M. Zerwas, *Measuring the $H t \bar{t}$ coupling in e^+e^- collisions*, *Mod. Phys. Lett. A* **7** (1992) 1765; A. Juste and G. Merino, *Top-Higgs Yukawa coupling measurement at a linear e^+e^- collider*, [[hep-ph/9910301](#)] (and references therein); M. Battaglia, A. Ferrari, A. Kiiskinen and T. Maki, *Pair production of charged Higgs bosons at future linear e^+e^- colliders*, in *Proc. of the APS/DPF/DPB Summer Study on the Future of Particle Physics (Snowmass 2001)* ed. R. Davidson and C. Quigg, [[hep-ex/0112015](#)]; S. Moretti, *Detection of heavy charged Higgs bosons at future linear colliders*, [[hep-ph/0206208](#)]; *Higgs radiation off top-antitop pairs at future Linear Colliders: a background study*, [[hep-ph/9911501](#)]; S. Moretti, *The process $e^+e^- \rightarrow H t \bar{t}$ and its backgrounds at future electron positron colliders*, *Phys. Lett. B* **452** (1999) 338 [[hep-ph/9902214](#)].
- [66] A.H. Mueller and W.K. Tang, *High-energy parton-parton elastic scattering in QCD*, *Phys. Lett. B* **284** (1992) 123.
- [67] J. F. Gunion and Z. Kunszt, *Lepton correlations in gauge boson pair production and decay*, *Phys. Rev. D* **33** (1986) 665.
- [68] R. Kleiss and W. J. Stirling, *Spinor techniques for calculating $p\bar{p} \rightarrow W^\pm/Z^0 + jets$* , *Nucl. Phys. B* **262** (1985) 235.
- [69] B. van Eijk and R. Kleiss, *On the calculation of the exact $gg \rightarrow Z b\bar{b}$ cross-section including Z decay and b quark mass effects*, in *Proc. LHC Workshop, Aachen 1990*, vol. 2 183-194.
- [70] F. A. Berends, R. Pittau and R. Kleiss, *Excalibur: a Monte Carlo program to evaluate all four fermion processes at LEP-200 and beyond*, *Comput. Phys. Commun.* **85** (1995) 437 [[hep-ph/9409326](#)].
- [71] R. Kleiss and R. Pittau, *Weight optimization in multichannel Monte Carlo*, *Comput. Phys. Commun.* **83** (1994) 141 [[hep-ph/9405257](#)].
- [72] E. Eichten, I. Hinchliffe, K. Lane and C. Quigg, *Super collider physics*, *Rev. Mod. Phys.* **56** (1984) 579; erratum *ibid.* **58** (1986) 1065.
- [73] S. Dawson, E. Eichten and C. Quigg, *Search for supersymmetric particles in hadron-hadron collisions*, *Phys. Rev. D* **31** (1985) 1581.
- [74] A. Dedes and S. Moretti, *Eur. Phys. J. C* **10** (1999) 515; preprint RAL-TR-1999-067, June 1999, [[hep-ph/9909526](#)]; A. Djouadi *et al.*, preprint February 2000, [[hep-ph/0002258](#)].
- [75] A. Dedes and S. Moretti, *Phys. Rev. D* **60** (1999) 015007; A. Djouadi, J.-L. Kneur and G. Moutaka, *Phys. Rev. Lett.* **80** (1998) 1830; *Nucl. Phys. B* **569** (2000) 53; G. Bélanger, F. Boudjema and K. K. Sridhar, *Nucl. Phys. B* **568** (2000) 3.

- [76] A.A. Barrientos-Bendezù and B.A. Kniehl, $W^\pm H^\mp$ associated production at the Large Hadron Collider, *Phys. Rev. D* **59** (1999) 015009 [hep-ph/9807480];
S. Moretti and K. Odagiri, *The phenomenology of $W^\pm H^\mp$ production at the Large Hadron Collider*, *Phys. Rev. D* **59** (1999) 055008 [hep-ph/9809244].
- [77] S. Moretti and K. Odagiri, *Phys. Rev. D* **55** (1997) 5627.
- [78] M. Spira, *Fortsch. Phys.* **46** (1998) 203.
- [79] D. Dicus, T. Stelzer, Z. Sullivan and S. Willenbrock, *Phys. Rev. D* **59** (1999) 094016.
- [80] F. Borzumati, J.-L. Kneur and N. Polonsky, *Phys. Rev. D* **60** (1999) 115011;
S. Moretti and D.P. Roy, *Phys. Lett. B* **470** (1999) 209.
- [81] M. Carena *et al.*, *Report of the Tevatron Higgs working group*, hep-ph/0010338.
- [82] D.J. Miller, S. Moretti, D.P. Roy and W.J. Stirling, *Detecting heavy charged Higgs bosons at the LHC with four b quark tags*, *Phys. Rev. D* **61** (2000) 055011.
- [83] B.C. Allanach, K. Odagiri, M.A. Parker and B.R. Webber, *Searching for narrow graviton resonances with the ATLAS detector at the large hadron collider*, *J. High Energy Phys.* **09** (2000) 019.
- [84] A. Donnachie and P.V. Landshoff, *Total cross sections*, *Phys. Lett. B* **296** (1992) 227 [hep-ph/9209205].
- [85] S. Moch, A. Ringwald and F. Schrempp, *Instantons in deep-inelastic scattering. The simplest process*, *Nucl. Phys. B* **507** (1997) 134 [hep-ph/9609445]; *Instanton induced cross-sections in deep inelastic scattering*, *Phys. Lett. B* **438** (1998) 217 [hep-ph/9806528].
- [86] M. Gibbs, A. Ringwald and F. Schrempp, *QCD-instanton induced final states in deep inelastic scattering*, in Proc. DIS 1995 (Paris), pp. 341-344 [hep-ph/9506392];
A. Ringwald and F. Schrempp, *QCDINS 2.0: a Monte Carlo generator for instanton-induced processes in deep-inelastic scattering*, *Comput. Phys. Commun.* **132** (2000) 267 [hep-ph/9911516]
- [87] M.H. Seymour, *Heavy quark production in jets*, *Z. Physik C* **63** (1994) 99.
- [88] S. Jadach, Z. Was, R. Decker and J. H. Kuhn, *The tau decay library TAUOLA: Version 2.4*, *Comput. Phys. Commun.* **76** (1993) 361; Z. Was, *TAUOLA the library for tau lepton decay, and KKMC/KORALB/KORALZ/ status report*, *Nucl. Phys. B* **98** (Proc. Suppl.) (2001) 96. [hep-ph/0011305].
- [89] E. Boos *et al.*, *Generic user process interface for event generators*, [hep-ph/0109068].
- [90] T. Sjostrand, P. Eden, C. Friberg, L. Lonnblad, G. Miu, S. Mrenna and E. Norrbin, *High-energy-physics event generation with PYTHIA 6.1*, *Comput. Phys. Commun.* **135** (2001) 238 [hep-ph/0010017]; T. Sjostrand, L. Lonnblad and S. Mrenna, *PYTHIA 6.2: Physics and manual*, [hep-ph/0108264].

- [91] M. L. Mangano, M. Moretti, F. Piccinini, R. Pittau and A. D. Polosa, ALPGEN, *a generator for hard multiparton processes in hadronic collisions*, hep-ph/0206293.
- [92] T. Ohl, *CIRCE version 1.0: Beam spectra for simulating linear collider physics*, *Comput. Phys. Commun.* **101** (1997) 269 [hep-ph/9607454].
- [93] B. C. Allanach *et al.*, *The Snowmass points and slopes: Benchmarks for SUSY searches*, in *Proc. of the APS/DPF/DPB Summer Study on the Future of Particle Physics (Snowmass 2001)* ed. R. Davidson and C. Quigg, *Eur. Phys. J. C* **25** (2002) 113 [hep-ph/0202233].
- [94] A. Djouadi, J. Kalinowski and M. Spira, *HDECAY: A program for Higgs boson decays in the standard model and its supersymmetric extension*, *Comput. Phys. Commun.* **108** (1998) 56 [hep-ph/9704448].
- [95] S. Frixione and B. R. Webber, *Matching NLO QCD computations and parton shower simulations*, *J. High Energy Phys.* **0206** (2002) 029 [hep-ph/0204244]; *The MC@NLO event generator*, [hep-ph/0207182].
- [96] S. Frixione, P. Nason and B. R. Webber, *Matching NLO QCD computations and parton showers in heavy quark production*, in preparation.